

4332

UNIVERSITY OF HAWAII LIBRARY

GEOCHEMICAL VARIATIONS OF KAUA'I ISLAND AND SOUTH KAUA'I
SWELL VOLCANICS

A THESIS SUBMITTED TO THE GRADUATE DIVISION OF THE
UNIVERSITY OF HAWAII IN PARTIAL FULFILLMENT
OF THE REQUIREMENTS FOR THE DEGREE OF

MASTER OF SCIENCE

IN

GEOLOGY AND GEOPHYSICS

AUGUST 2008

By:

Lisa F. Swinnard

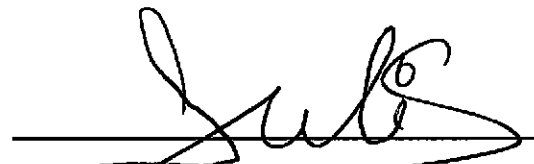

Thesis Committee:

Michael O. Garcia, Chairperson
Dominique Weis
Scott Rowland

We certify that we have read this thesis and that, in our opinion, it is satisfactory in scope and quality as a thesis for the degree of Master of Science in Geology and Geophysics.

THESIS COMMITTEE


Chairperson

ACKNOWLEDGEMENTS

I would like to thank Chuck Blay for his assistance in the field, Ian McDougall for supplying the post-shield Kaua'i samples, and Mike Vollinger and Mike Rhodes at the University of Massachusetts for the XRF analyses. Special thanks go out to Vivian Lai for all her assistance with the ICP-MS trace element analysis, to Bruno Kieffer for the Sr and Nd isotope analyses on the Triton TIMS and to Jane Barling and Alyssa Shiel for their assistance with the Pb and Hf isotopic analyses on the Nu Plasma MC-ICP-MS. Mahalo to all the cruise participants for making it an amazing and unforgettable experience, and for helping to document all the submarine samples. Thanks to Lindsey Spencer for all her long hours helping me prepare and process my samples for geochemical analysis. I would like to extend my deepest gratitude to my committee members, Michael Garcia, Dominique Weis and Scott Rowland. I appreciate all the time they spent with me discussing the project, answering my questions and revising all sections of this thesis. Finally, I would like to thank my family and friends for all the moral and emotional support and encouragement they provided over the past two years: Wendy Stovall, Andrea Steffke, Kelly Mitchell, Chris Wattam and Keli and Dave Swinnard. This project was fully funded by NSF grant EAR05-10482 to M.G.

ABSTRACT

This study addresses two enigmatic volcanic features of volcanism on and south of the island of Kauaʻi: (1) the long-lived (2.4 m.y.) and voluminous ($\sim 58 \text{ km}^3$) rejuvenated volcanism (Kōloa Volcanics), and (2) the prominent bathymetric swell south of Kauaʻi (SKS). A new suite of K-Ar dated late-shield, post-shield and rejuvenated lavas from Kauaʻi, and a suite of undated samples collected from the SKS are characterized for major and trace elements, and Pb, Sr, Nd and Hf isotopes to determine their sources and origins of formation. The geochemical relationships between the three stages of volcanism on Kauaʻi (shield, post-shield and rejuvenated) and the Pacific lithosphere indicate that the Kōloa Volcanics were derived solely from the Hawaiian mantle plume. A mantle plume source and the duration and composition of the Kōloa lavas are consistent with a combination of the flexure-induced melting model and the secondary zone of mantle plume melting model as the mechanisms responsible for the voluminous and long-lived Kōloa Volcanics. Geochemical relationships between the three stages of onshore Kauaʻi volcanism and the SKS volcanics are used in concert with morphological and geological data to evaluate the origin of the $\sim 5000 \text{ km}^2$ and 3000 km^3 swell. Its origin is controversial: landslide, secondary volcanism or separate shield? Lithologic, geochemical and gravity results are consistent with a huge landslide from an early Kauaʻi shield and a separate submarine shield that experienced extensive explosive volcanism. However, the absence of a scar and the two available K-Ar ages are not consistent with a landslide origin. Thus, a satellite shield model best explains the geological, geochemistry and geophysical data for the SKS.

TABLE OF CONTENTS

Acknowledgements.....	iii
Abstract	iv
List of Tables	vi
List of Figures	vii
 Part I: Geochemistry of Rejuvenated, Post-shield and Late-shield Volcanism on the Island of Kauaʻi, Hawaiʻi	
1.0: Introduction.....	2
2.0: Rejuvenated Volcanism Models	6
3.0: Samples and Analytical Techniques	9
4.0: Results.....	12
4.1 Major and Trace Element Compositions	12
4.2 Isotopic Compositions of the Post-shield and Kōloa Volcanics	23
5.0: Discussion.....	33
5.1 Sources of the Late-shield and Post-shield Stages of Kauaʻi Volcanism	33
5.2 Sources of the Kōloa Volcanics	34
5.3 Kauaʻi's Evolution and Plume Structure	36
5.4 Implications of Isotopic Results for Rejuvenated Volcanism Models ...	41
6.0: Conclusions.....	45
 Part II: Geochemical Inferences for the Origin of the South Kauaʻi Swell	
7.0: Introduction	48
8.0: Sampling and Analytical Techniques	51
9.0: Results	53
9.1 Major and Trace Element Compositions of the South Kauaʻi Swell Volcanics	53
9.2 Isotopic Compositions of the South Kauaʻi Swell Volcanics	64
10.0: Discussion	70
11.0: Conclusions	77
 Appendix A: Location and Sample Descriptions for SKS Volcanics	78
Appendix B: Leaching Information	88
Appendix C: Point Counting Petrography for Dive 252 Volcanics.....	90
References	91

LIST OF TABLES

Table	Page
1. XRF major and trace element compositions of the Kōloa Volcanics	15
2. XRF major and trace element compositions of the late-shield and post-shield stages of volcanism on Kauaʻi	17
3. ICP-MS trace element compositions of the Kōloa Volcanics	18
4. ICP-MS trace element compositions of the late-shield and post-shield stages of volcanism on Kauaʻi	20
5. Pb, Sr, Nd and Hf isotope data for the rejuvenated, post-shield and late-shield stages of Kauaʻi	26
6. XRF major and trace element compositions of the South Kauaʻi Swell volcanics	56
7. ICP-MS trace element compositions of the South Kauaʻi Swell volcanics	60
8. Pb, Sr, Nd and Hf isotope data for the South Kauaʻi Swell volcanics	66

LIST OF FIGURES

Figure	Page
1. Geological map of the island of Kauaʻi	5
2. Block diagram illustrating mechanisms for rejuvenated volcanism and inferred mantle structure	8
3. Total alkalis vs. silica diagram for Kauaʻi's late-shield and post-shield stages, and the Kōloa Volcanics	14
4. Major and trace element ratio plots comparing the three stages of volcanism on Kauaʻi: shield/late-shield, post-shield and rejuvenated	21
5. Comparison of Pb, Hf, Sr and Nd isotopic ratios for the three stages of Kauaʻi volcanism with recent EPR MORB lavas and ~110 Ma-old Pacific lithosphere from ODP Site 843	27
6. Comparison of Pb, Hf, Sr and Nd isotopic ratios from the different stages of Kauaʻi volcanism and rejuvenated volcanism (Kōloa, Honolulu, Kalaupapa and Lahaina Volcanics) with other Hawaiian shield volcanoes	28
7. Comparison of the different stages of Kauaʻi volcanism and rejuvenated volcanism from other Hawaiian Islands with the Loa-Kea compositional boundary	31
8. Pb, Sr and Nd isotopic ratios vs. age diagram for the Kōloa Volcanics, post-shield and late-shield stages of Kauaʻi	32
9. Cartoon illustrating the plume structure during the evolution of the island of Kauaʻi from the shield stage to the rejuvenated stage	40
10. Qualitative representation of the predicted rate of uplift of the flexural arch with distance from the load. Histogram of rock types vs. age in 0.50 Ma bins for the Kōloa Volcanics.....	44
11. Bathymetric map of the South Kauaʻi Swell showing the sample locations	50
12. Total alkalis vs. silica diagram for South Kauaʻi Swell volcanics	55
13. Major element ratio plots comparing the South Kauaʻi Swell volcanics to the different stages of volcanism on Kauaʻi	62

14. Trace element ratio plots comparing the South Kaua'i Swell volcanics to the different stages of volcanism on Kaua'i	63
15. Comparison of Pb, Hf, Sr and Nd isotopic ratios for the South Kaua'i Swell volcanics with the onshore Kaua'i lavas, the recent EPR MORB lavas and ~110 Ma-old Pacific lithosphere from ODP Site 843.....	67
16. Bathymetric map of the southeast part of the South Kaua'i Swell showing the numerous conical seamounts	71
17. $^{206}\text{Pb}/^{204}\text{Pb}$ vs. longitude for the South Kaua'i Swell and Kaua'i shield volcanics	73
18. Comparison of Pb, Hf, Sr and Nd isotopic ratios from the South Kaua'i Swell with other Hawaiian shield volcanoes	75

PART I

**GEOCHEMISTRY OF REJUVENATED, POST-SHIELD
AND LATE-SHIELD VOLCANISM ON THE ISLAND
OF KAUA'I, HAWAI'I**

1.0 INTRODUCTION

Rejuvenated volcanism is an enigmatic aspect of plume volcanism. It occurs hundreds of kilometers downstream from the ascending plume stem, which generates the vast bulk (>99 vol. %) of many oceanic island volcanoes (Macdonald et al., 1983).

Rejuvenated stage volcanism has occurred on many oceanic islands including Samoa (Wright and White, 1987), Kerguelen (Weis et al., 1998), the Canary Islands (Paris et al., 2005), and Mauritius (Paul et al., 2005). In Hawai'i, rejuvenated volcanism is found on the older (~5.5 Ma – 2 Ma) six of the nine main islands (Ka'ula, Ni'ihau, Kaua'i, O'ahu, Moloka'i and Maui; Macdonald et al., 1983; Garcia et al., 1986; Ozawa et al., 2005).

Rejuvenated lavas exhibit paradoxical trace element and isotopic signatures. Their high incompatible element abundances and ratios paired with depleted isotopic signatures spurred models incorporating varying amounts of metasomatic fluids from either an enriched or depleted mantle reservoir interacting with a lithospheric component (e.g., Clague and Frey, 1982; Maaloe, 1992; Reiners and Nelson, 1998).

The magma generation mechanism(s) and source components for rejuvenated volcanism remain controversial. Four components within the Hawaiian plume, Lō'ihi, Ko'olau, Kea and depleted mantle, are thought to be required to explain the overall isotopic variability of Hawaiian lavas (e.g., Hauri, 1996; Eiler et al., 1998; Mukhopadhyay, 2003; Frey et al., 2005; Fekiacova et al., 2007). However, only three geochemical end-members normally contribute to the lavas at individual volcanoes. For example, Kaua'i lavas involved the Lō'ihi, Ko'olau and DM components. The depleted mantle component is rarely sampled during the shield stage (Mukhopadhyay et al., 2003; Frey et al., 2005), although it is extensively represented in the rejuvenated stage of

Kauaʻi volcanism. To better understand this mantle component, its relationship to the Hawaiian plume and the causes of rejuvenated volcanism, we have studied the Kōloa Volcanics on Kauaʻi, the most voluminous ($\sim 58 \text{ km}^3$; Gandy et al., in review) and longest-lived (2.45 m.y.; Tagami et al., 2005) example of Hawaiian rejuvenated volcanism (Figure 1).

Kauaʻi is the northernmost and second oldest of the eight principal islands in the Hawaiian chain. Kauaʻi is commonly thought to represent a single shield volcano (Macdonald et al., 1960; Macdonald et al., 1983), although structural features and systematic geochemical variations led to the suggestion that it actually represents two shields (Holcomb et al., 1997). The subaerial shield building tholeiitic lavas ($>99 \text{ vol\%}$ of total island volume) erupted between 5.1 – 4.0 Ma (McDougall, 1979). Together, the subaerial lavas of the Nāpali, Makaweli, Olokele and Hāʻupu members form the Waimea Canyon Basalts (WCB; Macdonald et al., 1960). The oldest member is the Nāpali and it constitutes the major part of the shield (McDougall, 1964). Near the end of shield volcanism, a caldera close to the center of the island collapsed and was subsequently filled with Olokele member lavas. Caldera-filling lava breached the rim of the main caldera and flowed into a graben on the southwest of the island forming the Makaweli member. The Makaweli and Olokele members were subsequently partially capped by post-shield tholeiitic and alkalic lavas erupted from 3.95 – 3.58 Ma (McDougall, 1964; Clague and Dalrymple, 1988; Tagami et al., 2005). The smaller Hāʻupu member, on the southeast flank of the island, erupted at approximately the same time as the Makaweli and Olokele members (Macdonald et al., 1960). After a $\sim 1 \text{ Ma}$ period of quiescence, an

alkalic rejuvenated stage (Kōloa Volcanics) began and continued to at least 0.15 Ma (Macdonald et al., 1960; Tagami et al., 2005).

To understand the source components of rejuvenated volcanism better, as well as the mechanisms of its formation and the evolution of the Hawaiian mantle plume structure, we examined the geochemistry of a suite of Kauaʻi's shield and rejuvenated lavas spanning over 4 m.y. (from late-shield and post-shield to rejuvenated lavas). This study utilizes new samples collected during an extensive field and geochronological study that focused mainly on Kōloa Volcanics (Gandy et al., in review; Tagami et al., 2005). Major and trace element, and radiogenic isotope (Pb, Sr, Nd and Hf) data for K-Ar dated lavas from the late-shield (4 samples), post-shield (6 samples) and rejuvenated stages (16 samples) of Kauaʻi (McDougall, 1964; Tagami et al., 2005) are utilized here to evaluate the long-term geochemical evolution of Kauaʻi and the Hawaiian mantle plume.

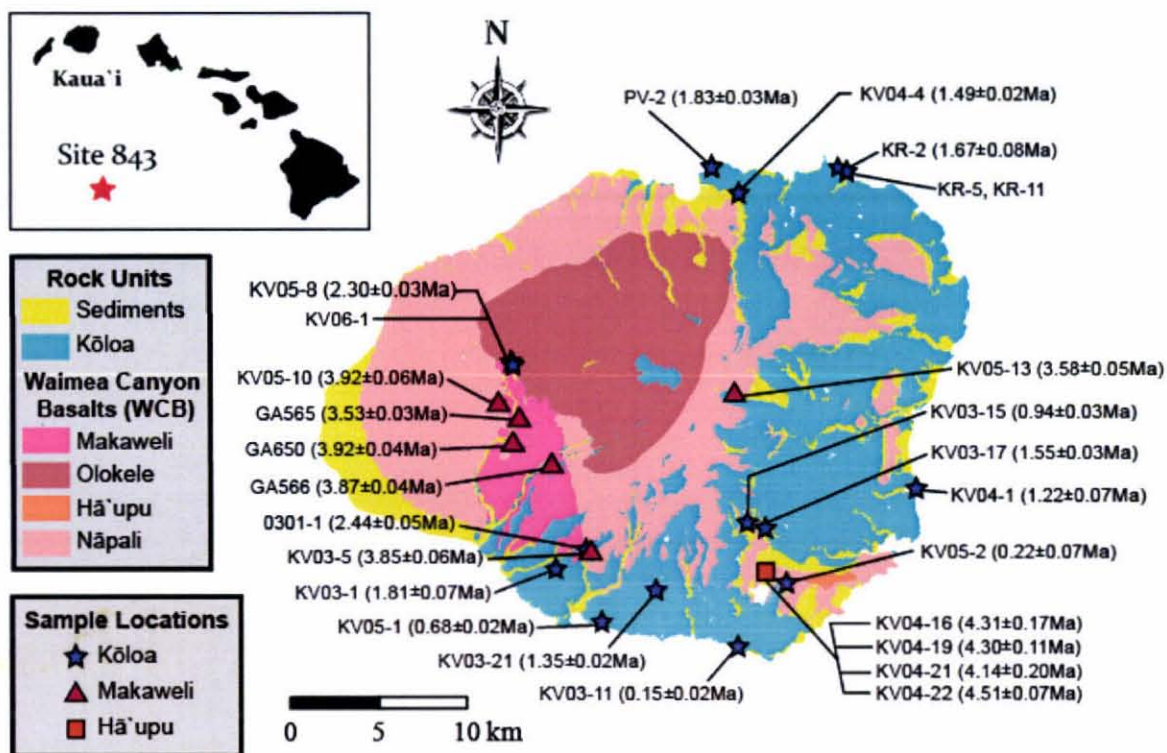


Fig. 1: Geological map of the island of Kaua'i showing the locations of the samples used in this study and their respective ages (modified from Sano, 2006). Blue stars indicate Kōloa Volcanics samples, pink triangles indicate post-shield samples and the orange square indicates the Hā'upu Tunnel samples. The inset map shows the Hawaiian Island chain and the location of the Ocean Drilling Program (ODP) Site 843.

2.0 REJUVENATED VOLCANISM MODELS

The three current models for the origin of rejuvenated volcanism are: (1) Lithospheric melting by conductive heating (Figure 2a); (2) Secondary zone of mantle plume melting from decompression uplift resulting from lateral spreading of the plume beneath the lithosphere (Figure 2a); and (3) Flexure-induced decompression melting (Figure 2b). Lithospheric melting by conductive heating proposes that rejuvenated volcanism occurred as a result of the ambient asthenosphere being quickly replaced by the hot Hawaiian mantle plume, which conductively heated and melted the lower lithosphere (Gurriet, 1987). This model predicts a greater volume ($<100 \text{ km}^3/\text{m.y.}$) and a longer duration ($\sim 5 \text{ Ma}$) of rejuvenated volcanism than has been observed on any Hawaiian volcano, including Kaua'i (Gandy et al., in review). Also, it fails to explain the observed $\sim 1+$ m.y. volcanic hiatus following the shield stage (Ozawa et al., 2005).

The model involving a secondary zone of mantle plume melting was designed to account for the significant volcanic hiatus ($\sim 1 \text{ m.y.}$) and duration of $\sim 1-2 \text{ m.y.}$ of rejuvenated volcanism 300-500 km downwind of the vertical plume stem (Ribe and Christensen, 1999). These features are thought to occur naturally as a result of the buoyant plume material spreading laterally and rising downstream of the plume stem (Ribe and Christensen, 1999). However, the model predicts both a smaller erupted volume and lower eruption rate for rejuvenated lavas than has been observed for Kaua'i (Gandy et al., in review).

The third model involves flexure-induced decompression melting of the chemically and isotopically heterogeneous mantle plume to produce the rejuvenated stage lavas (Jackson and Wright, 1970; Bianco et al., 2005). This decompression melting

occurs when a volcanic load above the plume stem causes flexural uplift of the surrounding hot elastic lithosphere (Bianco et al., 2005). This model successfully predicts the length of the volcanic hiatus, but not the 2.45 m.y. duration of Kaua'i's rejuvenated volcanism (Gandy et al., in review).

Isotopic compositions of Kōloa rejuvenated lavas are useful in determining their source components (lithosphere vs. mantle plume; Lassiter et al., 2000; Fekiacova et al., 2007), and thus may help to eliminate inadequate models. While the previous Kōloa Volcanics study (Gandy, 2006) evaluated the models based on volume flux, volcanic hiatus and duration of volcanism, this study incorporates new isotopic data for the Kōloa Volcanics. A viable model must explain the volume, age, compositional and isotopic data for rejuvenated volcanism. Here the current models will be evaluated using new high precision isotopic and other geochemical data.

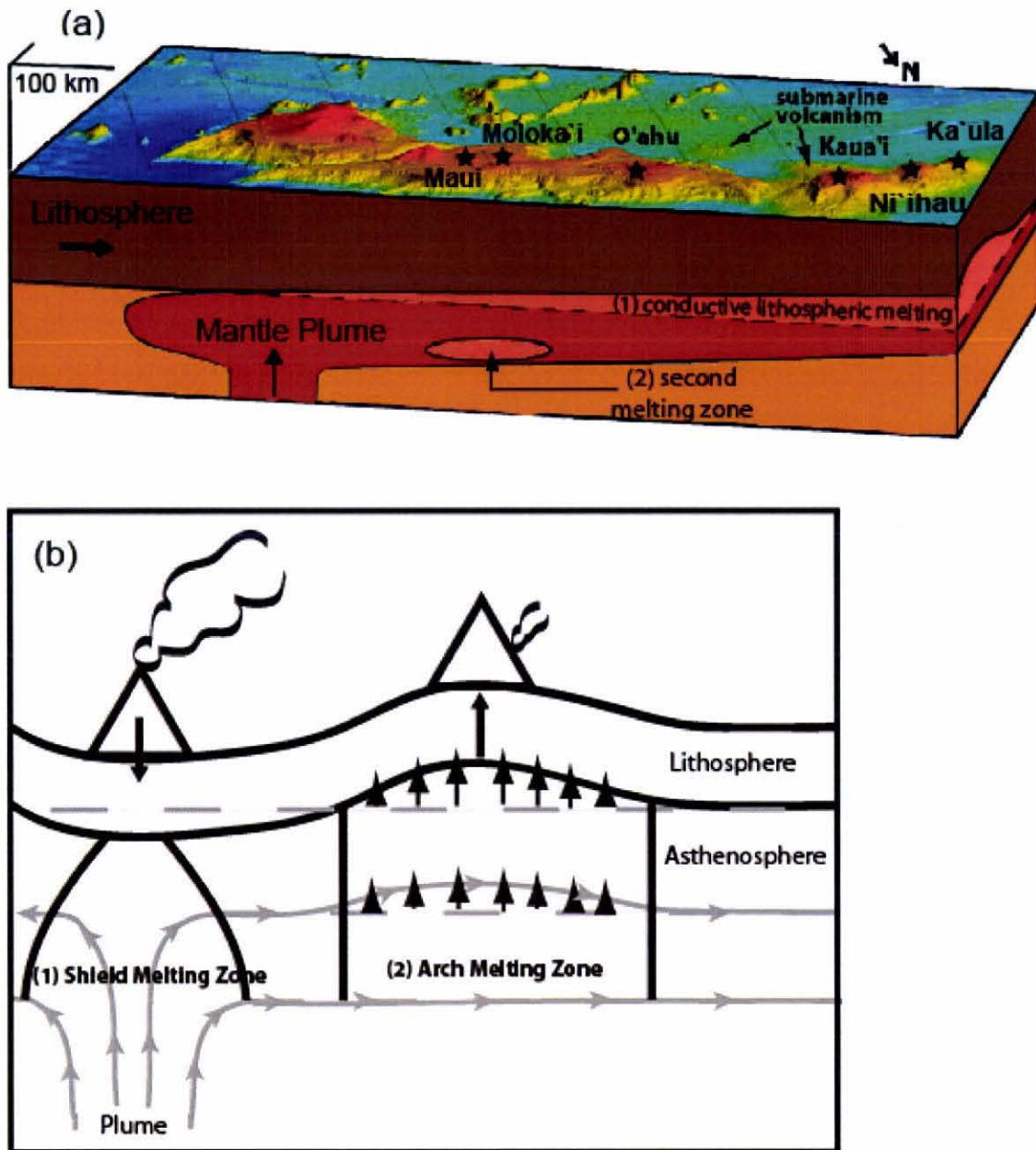


Fig. 2: (a) Block diagram illustrating mechanisms for rejuvenated volcanism and inferred mantle structure after Li et al. (2004), Ribe (2004), and B. Taylor (pers. comm., 2007). Black stars indicate volcanoes that have experienced rejuvenated volcanism. Mechanism (1) – lithospheric melting by conductive heating. Mechanism (2) – secondary melting zone of mantle plume. (b) Schematic representation of the flexure model for rejuvenated volcanism (modified from Bianco et al., 2005).

3.0 SAMPLES AND ANALYTICAL TECHNIQUES

The Kōloa samples were chosen from a suite of 129 new samples collected during an extensive field program (Gandy et al., in review). Thin section analysis identified 60 unaltered or weakly altered samples (minor iddingsite on olivine, and/or calcite and zeolites in vesicles) for XRF analysis. From this group, 16 samples were selected for ICP-MS trace element, and Pb, Sr, Nd and Hf isotopic analysis to cover the entire age (2.6 – 0.15 Ma), compositional (weakly alkalic to foidite), and spatial ranges for the Kōloa Volcanics. In addition, ten K-Ar dated (McDougall, 1964; Tagami et al., 2005) and XRF analyzed samples of the late-shield and post-shield stages were chosen for comparison with the Kōloa lavas. The post-shield stage of volcanism on Kauaʻi was poorly defined geochemically prior to this study. McDougall (1964) and Clague and Dalrymple (1988) each dated four post-shield samples using the K-Ar technique. The Clague and Dalrymple (1988) suite was also analyzed for major and trace elements, and Sr and Nd isotopes, whereas the McDougall (1964) suite (GA prefix) had not been further geochemically studied. We collected three additional post-shield samples and included three of the McDougall samples, all from the Makaweli Member on the western side of the island, in our study. One sample, a hawaiite (GA566), is distinct in most geochemical systematics. The four late-shield samples are from a tunnel into Hāʻupu Ridge on the southeast side of the island (Figure 1) and are the first samples reported from this area. Two late-shield samples are from lava flows, whereas the other two are from cross-cutting dikes. They were collected below the surface weathering zone and appear unaltered in thin section.

During sample preparation, fragments with signs of alteration were removed to ensure only the freshest parts were analyzed. The success of the selection process was confirmed by the low loss-on-ignition (LOI) values for most samples (Tables 1 and 2). However, two post-shield samples with suspect ages were included due to the limited availability of post-shield samples. Sample GA650 has low K_2O/P_2O_5 (1.0) and Rb (1.7 ppm) indicating significant alteration. Sample GA565 has an anomalously young age for its position in the stratigraphic section (McDougall, 1964).

For the ICP-MS trace element analysis, the powdered samples were digested in concentrated sub-boiled HF and HNO_3 for 48 hours and then digested in 6N sub-boiled HCl for 24 hours. Once dried, they were re-dissolved in concentrated HNO_3 , dried down again and diluted 5000 times using a 10 ppb Indium, 1% HNO_3 solution. The trace elements were analyzed using a Finnigan Element2 high-resolution inductively-coupled plasma mass spectrometer (HR-ICP-MS) at the Pacific Centre for Isotopic and Geochemical Research (PCIGR) at the University of British Columbia (Pretorius et al., 2006). For the isotopic analyses, the powdered samples were extensively acid-leached using methods outlined in Weis and Frey (1991, 1996) and Weis et al. (2005) to remove any post-eruptive alteration. After a 48 hour period of digestion in concentrated sub-boiled HF and HNO_3 and a 24 hour period of digestion in 6N sub-boiled HCl, the samples were purified using Pb, Sr, Nd and Hf anionic exchange columns to separate these elements (see Weis et al., 2006, 2007 and Connelly et al., 2006 for detailed procedure). The Pb and Hf isotopes were analyzed using a Nu Plasma multi collector inductively-coupled plasma mass spectrometer (MC-ICP-MS) and the Sr and Nd isotopes were analyzed using a Finnigan Triton thermal-ionization mass spectrometer (TIMS),

both at the PCIGR. Complete procedural duplicates were analyzed for one Kōloa sample and one post-shield sample, yielding an external reproducibility for the Pb, Sr, Nd and Hf of 320 – 395, 16-26, 3 and 41 ppm, respectively.

4.0 RESULTS

4.1 Major and Trace Element Compositions

The Kōloa, post-shield and late-shield lavas show a wide compositional range (Tables 1 and 2). A total alkali vs. silica (TAS) diagram indicates that the newly collected Kōloa Volcanics samples (Gandy, 2006) are exclusively alkalic, ranging from alkali basalts to foidites (Figure 3). The major-element trends show wider ranges than previously reported for Kōloa Volcanics, except for K_2O , which may result from alteration of the previous samples (Figure 4; Macdonald et al., 1960; Macdonald, 1968; Palmiter, 1975; Feigenson, 1984; Clague and Dalrymple, 1988; Maaloe et al., 1992; Reiners and Nelson, 1998). The new samples have lower LOI values, generally ≤ 1.0 wt%. The six new post-shield stage lavas range from tholeiite and basanite to hawaiite (Figure 3). The four other previously reported post-shield lavas include an alkalic basalt, two hawaiites and a mugearite (Clague and Dalrymple, 1988). The late-shield lavas are exclusively tholeiites. The shield/late-shield and rejuvenated stage lavas form two distinct fields on SiO_2 , CaO/Al_2O_3 and K_2O vs. MgO graphs (Figure 4). The late-shield samples plot amongst the shield lavas, except they have slightly higher K_2O values as they have experience less K_2O removal due to alteration than the older Kaua'i shield lavas. Our late-shield samples have K_2O/P_2O_5 ratios of 1.4 – 1.8, whereas the Kaua'i shield samples have K_2O/P_2O_5 ratios of 0.4 – 1.4 (Mukhopadhyay et al., 2003). On the major element plots, the tholeiitic post-shield samples plot with the shield lavas, whereas two alkalic post-shield samples are geochemically similar to Kōloa Volcanics, and the other two alkalic post-shield samples have lower MgO ratios due to olivine fractionation (Figure 4).

The Kōloa Volcanics are enriched in incompatible elements (Table 3; Figure 4). Two geochemically distinct groups can be distinguished within the post-shield lavas based on plots of Ba/Sr vs. Zr/Nb and Nb/Y vs. Ce (Table 4; Figures 4d and 4e). The alkalic post-shield samples plot near the Kōloa lavas field and the tholeiitic post-shield samples plot within the shield field. The Kōloa lavas decrease in Nb/Y with increased degree of partial melting. There is a correlation between Nb/Y and rock type indicating that the foidites result from low degrees of partial melting, whereas alkalic basalts result from higher degrees of partial melting. Similar partial melting vs. rock type correlations have been observed for the Honolulu Volcanics (Clague and Frey, 1982).

The rare-earth element patterns for the alkalic post-shield and rejuvenated lavas show strong light-rare-earth element enrichment, whereas the late-shield lavas display moderate enrichment (Figure 4f). The Kōloa Volcanics exhibit crossing patterns, with the foidic rocks having higher light-rare-earth element (LREE) abundances and lower heavy-rare-earth element (HREE) abundance than the basanites and alkali basalts. The tholeiitic late-shield lavas have significantly lower LREE abundances and slightly higher HREE abundances than the post-shield and rejuvenated lavas (Figure 4f).

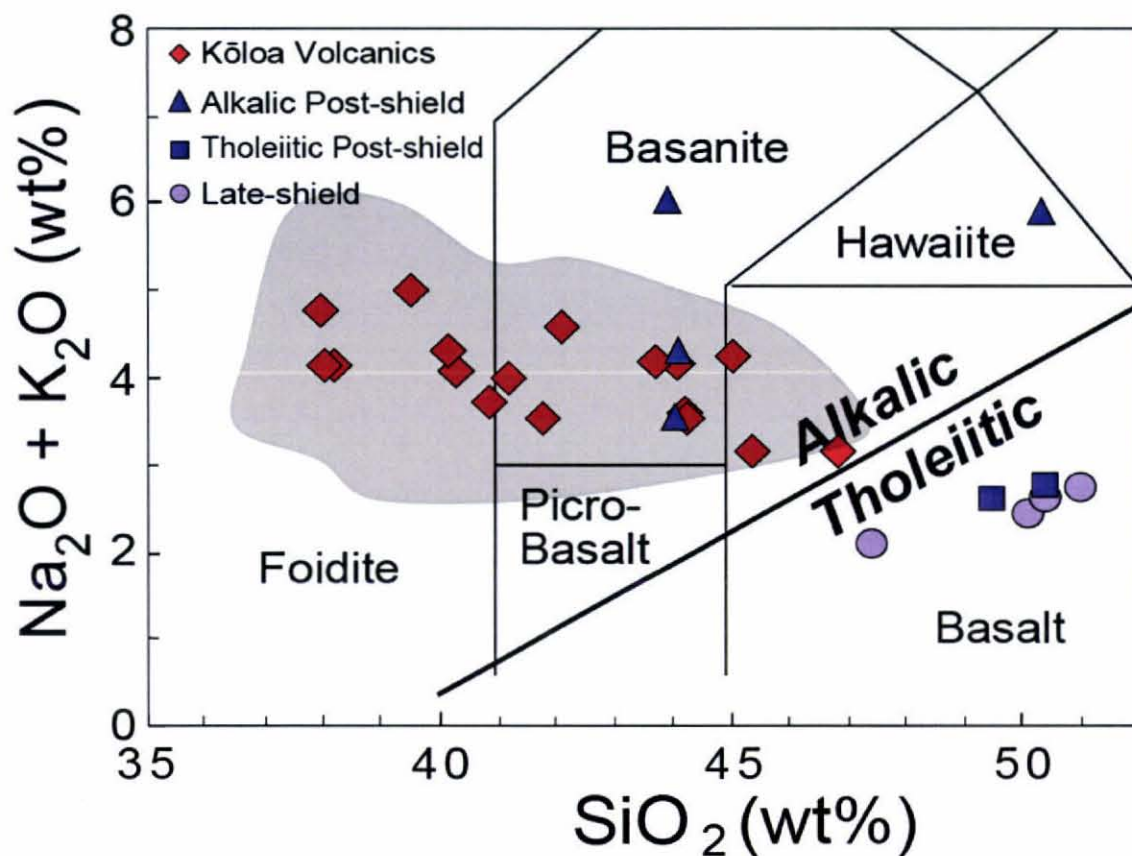


Fig. 3: Total alkalis vs. silica diagram for Kaua'i's late-shield and post-shield stages, and the Kōloa Volcanics. The grey field outlines the 60 Kōloa lavas analyzed by Gandy (2006). The red diamonds indicate samples that were analyzed in this study for the entire trace element (ICP-MS) and isotopic suite. The late-shield lavas are tholeiitic and the Kōloa Volcanics are exclusively alkalic ranging in composition from alkali basalts to foidites. The post-shield lavas range from tholeiitic basalt and basanite to hawaiite. The tholeiitic-alkalic dividing line is from Macdonald and Katsura (1964).

Table 1. XRF major and trace element compositions of the Kōloa Volcanics

Sample Name:	KR-11	KV06-1	0301-1	KV05-8	PV-2	KV03-1	KR-2	KR-5
Rock Type:	F	B	B	F	AB	F	F	F
Age (Ma):	-	-	2.44 ± 0.05	2.30 ± 0.03	1.83 ± 0.03	1.81 ± 0.07	1.67 ± 0.08	1.67 ± 0.08
SiO ₂	37.92	41.77	43.67	40.84	45.34	39.48	40.26	38.15
TiO ₂	3.473	3.308	2.550	3.306	2.002	3.544	3.320	3.467
Al ₂ O ₃	9.29	10.93	11.42	10.83	12.45	9.54	10.07	9.31
Fe ₂ O ₃	15.46	14.26	13.68	14.24	13.21	15.28	14.34	15.33
MnO	0.23	0.21	0.19	0.20	0.20	0.20	0.20	0.21
MgO	14.2	13.28	12.38	13.11	11.04	13.38	14.27	15.04
CaO	13.31	12.43	11.32	12.41	11.57	12.02	12.71	13.24
Na ₂ O	3.31	3.16	3.08	2.55	2.46	3.33	3.56	3.11
K ₂ O	1.455	0.388	1.118	1.187	0.705	1.674	0.523	1.028
P ₂ O ₅	0.920	0.517	0.443	0.531	0.497	0.696	0.690	0.960
Total	99.57	100.25	99.85	99.20	99.47	99.14	99.94	99.84
LOI	0.98	0.60	0.09	1.03	0.21	0.59	1.36	1.29
La	61	36	30	30	36	47	46	59
Ce	133	75	66	76	73	102	98	127
V	315	331	286	336	235	315	270	323
Ni	315	300	314	354	275	387	331	329
Cr	466	597	526	664	431	539	528	493
Zn	140	106	112	113	113	144	111	135
Ga	20	19	19	19	19	21	18	20
Rb	31.4	42.4	24.4	38.8	16.6	39.2	10.4	27.1
Sr	1176	631	601	653	629	761	802	1085
Y	27.1	21.6	22.5	19.9	27.9	23.6	22.0	25.4
Zr	302	196	164	182	125	252	203	292
Nb	91.5	58.9	42.8	61.5	36.3	73.5	69.1	88.4
Ba	1068	518	566	675	672	924	763	991

Table 1. (Continued) XRF major and trace element compositions of the Koloa Volcanics

Sample Name:	KV03-17	KV04-4	KV03-21	KV04-1	KV03-15	KV05-1	KV05-2	KV03-11
Rock Type:	B	B	B	AB	F	B	B	AB
Age (Ma):	1.55 ± 0.03	1.49 ± 0.02	1.35 ± 0.02	1.22 ± 0.07	0.94 ± 0.03	0.68 ± 0.02	0.22 ± 0.03	0.15 ± 0.02
SiO ₂	42.10	44.22	44.17	46.82	40.14	41.16	44.06	45.01
TiO ₂	2.320	2.112	2.702	1.630	2.892	2.947	2.206	2.483
Al ₂ O ₃	10.89	11.66	12.04	11.45	9.76	10.75	11.79	12.97
Fe ₂ O ₃	13.98	13.55	13.44	12.79	14.01	14.02	13.32	13.07
MnO	0.20	0.20	0.19	0.18	0.22	0.20	0.20	0.19
MgO	13.51	13.08	11.11	13.64	15.25	13.24	12.27	8.82
CaO	11.54	11.26	11.91	10.15	12.47	12.50	11.11	12.56
Na ₂ O	3.46	2.65	2.41	2.58	3.18	3.14	3.18	3.23
K ₂ O	1.132	0.890	1.195	0.580	1.133	0.854	0.998	1.020
P ₂ O ₅	0.527	0.390	0.542	0.251	0.634	0.647	0.391	0.449
Total	99.66	100.01	99.71	100.07	99.69	99.46	99.53	99.80
LOI	-0.55	0.19	1.70	0.41	0.74	2.15	-0.37	0.04
La	38	24	41	18	40	46	21	27
Ce	83	57	84	38	89	96	55	58
V	281	262	261	207	303	267	267	283
Ni	370	348	291	505	413	422	324	169
Cr	594	575	437	698	648	722	529	330
Zn	120	115	125	107	122	108	113	113
Ga	18	19	20	17	18	18	19	20
Rb	28.5	22.5	28.8	13.4	32.8	25.0	24.8	26.1
Sr	686	560	751	404	790	702	548	638
Y	20.4	19.9	31.0	25.0	20.6	23.2	20.3	23.0
Zr	139	112	169	85	168	203	125	119
Nb	52.2	39.5	54.5	23.2	63.4	67.5	40.3	41.1
Ba	678	487	762	345	669	667	479	552

Samples listed oldest to youngest except for the first two samples, which have no age data

Samples were analyzed using XRF at University of Massachusetts (see Rhodes and Vollinger (2004) for analytical procedure)

Major element concentrations in wt%, trace element concentrations in ppm

AB, alkali basalt; B, basanite; F, foidite; names from TAS diagram (Figure 3)

Ages determined by Sano (2006) using the unspiked K-Ar method for KV series; ages by McDougall (1964) for GA series

Table 2. XRF major and trace element compositions of the late-shield and post-shield stages of volcanism on Kaua'i

Sample Name:	KV04-22	KV04-16	KV04-19	KV04-21	KV05-10	GA650	KV03-5	GA566	KV05-13	GA565
Rock Type:	Thol	Thol	Thol	Thol	B	Thol	B	Haw	B	Thol
Age (Ma):	4.51 ± 0.07	4.31 ± 0.17	4.30 ± 0.11	4.1 ± 0.2	3.92 ± 0.06	3.92 ± 0.03*	3.85 ± 0.06	3.87 ± 0.04	3.58 ± 0.05	3.53 ± 0.02*
SiO ₂	50.12	47.40	50.40	51.02	44.09	49.51	44.06	50.33	43.91	50.41
TiO ₂	2.278	2.147	2.369	2.402	2.667	2.581	2.619	3.279	4.138	2.375
Al ₂ O ₃	12.44	10.05	12.75	13.13	12.67	13.63	11.93	20.84	15.98	13.44
Fe ₂ O ₃	12.33	12.83	11.96	12.31	13.84	12.81	14.09	13.89	13.78	12.67
MnO	0.17	0.17	0.17	0.17	0.19	0.18	0.19	0.17	0.21	0.18
MgO	10.49	17.54	9.89	8.01	11.17	7.73	12.18	1.77	5.59	7.71
CaO	9.65	7.48	9.70	10.04	10.91	10.56	10.51	2.51	9.04	10.54
Na ₂ O	2.01	1.73	2.20	2.26	3.36	2.41	2.65	3.56	4.57	2.44
K ₂ O	0.438	0.376	0.426	0.484	0.906	0.234	0.889	2.315	1.448	0.374
P ₂ O ₅	0.238	0.261	0.261	0.264	0.472	0.237	0.449	1.332	0.701	0.233
Total	100.16	99.99	100.12	100.09	100.28	99.88	99.57	100.00	99.37	100.37
LOI	-0.10	-0.20	-0.06	-0.11	-0.30	0.33	0.03	6.60	0.08	0.36
La	11	10	10	10	25	9	31	41	37	13
Ce	33	30	29	28	59	30	68	104	92	32
V	259	207	247	263	291	245	290	140	233	242
Ni	287	818	245	114	295	123	359	17	12	107
Cr	632	939	558	358	575	326	638	10	0	323
Zn	116	128	113	115	109	109	119	137	123	106
Ga	19	17	19	20	19	21	19	30	21	19
Rb	7.0	5.7	7.0	8.7	22.1	1.7	20.4	45.3	30.8	6.5
Sr	312	317	322	316	661	330	661	608	1203	310
Y	22.4	19.0	23.0	23.7	32.8	25.8	27.1	105.5	31.0	25.3
Zr	129	137	143	139	139	146	151	543	200	143
Nb	14.0	13.2	14.3	12.7	34.3	13.7	35.0	79.3	58.0	14.7
Ba	94	89	103	101	417	94	503	688	686	92

Samples listed oldest to youngest. KV04- series samples are from the Haupu Tunnel. Other samples from Makaweli member, near Waimea Canyon.

Samples were analyzed using XRF at University of Massachusetts (see Rhodes and Vollinger (2004) for analytical procedure)

Major element concentrations in wt%, trace element concentrations in ppm

Thol, tholeiite; Haw, hawaiite; B, basanite; names from TAS diagram (Figure 3)

Ages determined by Sano (2006) using the unspiked K-Ar method for KV series; ages by McDougall (1964) for GA series (adjusted to newer age constants)

Samples ages marked with * are suspect based on low K and Rb contents due to alteration or misfit in stratigraphic age order

Table 3. ICP-MS trace element compositions of the Koloa Volcanics

Sample Name:	KR-11	0301-1	KV05-8	PV-2	KV03-1	KR-2	KR-5	KV03-17
Li	8.22	5.50	5.07	5.43	6.91	7.62	7.34	6.57
Sc	21.7	26.3	25.9	26.0	21.2	22.7	22.0	23.2
Ni	324	333	350	269	412	346	348	360
Ga	18.6	19.2	18.7	17.2	21.0	18.1	19.1	16.9
Y	27.7	22.3	21.3	22.6	34.7	23.5	28.0	20.6
Zr	279	166	181	121	248	195	299	136
Nb	90.9	38.1	55.0	34.8	72.8	66.6	90.3	46.9
Sb	0.07	0.02	0.01	0.04	0.04	0.03	0.07	0.03
Cs	0.36	0.29	0.35	0.22	0.19	0.88	0.30	0.30
Ba	967	471	672	554	761	716	964	587
Ta	5.74	2.62	3.80	2.28	4.52	4.16	5.58	3.07
Th	6.57	3.16	3.99	2.83	5.66	6.01	7.64	3.83
U	1.97	0.71	0.97	0.86	1.02	1.25	1.79	1.14
La	54.8	33.9	38.7	27.7	52.5	47.8	69.4	31.3
Ce	117	62.4	73.8	53.1	102	94.0	133	62.3
Pr	13.9	7.25	8.53	7.01	12.7	10.5	14.7	7.79
Nd	63.2	28.9	33.2	31.8	52.5	40.3	55.0	34.6
Sm	12.4	6.10	6.87	6.83	10.6	8.18	10.5	7.28
Eu	3.79	2.08	2.24	2.25	3.42	2.77	3.54	2.42
Gd	16.3	5.66	6.31	8.96	10.5	7.32	8.99	9.55
Tb	1.27	0.87	0.92	0.91	1.33	1.07	1.27	0.86
Dy	6.79	4.46	4.69	4.97	6.47	5.55	6.12	4.80
Ho	1.10	0.73	0.74	0.88	1.05	0.81	0.90	0.85
Er	2.58	1.90	1.83	2.32	2.43	2.02	2.22	2.08
Tm	0.28	0.22	0.21	0.27	0.26	0.23	0.23	0.24
Yb	1.77	1.38	1.24	1.79	1.42	1.31	1.33	1.57
Lu	0.18	0.19	0.17	0.21	0.17	0.18	0.16	0.17

Table 3. (Continued) ICP-MS trace element compositions of the Koloa Volcanics

Sample Name:	KV04-4	KV03-21	KV04-1	KV03-15	KV05-1	KV05-2	KV03-11
Li	5.40	6.33	4.66	6.82	5.09	5.42	6.11
Sc	25.3	22.9	24.4	23.4	25.3	25.4	27.1
Ni	339	260	430	372	357	367	226
Ga	15.3	17.1	13.8	17.4	18.4	18.3	19.9
Y	21.3	29.4	22.9	22.1	22.3	19.6	23.4
Zr	113	145	77.2	169	123	114	125
Nb	34.5	47.4	19.1	62.5	32.9	35.1	35.7
Sb	0.03	0.03	0.00	0.05	0.00	0.02	0.01
Cs	0.32	0.27	0.15	0.55	0.20	0.27	0.13
Ba	431	663	295	601	438	431	478
Ta	2.42	2.94	0.97	3.96	2.09	2.21	2.06
Th	3.22	4.46	1.96	4.70	2.88	2.90	3.11
U	0.77	1.09	0.52	1.16	0.70	0.72	0.61
La	29.1	41.1	19.8	37.0	27.8	25.3	28.9
Ce	54.0	83.4	35.2	77.2	49.8	45.6	52.9
Pr	6.62	9.98	4.69	9.58	5.86	5.75	6.64
Nd	26.8	39.9	19.9	42.8	23.4	23.8	26.4
Sm	5.80	8.31	4.62	8.93	5.31	5.28	6.00
Eu	1.93	2.87	1.66	2.85	1.87	1.82	2.19
Gd	5.77	8.67	4.77	10.9	5.09	5.50	6.03
Tb	0.80	1.15	0.75	1.00	0.76	0.71	0.91
Dy	4.54	6.19	4.33	5.62	4.45	4.13	4.83
Ho	0.81	1.04	0.81	0.90	0.74	0.72	0.83
Er	2.18	2.68	2.20	2.18	1.96	1.87	2.16
Tm	0.26	0.31	0.27	0.24	0.23	0.23	0.26
Yb	1.64	1.86	1.64	1.57	1.40	1.40	1.57
Lu	0.22	0.24	0.23	0.17	0.20	0.18	0.21

Samples listed oldest to youngest except for the first sample, which has no age data

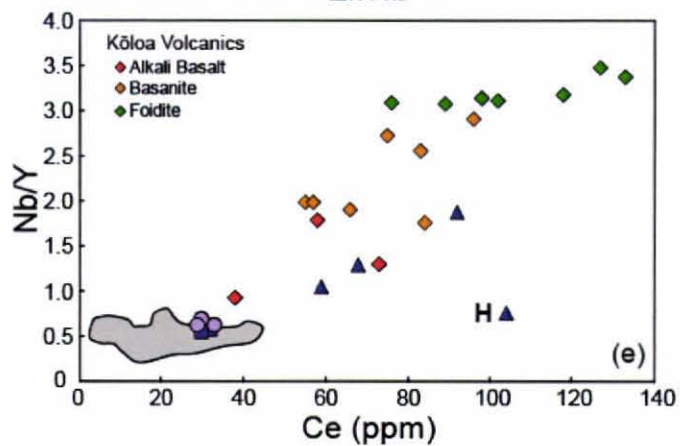
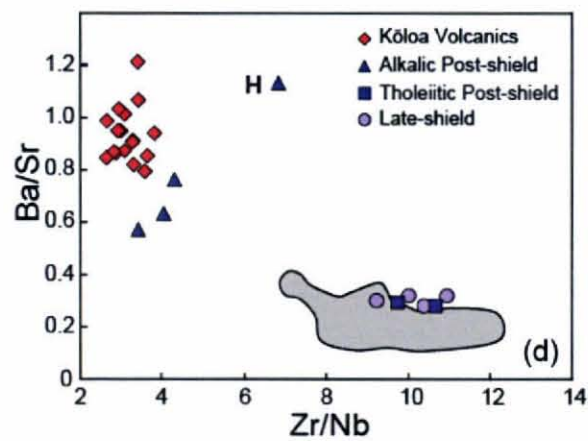
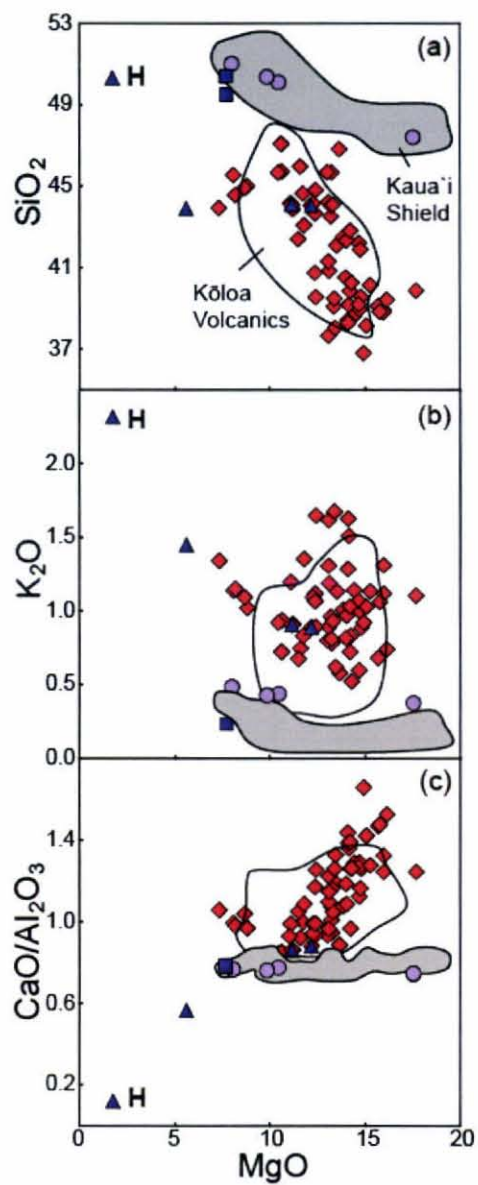
Trace element concentrations in ppm

Table 4. ICP-MS trace element compositions of the late-shield and post-shield stages of volcanism on Kauaʻi

Sample Name:	KV04-22	KV04-16	KV04-19	KV04-21	KV05-10	GA650	KV03-5	GA566	KV05-13	GA565
Li	3.21	4.15	5.32	6.09	4.44	5.09	5.05	7.22	7.29	4.14
Sc	28.6	21.0	28.6	29.4	24.8	32.4	24.4	11.3	14.0	31.3
Ni	328	882	283	123	315	130	350	15.8	15.8	138
Ga	17.6	13.8	18.7	19.2	18.7	17.9	18.4	27.9	20.9	19.4
Y	23.6	18.8	24.3	24.8	34.9	25.6	26.7	104.4	33.8	25.3
Zr	125	112	142	134	147	134	143	538	223	136
Nb	14.0	8.5	14.8	12.5	33.4	13.0	34.4	77.6	56.8	15.3
Sb	0.01	0.01	0.02	0.02	0.01	-	0.04	0.03	0.01	0.03
Cs	0.01	0.05	0.07	0.10	0.23	0.02	0.28	0.19	0.32	0.06
Ba	86.7	82.9	94.7	96.7	399	77.3	423	636	667	83.1
Ta	0.90	0.62	1.01	0.87	2.09	-	2.10	4.89	3.64	1.02
Th	1.00	0.73	0.94	0.79	2.61	0.76	2.31	6.88	3.94	1.01
U	0.24	0.23	0.22	0.22	0.62	0.18	0.55	1.50	0.93	0.22
La	13.6	9.7	13.4	11.5	32.5	10.7	33.0	49.7	41.6	13.9
Ce	32.9	24.3	32.6	28.9	59.3	26.8	64.6	105	90.0	32.2
Pr	3.96	3.51	4.09	3.80	7.41	4.10	7.25	14.2	10.7	4.18
Nd	16.6	17.9	17.7	17.1	29.3	19.7	29.0	61.7	44.0	17.4
Sm	4.41	4.73	4.83	4.78	6.64	5.42	6.64	14.6	10.0	4.80
Eu	1.57	1.60	1.71	1.70	2.37	1.89	2.20	5.16	3.24	1.66
Gd	4.09	5.54	4.49	4.56	6.11	5.99	6.08	14.3	8.68	4.52
Tb	0.77	0.66	0.84	0.83	0.96	0.90	0.94	2.61	1.33	0.76
Dy	4.34	4.13	4.91	4.74	5.09	5.57	5.16	15.71	6.92	5.10
Ho	0.75	0.74	0.80	0.83	0.87	1.02	0.84	3.07	1.12	0.83
Er	2.13	1.96	2.21	2.35	2.34	2.80	2.23	8.84	2.91	2.33
Tm	0.26	0.24	0.27	0.29	0.25	0.35	0.26	1.09	0.34	0.29
Yb	1.67	1.58	1.71	1.82	1.51	2.27	1.53	6.15	2.07	1.79
Lu	0.25	0.18	0.26	0.26	0.21	0.29	0.23	0.74	0.29	0.29

Samples listed oldest to youngest.

Trace element concentrations in ppm



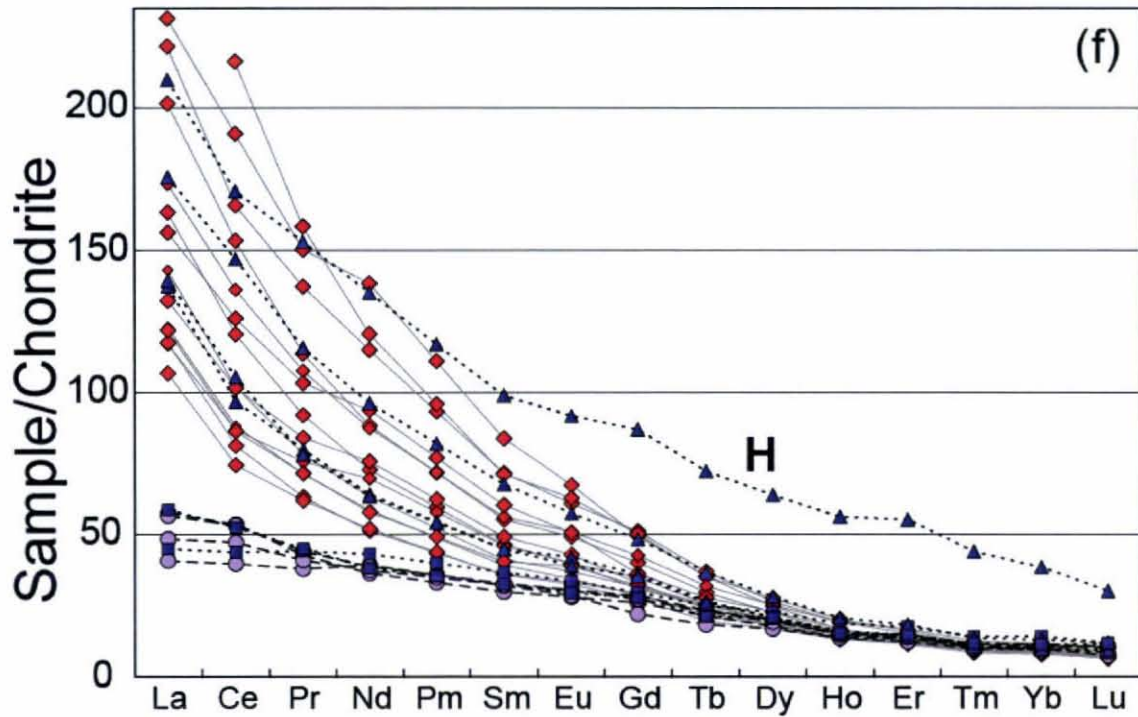


Fig. 4: Major and trace element ratio plots comparing the three stages of volcanism on Kauaʻi: shield/late-shield, post-shield and rejuvenated. The “H” on the plots represents the geochemically distinct hawaiite sample (GA 566). (a) SiO_2 vs. MgO . (b) K_2O vs. MgO . (c) $\text{CaO}/\text{Al}_2\text{O}_3$ vs. MgO . Kōloa Volcanics from previous studies outlined; data from Clague and Dalrymple (1988), Maaloe (1992), and Reiners and Nelson (1998). Kōloa Volcanics represented by the red diamonds are from Gandy (2006). (d) Ba/Sr vs. Zr/Nb (XRF data). The shield and rejuvenated stages define two distinct groups. The post-shield lavas also form two groups, the tholeiitic samples plot near the shield stage lavas whereas the alkalic samples plot near to the rejuvenated stage lavas. (e) Nb/Y vs. Ce (XRF data). Rock type correlates with Nb/Y indicating foidites result from low degrees of partial melting and alkalic basalts result from higher degrees of partial melting. Kauaʻi shield represented by grey outline; data from Mukhopadhyay et al. (2003). (f) Rare-earth element diagram (ICP-MS data). REE values normalized to chondrite values from McDonough and Sun (1995).

4.2 Isotopic Compositions of the Late-shield, Post-shield and Kōloa Volcanics

The new isotopic data for the Kōloa Volcanics extend their previously known ranges for Pb, Sr, Nd and Hf ratios (Table 5). Kōloa Volcanics form a well-defined linear array (correlation coefficient R^2 of 0.99) in $^{208}\text{Pb}/^{204}\text{Pb}$ vs. $^{206}\text{Pb}/^{204}\text{Pb}$ space (Figure 5a). Two samples from the same lava flow (KR-5, KR-11) have higher $^{206}\text{Pb}/^{204}\text{Pb}$ ratios than previously reported for rejuvenated lavas, and are among the highest reported for any Hawaiian lava (Figure 6). With the exception of these two highly radiogenic samples, the Pb ratios of the Kōloa Volcanics overlap with Kaua'i shield stage lavas. None of the post-shield samples plot directly on the trend defined by the Kōloa lavas; the tholeiitic post-shield and late-shield samples have higher $^{208}\text{Pb}/^{204}\text{Pb}$ ratios for a given $^{206}\text{Pb}/^{204}\text{Pb}$ ratio, whereas the alkalic post-shield samples have slightly lower $^{208}\text{Pb}/^{204}\text{Pb}$ ratios for a given $^{206}\text{Pb}/^{204}\text{Pb}$ ratio. A clearer distinction between the alkalic and tholeiitic post-shield lavas is seen in radiogenic $^{208}\text{Pb}^*/^{206}\text{Pb}^*$ space; the alkalic lavas have low (~ 0.938) radiogenic Pb values, whereas the tholeiitic lavas have high (~ 0.95) radiogenic Pb values (Figure 7a). Pb isotopes appear to show a bilateral asymmetry in the Hawaiian plume south of the Moloka'i fracture zone, with a clear difference in $^{208}\text{Pb}^*/^{206}\text{Pb}^*$ for volcanoes belonging to the Loa and Kea trends (Figure 6a; Tatsumoto, 1978; Abouchami et al., 2005). Radiogenic Pb also offers a clear distinction between the shield and late-shield stages of Kaua'i (Figure 7a). Most shield and post-shield stage lavas plot in the Kea field, whereas, the late-shield samples from the Hā'upu Tunnel, and the tholeiitic post-shield samples plot in or near the Loa field (Figure 7a). No spatial relationship between the late-shield lavas and the post-shield lavas can account for the Loa-like signature (Figure 1). On a $^{208}\text{Pb}/^{204}\text{Pb}$ vs. $^{206}\text{Pb}/^{204}\text{Pb}$ diagram (Figure 7b), the Kōloa Volcanics plot in both Loa and

Kea fields; samples with $^{206}\text{Pb}/^{204}\text{Pb}$ ratios <18.3 plot in the Kea field, whereas those with higher ratios plot in the Loa field. A trend line through Kōloa Pb-Pb values has an $R^2 = 0.99$ and cross cuts the Kea-Loa dividing line, unlike Kalaupapa and Honolulu Volcanics (the rejuvenated stages of East Molokaʻi and Koʻolau Volcano of Oʻahu, respectively), both of which plot only on the Kea side (Xu et al., 2005; Fekiacova et al., 2007; Figure 7b). Prior to the recognition of late-shield and rejuvenated Loa-type lavas on Kauaʻi, it was thought that the Loa signature was restricted to the last 3 Myr of Hawaiian volcanism (e.g., Jackson et al., 1999, Tanaka et al., 2002, Haskins and Garcia, 2004, Tanaka et al., 2008).

The Hf isotopic data (Table 5) are the first for the late-shield and post-shield stages of Kauaʻi, and supplement six previous values for Kōloa Volcanics (Stracke et al., 1999). The ϵ_{Hf} vs. $^{206}\text{Pb}/^{204}\text{Pb}$ plot (Figure 5b) displays a clear distinction between the tholeiitic samples (positive trend) and the alkalic samples (negative trend). Figure 6b shows that the tholeiitic Kauaʻi lavas plot along the mixing hyperbola defined by all Hawaiian shield volcanoes, whereas the alkalic Kauaʻi lavas and all other Hawaiian rejuvenated lavas trend away from this hyperbola towards higher ϵ_{Hf} values. A similar divergent trend is exhibited by the Hualālai post-shield lavas (Hanano et al., 2005). This pattern indicates a minimum of three end-member components were sampled by the Kauaʻi lavas.

The ϵ_{Nd} vs. $^{206}\text{Pb}/^{204}\text{Pb}$ plot (Figure 5c) exhibits a very similar pattern to the ϵ_{Hf} vs. $^{206}\text{Pb}/^{204}\text{Pb}$ plot (Figure 5b). The late-shield lavas show distinctly lower ϵ_{Nd} values than the shield lavas (Figure 5c). As expected, due to the similarity between the Nd and Hf

systematics, the late-shield, post-shield and rejuvenated samples form a positive linear trend on the ϵ_{Hf} vs. ϵ_{Nd} plot (Figure 5d).

The Kōloa Volcanics exhibit lower Sr isotopic ratios (0.70296-0.70325) than the shield stage lavas (0.70345-0.70381; Figure 5e; Figure 6d), which is consistent with results from previous studies (e.g., Reiners and Nelson, 1998; Maaloe, 1992; Reiners et al., 1999). There is also a distinction between the alkalic and tholeiitic post-shield samples in Sr isotopic ratios (Figure 5e). As in other plots, the tholeiitic post-shield samples plot within the Kauaʻi shield field, whereas the alkalic post-shield samples plot with the Kōloa Volcanics.

The $^{206}\text{Pb}/^{204}\text{Pb}$, $^{87}\text{Sr}/^{86}\text{Sr}$ and $^{143}\text{Nd}/^{144}\text{Nd}$ isotopic ratios of the Kōloa Volcanics are significantly more variable in rocks older than 1.5 Ma (Figure 8). The younger samples, regardless of location, define a narrower range in these three isotopic ratios. The $^{87}\text{Sr}/^{86}\text{Sr}$ and $^{143}\text{Nd}/^{144}\text{Nd}$ ratios have remained essentially constant for the past 1.5 Ma, whereas the $^{206}\text{Pb}/^{204}\text{Pb}$ ratios show a decreasing trend. The post-shield lavas of Kauaʻi are isotopically diverse, as seen for all the post-1.5 Ma Kōloa lavas. In contrast, the Honolulu Volcanics do not exhibit a similar narrowing pattern in their isotopic ratios (Fekiacova et al., 2007).

Table 5. Pb, Sr, Nd and Hf isotope data for the rejuvenated, post-shield and late-shield stages of Kaua'i

Sample Name	$^{206}\text{Pb}/^{204}\text{Pb}$	$\pm 2\sigma$	$^{207}\text{Pb}/^{204}\text{Pb}$	$\pm 2\sigma$	$^{208}\text{Pb}/^{204}\text{Pb}$	$\pm 2\sigma$	$^{87}\text{Sr}/^{86}\text{Sr}$	$\pm 2\sigma$	$^{143}\text{Nd}/^{144}\text{Nd}$	$\pm 2\sigma$	ϵ^{Nd}	$^{178}\text{Hf}/^{177}\text{Hf}$	$\pm 2\sigma$
<i>Koia Volcanics</i>													
KR-11	18.5714	0.0049	15.4848	0.0045	38.3315	0.0109	0.703113	0.000007	0.513012	0.000007	7.29	-	-
Q301-1	18.2023	0.0008	15.4405	0.0007	37.9104	0.0019	0.703248	0.000007	0.513019	0.000006	7.43	-	-
KV05-8	18.1984	0.0008	15.4483	0.0009	37.8518	0.0023	0.702959	0.000008	0.513077	0.000008	8.56	-	-
PV-2	18.2932	0.0007	15.4539	0.0006	37.9961	0.0016	0.703243	0.000007	0.513025	0.000005	7.55	-	-
KV03-1	18.3206	0.0016	15.4603	0.0015	38.0253	0.0033	0.703130	0.000008	0.513016	0.000007	7.37	-	-
KR-2	18.2239	0.0007	15.4486	0.0007	37.8731	0.0021	0.703055	0.000007	0.513059	0.000006	8.21	-	-
KR-5	18.6136	0.0017	15.4771	0.0015	38.3757	0.0044	0.703112	0.000008	0.513006	0.000006	7.52	0.283083	0.000007
KR-5 (2) ^M	18.6044	0.0017	15.4777	0.0018	38.3575	0.0042	0.703092	0.000008	0.513024	0.000007	7.29	-	-
KV03-17	18.1404	0.0008	15.4386	0.0007	37.7642	0.0019	0.703008	0.000009	0.513072	0.000006	8.47	0.283165	0.000006
KV04-4	18.1402	0.0015	15.4426	0.0014	37.7670	0.0040	0.703070	0.000008	0.513087	0.000006	8.76	-	-
KV03-21	18.2423	0.0014	15.4546	0.0013	37.9105	0.0036	0.703176	0.000007	0.513048	0.000007	8.00	-	-
KV04-1	18.2130	0.0006	15.4509	0.0005	37.8613	0.0015	0.703162	0.000007	0.513055	0.000006	8.13	-	-
KV03-15	18.1754	0.0023	15.4552	0.0021	37.8472	0.0051	0.703156	0.000009	0.513044	0.000007	7.92	0.283149	0.000011
KV05-1	18.1373	0.0007	15.4356	0.0006	37.7840	0.0017	0.703165	0.000007	0.513049	0.000008	8.02	-	-
KV05-2	18.0895	0.0011	15.4316	0.0010	37.7794	0.0027	0.703165	0.000007	0.513048	0.000005	8.00	-	-
KV03-11	18.1361	0.0021	15.4474	0.0020	37.7857	0.0054	0.703201	0.000007	0.513061	0.000006	8.25	-	-
KV03-11 (dup)	18.1402	0.0009	15.4517	0.0013	37.7957	0.0047	0.703209	0.000009	0.513060	0.000007	8.23	-	-
<i>Post-Shield Kaua'i Volcanics</i>													
KV05-10*	18.1859	0.0007	15.4568	0.0005	37.7986	0.0017	0.703167	0.000008	0.513067	0.000006	8.37	0.283166	0.000005
GA650 ^M	18.1794	0.0007	15.4481	0.0007	37.9005	0.0018	0.703681	0.000007	0.512963	0.000007	6.33	0.283079	0.000004
GA650 (rep)	18.1791	0.0008	15.4488	0.0008	37.9017	0.0016	-	-	-	-	-	-	-
GA566 ^{M*}	18.3290	0.0006	15.4697	0.0005	37.9403	0.0014	0.703405	0.000007	0.513045	0.000009	7.93	0.283127	0.000013
KV03-5*	18.1198	0.0019	15.4432	0.0013	37.7380	0.0030	0.703152	0.000008	0.513058	0.000006	8.19	0.283175	0.000005
KV05-13 *	18.1989	0.0008	15.4537	0.0006	37.8285	0.0016	0.703226	0.000006	0.513049	0.000006	8.02	-	-
GA565 ^M	18.1848	0.0005	15.4512	0.0005	37.9735	0.0013	0.703705	0.000008	0.512940	0.000003	5.88	0.283069	0.000005
<i>Late-Shield Kaua'i Volcanics</i>													
KV04-16	18.1857	0.0007	15.4540	0.0008	37.9563	0.0019	0.703742	0.000007	0.512940	0.000007	5.89	0.283059	0.000006
KV04-16 (dup) ^M	18.1855	0.0005	15.4542	0.0004	37.9565	0.0014	0.703729	0.000007	0.512949	0.000007	6.06	0.283068	0.000007
KV04-19	18.2133	0.0006	15.4555	0.0006	37.9697	0.0016	0.703729	0.000007	0.512964	0.000008	6.36	0.283081	0.000011
KV04-21	18.1116	0.0004	15.4478	0.0004	37.8834	0.0011	0.703755	0.000009	0.512942	0.000008	5.93	0.283059	0.000006
KV04-22	18.0861	0.0010	15.4453	0.0008	37.9250	0.0022	0.703811	0.000010	0.512891	0.000007	4.94	0.283046	0.000006
KV04-22 (rep)	18.0855	0.0005	15.4446	0.0005	37.9244	0.0013	-	-	-	-	-	-	-

Koia Volcanics listed oldest to youngest except for the first sample, which has no age data

All samples were leached using method outlined in Weis and Frey 1991, 1996; Weis et al., 2005

Samples were analyzed for Pb and Hf using the Nu Plasma Instruments MC-ICP-MS and for Sr using the Finnigan TRITON TIMS

Samples denoted with ^M were analyzed for Nd using MC-ICP-MS

Remaining samples analyzed for Nd using TRITON TIMS

Post-shield samples denoted with * are alkalic, remaining samples are tholeiitic

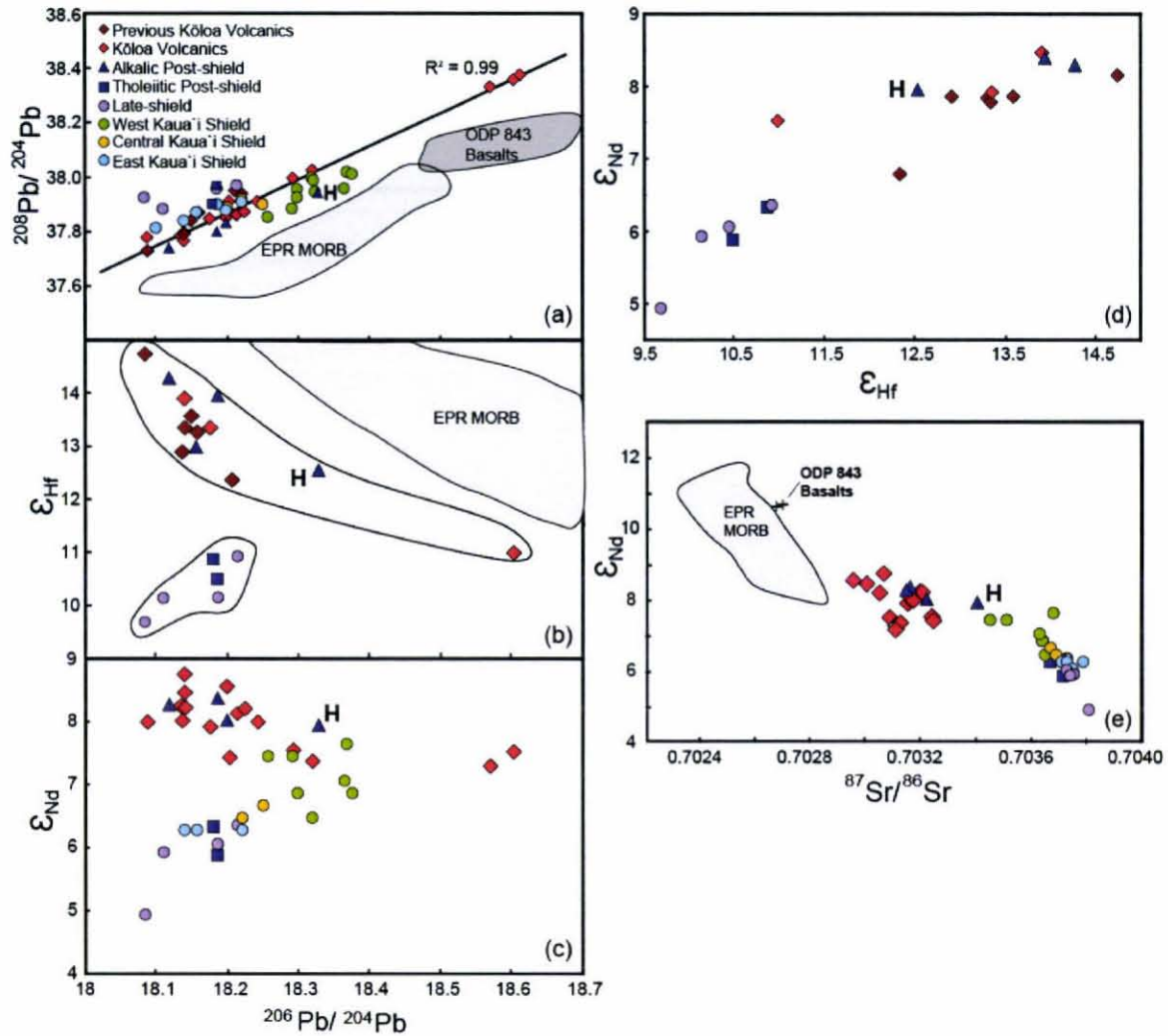
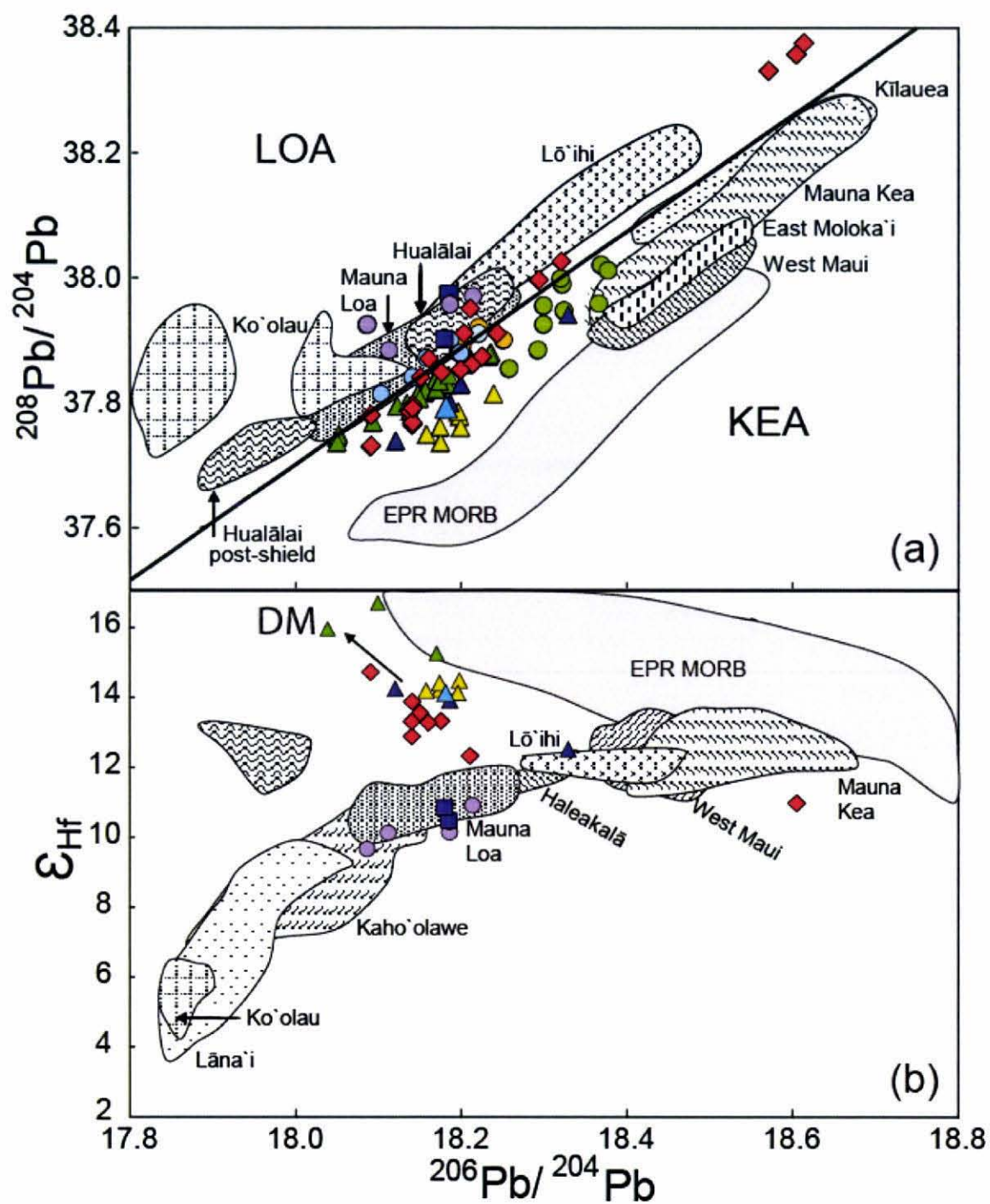


Fig. 5: Comparison of Pb, Hf, Sr and Nd isotopic ratios for the three stages of Kaua'i volcanism with recent EPR MORB lavas and ~110 Ma-old Pacific lithosphere from ODP Site 843. (a) $^{208}\text{Pb}/^{204}\text{Pb}$ vs. $^{206}\text{Pb}/^{204}\text{Pb}$. The Kōloa Volcanics form a well-defined linear array, above which the tholeiitic late-shield and post-shield samples plot, and below which the alkalic post-shield samples plot. The rejuvenated lavas overlap the field of Kaua'i shield lavas. The previous Kōloa Volcanics shown in the dark red diamonds are from Lassiter et al. (2000). (b) ϵ_{Hf} vs. $^{206}\text{Pb}/^{204}\text{Pb}$. The tholeiitic late-shield and post-shield samples form a positive trend, whereas the alkalic post-shield and rejuvenated samples form a negative trend. The Kōloa samples, represented by the dark red diamonds, are from Stracke et al. (1999). No Hf isotopic data exists for the Kaua'i shield or the ODP Site 843. (c) ϵ_{Nd} vs. $^{206}\text{Pb}/^{204}\text{Pb}$. (d) ϵ_{Nd} vs. ϵ_{Hf} . The late-shield, post-shield and rejuvenated samples form a positive linear trend. (e) ϵ_{Nd} vs. $^{87}\text{Sr}/^{86}\text{Sr}$. The late-shield samples plot with the field of the shield lavas, whereas the alkalic post-shield samples plot closer to, or within, the Kōloa field. Kaua'i shield data from Mukhopadhyay et al. (2003); EPR MORB data from Regelous et al. (1999) and Castillo (2000); ODP Site 843 data from Fekiacova et al. (2007).



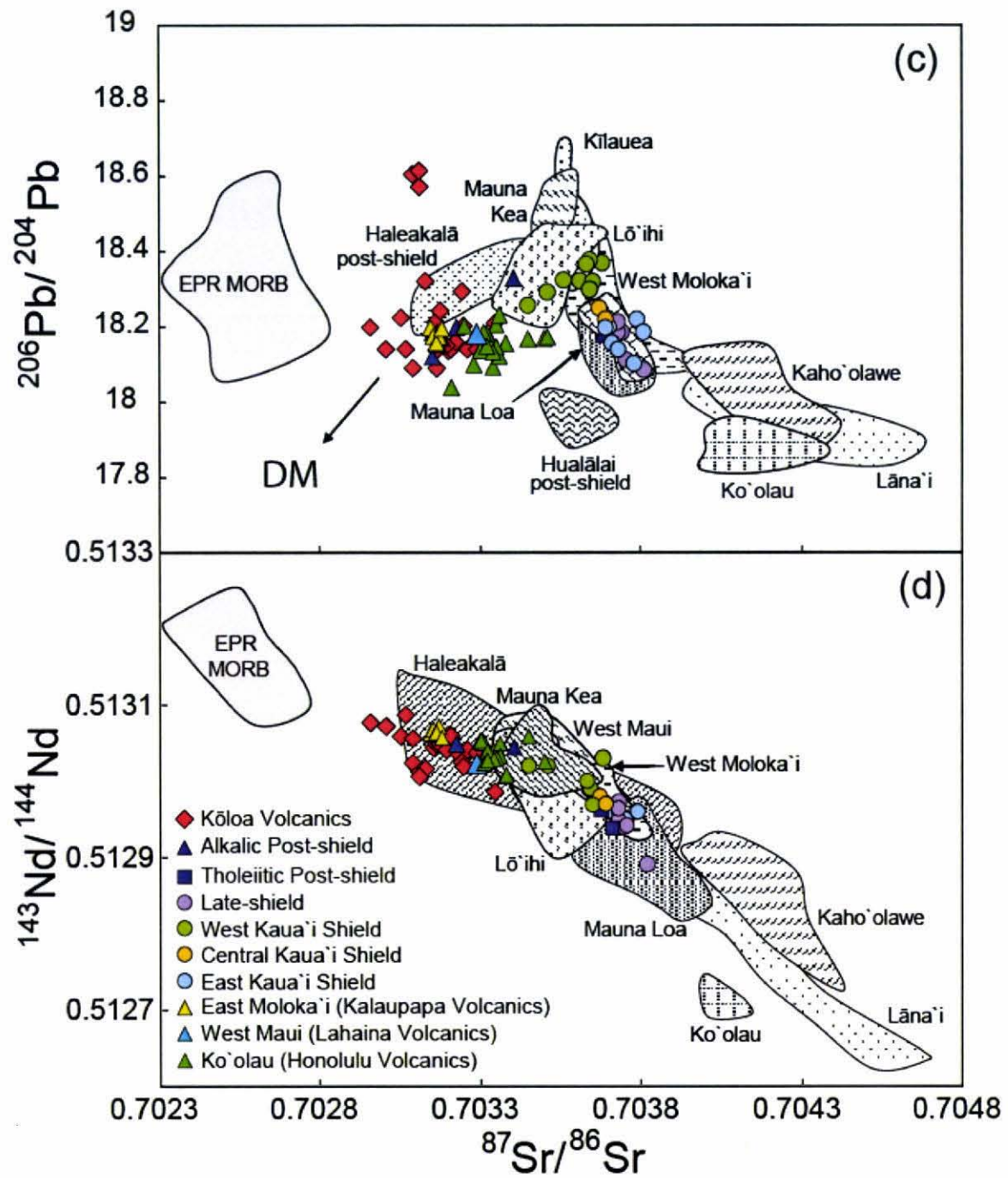


Fig. 6: Comparison of Pb, Hf, Sr and Nd isotopic ratios from the different stages of Kaua'i volcanism and rejuvenated volcanism (Kōloa, Honolulu, Kalaupapa and Lahaina Volcanics) with other Hawaiian shield volcanoes. (a) $^{208}\text{Pb}/^{204}\text{Pb}$ vs. $^{206}\text{Pb}/^{204}\text{Pb}$. The line on the graph is the Loa-Kea boundary. The Kaua'i shield volcanics tend to plot on the Kea side, but with lower Pb isotopic ratios than other Kea-like volcanoes. (b) ϵ_{Hf} vs. $^{206}\text{Pb}/^{204}\text{Pb}$. The tholeiitic late-shield Kaua'i lavas plot along the mixing hyperbola defined by the other Hawaiian shield volcanoes, whereas the alkalic Kaua'i lavas, Kōloa Volcanics and all other Hawaiian rejuvenated lavas trend away from this hyperbola to higher ϵ_{Hf} values. This pattern indicates a minimum of three end-member components were sampled by these lavas. The EPR MORB extends to higher ϵ_{Hf} values than shown on the diagram but the field does not extend to low enough $^{206}\text{Pb}/^{204}\text{Pb}$ ratios to plot above the trend of the Kōloa Volcanics. (c) $^{206}\text{Pb}/^{204}\text{Pb}$ vs. $^{87}\text{Sr}/^{86}\text{Sr}$. The Kaua'i shield lavas plot on the mixing hyperbola with the other Hawaiian shield lavas, with the exception of the west Kaua'i lavas which trend towards a more depleted component, also exhibited by the rejuvenated lavas. The rejuvenated (Kōloa, Honolulu, Kalaupapa and Lahaina) volcanics all trend towards a depleted component different from the EPR MORB. (d) $^{143}\text{Nd}/^{144}\text{Nd}$ vs. $^{87}\text{Sr}/^{86}\text{Sr}$. Isotopic data from the Hawaiian volcanoes (Pb, Sr, Nd, Hf) were compiled from the following: Kīlauea from Chen et al. (1996), Blichert-Toft et al. (1999) and Abouchami et al. (2005), Mauna Kea from Abouchami et al. (2000) and Blichert-Toft et al. (2003), Mauna Loa from Abouchami et al. (2000), Blichert-Toft et al. (2003), Tanaka et al. (2005), Wanless et al. (2006) and Marske et al. (2007), Lāna'i from Gaffney et al. (2005), Ko'olau from Stille et al. (1983), Roden et al. (1994), Abouchami et al. (2005) and Fekiacova et al. (2007), Kaho'olawe from Leeman et al. (1994) and Huang et al. (2005), Lō'ihi from Staudigel et al. (1984), Blichert-Toft et al. (1999) and Abouchami et al. (2005), Haleakalā from West et al. (1987), Chen et al. (1991) and Blichert-Toft et al. (1999), West Maui from Gaffney et al. (2004), East Moloka'i from Xu et al. (2005), West Moloka'i from Stille et al. (1986) and Xu et al. (2007) and Hualālai shield from D. Weis, pers. comm., (2005), Hualālai post-shield from Hanano et al. (2005).

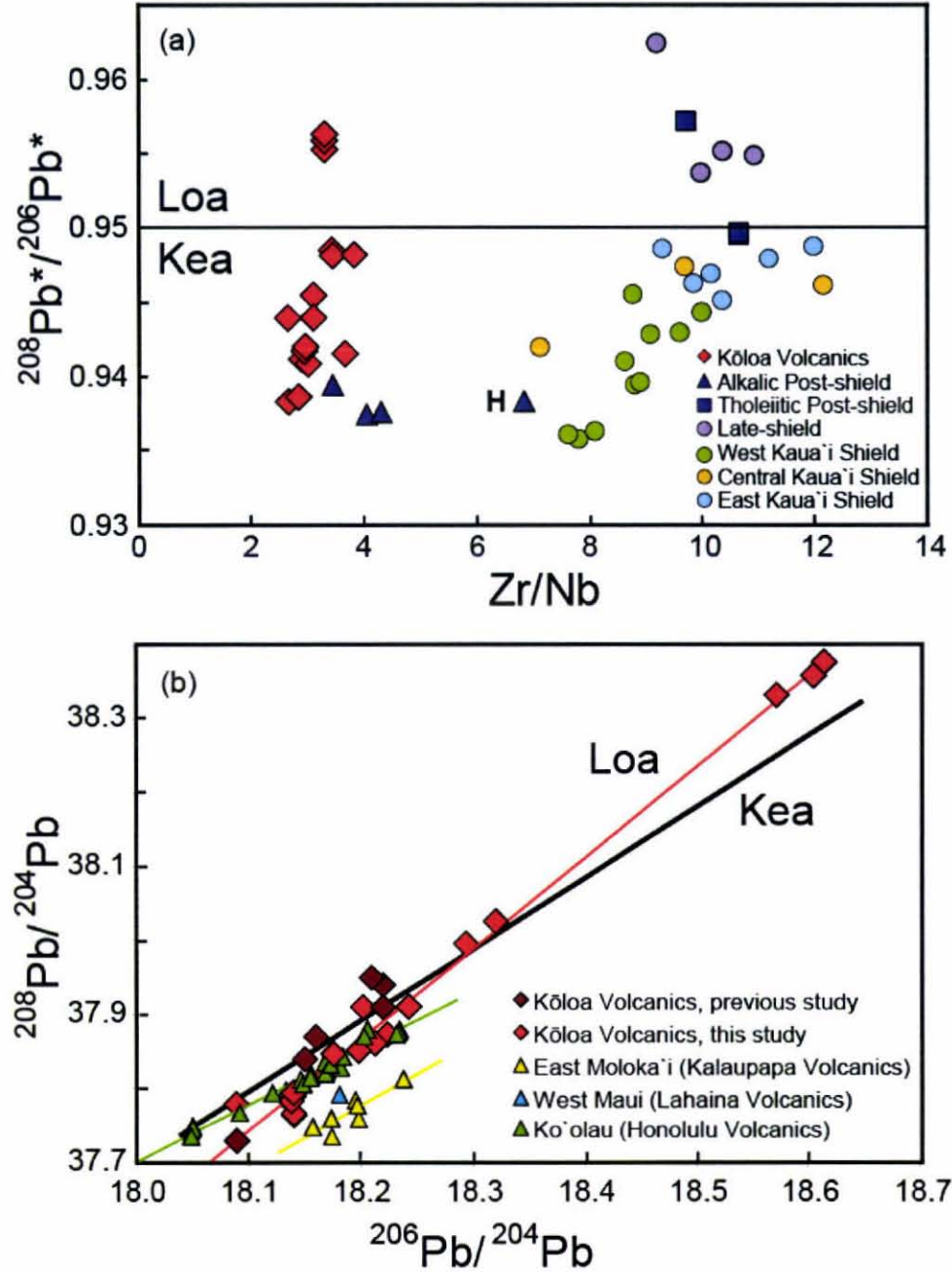


Fig. 7: Comparison of the different stages of Kaua'i volcanism and rejuvenated volcanism from other Hawaiian Islands with the Loa-Kea compositional boundary. The "H" on the plots represents the geochemically distinct hawaiite sample (GA 566). (a) $^{208}\text{Pb}^*/^{206}\text{Pb}^*$ vs. Zr/Nb . (b) $^{208}\text{Pb}/^{204}\text{Pb}$ vs. $^{206}\text{Pb}/^{204}\text{Pb}$. Rejuvenated volcanism on the Hawaiian Islands except Kaua'i is Kea-like, and the Kōloa Volcanics straddle the Loa-Kea boundary line defined by Abouchami et al. (2005). The previous Kōloa Volcanics shown in the dark red diamonds are from Lassiter et al. (2000). Kaua'i shield data from Mukhopadhyay et al. (2003); West Maui data from Gaffney et al. (2004); East Moloka'i data from Xu et al. (2005); Honolulu Volcanics data from Fekiacova et al. (2007).

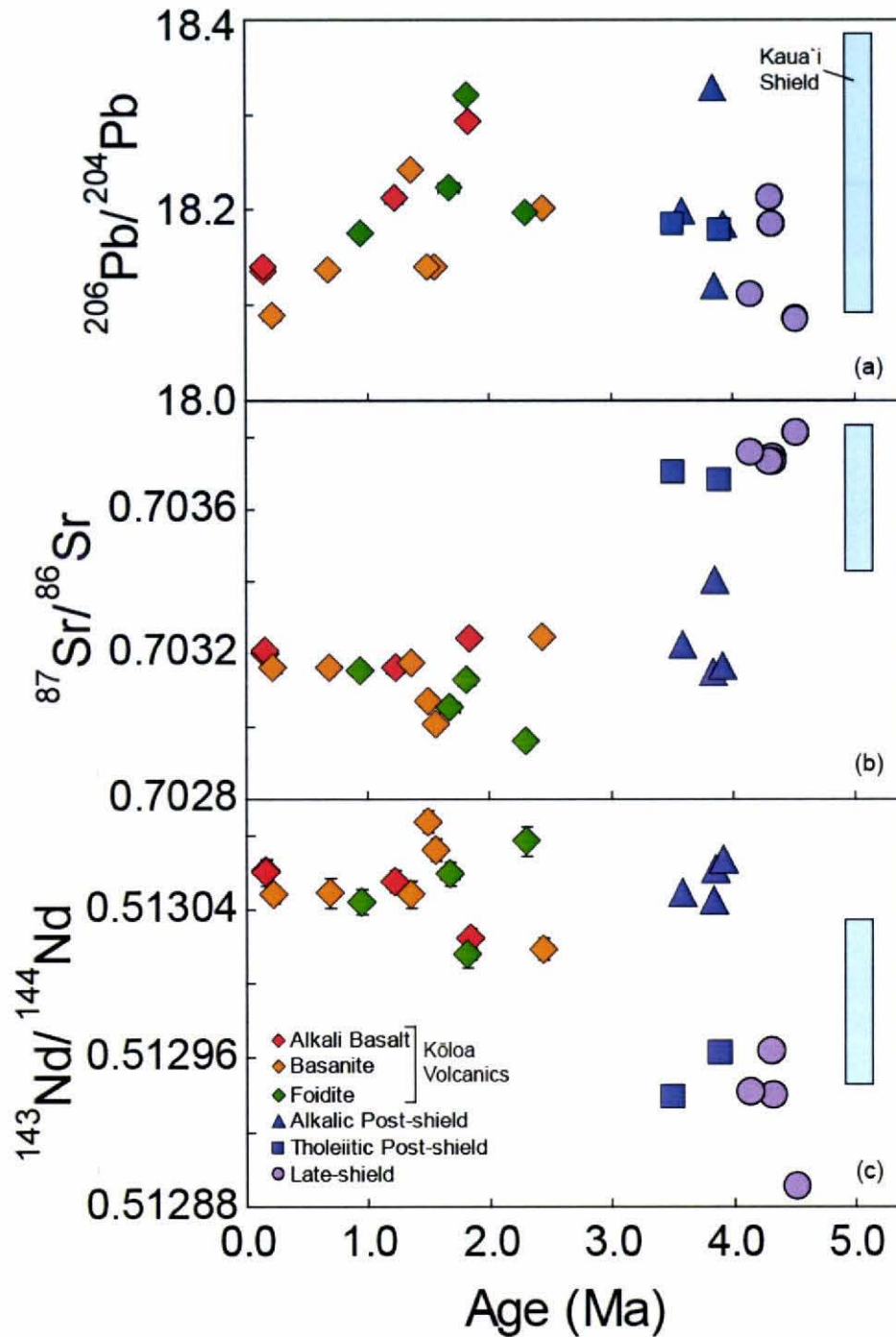


Fig. 8: Pb, Sr and Nd isotopic ratios vs. age for the Kōloa Volcanics, post-shield and late-shield stages of Kauaʻi. The blue bar represents the spread in isotopic ratios of the Kauaʻi shield lavas; no age data is available for these samples. During the rejuvenated stage, the isotopic heterogeneity decreased abruptly at 1.5 Ma. No correlation is seen between age and rock type. The late-shield samples exhibit similar Pb, higher Sr and lower Nd ratios. The post-shield samples exhibit a larger isotopic range over a small time scale. Unless visible, the 2σ error bars for the isotopic ratios and ages are within the size of the symbol. Kauaʻi shield data from Mukhopadhyay et al., 2003.

5.0 DISCUSSION

5.1 Sources of the Late-shield and Post-shield Stages of Kauaʻi Volcanism

A four component system (Lōʻihi, Koʻolau, Kea and DM, similar to that sampled during the rejuvenated stage) is required to adequately explain the isotopic compositions of all the Hawaiian shield lavas (Hauri, 1996; Eiler et al., 1998; Mukhopadhyay et al., 2003; Frey et al., 2005). Principal component analyses revealed that Lōʻihi, Koʻolau and DM end-members can reasonably explain the isotopic variability of the Kauaʻi shield (Mukhopadhyay et al., 2003). Our data show that these three end-member compositions are also sampled during the subsequent late-shield, post-shield and rejuvenated stages, although in varying amounts (Figure 6). The ~4.3 Ma late-shield lavas trend towards the enriched Koʻolau end-member, as do the older eastern Kauaʻi shield lavas (Figures 5 and 6), representing a mix of Lōʻihi and Koʻolau components.

The post-shield stage samples analyzed form two geochemical groups. The ~3.9 Ma tholeiitic samples are isotopically similar to the shield stage lavas, whereas the 3.9 - 3.6 Ma alkalic lavas are distinct in Ba/Sr but otherwise similar to the Kōloa Volcanics. Based on the observations from a limited sample suite, the post-shield stage of Kauaʻi began with a mixture of tholeiitic and alkalic lavas, and subsequently transitioned to alkalic lavas only. The presence of both tholeiitic and alkalic basalts in the post-shield stage is also observed on other Hawaiian shields (e.g., Haleakalā, Mauna Kea and East Molokaʻi; Chen et al., 1991; Frey et al., 1991; Xu et al., 2005).

The Kauaʻi post-shield lavas exhibit large isotopic heterogeneities (compared to the overall geochemical variability in Kauaʻi lavas) on a small spatial scale (few km),

indicating fluctuations in the relative proportions of the mixing of source components. This interpretation is supported by a change in the major and trace element ratios seen within the post-shield stage (Figure 4). Such isotopic variability within the post-shield is not common among Hawaiian volcanoes. The tholeiitic and alkalic post-shield lavas of Mauna Kea, Haleakalā and East Molokaʻi are isotopically similar (Kennedy et al., 1991; Chen et al., 1991; Xu et al., 2005). However, similar isotopic variations are reported over a small time scale for Kīlauea shield lavas (Marske et al., 2007). The isotopic distinction between tholeiitic and alkalic lavas of similar age erupted nearby (Figure 1) suggests Kauaʻi was tapping small-scale heterogeneities during the post-shield stage as has been noted for Kīlauea tholeiites (Garcia et al., 2000). Specifically, the post-shield tholeiitic samples were derived from larger degrees of partial melting from a source similar to the late-shield source (mostly Lōʻihi component with a little Koʻolau component), whereas the alkalic samples require a greater DM contribution but no Koʻolau component (Figures 5 and 6).

5.2 Sources of the Kōloa Volcanics

There has been an ongoing debate among geoscientists regarding the source of the Hawaiian rejuvenated volcanism (e.g. Jackson and Wright, 1970; Clague and Frey, 1982; Gurriet, 1987; Ribe and Christensen, 1999; Bianco et al., 2005). Rejuvenated lavas exhibit high Nd and low Sr isotopic values relative to the underlying Hawaiian shield stage, suggesting long term depletion of the source; however, this is inconsistent with the high concentrations and ratios of incompatible elements seen in these lavas (e.g. Clague and Dalrymple, 1988; Reiners and Nelson, 1998). To resolve the conflict between the

enriched trace element pattern and the depleted isotopic signatures, models have been invoked with varying amounts of metasomatic fluids from either depleted or enriched mantle reservoirs interacted with enriched or depleted reservoirs, respectively (Feigenson, 1984; Clague and Dalrymple, 1988; Maaloe, 1992; Reiners and Nelson, 1998; Lassiter et al., 2000). The depleted component was ascribed to the ~110 Ma oceanic lithosphere beneath Kaua'i. Our high precision Pb and Hf isotopic data (Table 3) for the Kōloa Volcanics do not support a lithospheric source component.

Pb and Hf isotopic data were not utilized previously as discriminating parameters in determining the source components of the Kōloa Volcanics because few high precision data for these isotopes were available. To evaluate the involvement of the oceanic lithosphere in the rejuvenated lavas, there are two readily testable lithospheric proxies: (1) the ~110 Ma lithosphere near Hawaii, sampled from ODP Site 843 (King et al., 1993; Fekiacova et al., 2007); and (2) present-day basalts from the East Pacific Rise (EPR) MOR (Fekiacova et al., 2007). The ϵ_{Hf} vs. $^{206}\text{Pb}/^{204}\text{Pb}$ plot shows that the Kōloa Volcanics trend toward a depleted mantle component with lower $^{206}\text{Pb}/^{204}\text{Pb}$ ratios than the EPR MORB (Figure 5b and 6b). Secondly, the trend line defined by the Kōloa Volcanics in Pb-Pb space does not intersect the ODP Site 843 lavas or the EPR MORB field (Figure 5a). Thus, these two isotopic systems indicate that a Pacific lithospheric component is not involved in the source for Kōloa lavas. Likewise, the Honolulu Volcanics show no isotopic relationship to any MORB-type material (Fekiacova et al., 2007). Alternatively, the source of the depleted component in rejuvenated lavas may be thermally entrained mantle in the upwelling Hawaiian plume (Frey et al., 2005; Fekiacova et al., 2007). Thermal accretion of deep-seated mantle material to the plume

core during ascent has been previously suggested by Hauri et al. (1994) to explain the depleted isotopic signature in other post-shield Hawaiian volcanics. The interpretation that the source is likely intrinsic to the Hawaiian plume is supported by the overlap of the Kōloa Volcanics and the alkalic post-shield lavas, which are thought to be entirely plume derived (Figures 3, 4, 5).

The Pb, Sr, Nd, and particularly the Hf isotopic ratios suggest a mixture of Lō`ihi and depleted mantle end-members contributed to the formation of the Kōloa Volcanics. However, two strongly alkaline Kōloa samples, from the same flow, with the extreme $^{206}\text{Pb}/^{204}\text{Pb}$ ratios (KR-5, KR-11) suggest the involvement of an additional seemingly short-lived, small-scale component. This component, characterized by coupled high $^{206}\text{Pb}/^{204}\text{Pb}$ ratios and $^{208}\text{Pb}/^{204}\text{Pb}$ ratios and lower than expected ϵ_{Hf} , is not sampled by any other Hawaiian volcano (Figure 6). These lavas represent the tapping of a previously unknown/unseen component in the Hawaiian mantle plume.

5.3 Kaua`i's Evolution and Plume Structure

Two basic models have been proposed for the geochemical structure of the Hawaiian plume: (1) radial zoning (Kurz et al., 1995; Hauri et al., 1996; Lassiter et al., 1996; Blichert-Toft et al., 2003; Bryce et al., 2005) and (2) bilateral asymmetry with vertically stretched isotopically heterogeneous “filaments” (Abouchami et al., 2005). A radially zoned plume, with geochemical variations in the horizontal dimension, is not adequate to explain the geochemical trends seen in the Kaua`i shield data; rather, time-varying geochemical heterogeneities in the vertical direction are required to explain the isotopic evolution of the Kaua`i shield lavas (Mukhopadhyay et al., 2003). The new late-

shield, post-shield and rejuvenated lava data are consistent with the need for a more elaborate plume structure.

The systematic shifts in components sampled throughout Kauaʻi's eruptive history reflect variations in source lithology. Simultaneous melting of varying proportions of the Loʻihi and Koʻolau components along with a third, depleted mantle component, is consistent with the isotopic compositions exhibited during Kauaʻi's eruptive history. Our isotopic and trace element data are consistent with the involvement of primitive mantle (Lōʻihi component) and, to a minor extent (< 15%), and enriched mantle (Koʻolau component) and the entrained depleted mantle (DM component). The enriched mantle component exists embedded in a plume of primarily peridotite (Gaffney et al., 2005). Numerical modeling and the observed geochemical variations suggest that the enriched mantle heterogeneities can be preserved in the plume over long time scales without being homogenized with the peridotite (van Keken and Zhong, 1999; du Vignaux and Fleitout, 2001; Kogiso et al., 2004a).

During the shield-building stage, the western Kauaʻi shield lavas preferentially sampled the Lōʻihi component (~95% Lōʻihi, ~5% DM), whereas the eastern Kauaʻi shield lavas sample a slightly higher proportion of the enriched Koʻolau component (<10% Koʻolau, >90% Lōʻihi; Mukhopadhyay et al., 2003). This systematic spatial isotopic variation of the Kauaʻi shield lavas indicates a change in the relative contribution of these two components from west to east across the island. As Kauaʻi transitioned into its late-shield stage, the volcano was located near the cooler periphery of the plume and lower degrees of melting produced a greater contribution from the Koʻolau end-member to form the late-shield lavas (<15%; Lassiter et al., 2000; Fekiacova et al., 2007). During

the post-shield stage, the isotopic variability suggests the volcano sampled the Ko`olau, Lō`ihi and DM components at the plumes edge. The tholeiitic lavas comprise a mixture of Lō`ihi (>90%) and Ko`olau (<10%) end-members, whereas the alkalic lavas comprise a mixture of Lō`ihi (~30-70%) and DM (~70-30%) end-members (Figures 5 and 6). The Ko`olau component was exhausted or otherwise absent in the melting zone during the latter portion of the post-shield stage, as it is not seen in the younger alkalic post-shield lavas or the subsequent rejuvenated volcanics. On Kaua`i, the Ko`olau component only contributes to the tholeiitic lavas. However, if it was present during the alkalic post-shield and rejuvenated stages it should have been sampled because pyroxenites and eclogites (lithologies commonly thought to be the Ko`olau component; Hauri et al., 1996; Pertermann and Hirschmann, 2003; Fekiacova et al., 2007) have lower solidi than peridotite (Lō`ihi), thus, lower degree partial melts should preferentially sample such components (Lassiter et al., 2000). The lack of the transient Ko`olau component is also observed in Ko`olau's rejuvenated volcanics (Fekiacova et al., 2007). The increased involvement of the DM component in the younger Kaua`i lavas is consistent with the volcano being located at the periphery of the plume during the post-shield stage. Isotopic and seismic evidence (Fekiacova et al., 2007; Woods et al., 1991), and numerical modeling of the plume-lithosphere interaction (Ribe and Christensen, 1999) suggest that the DM component sampled by Kaua`i lavas is asthenosphere entrained by the upwelling plume (Mukhopadhyay et al., 2003; Frey et al., 2005; Fekiacova et al., 2007).

The isotopic signature of the Kōloa Volcanics indicate they were derived from variable amounts of the Lō`ihi and DM end-members (Figures 5 and 6). The contribution of the DM component was highly variable, ranging from approximately 25 – 80%.

During the rejuvenated stage, the isotopic heterogeneity decreased abruptly at 1.5 Ma (Figure 8). The post 1.5 Ma lavas incorporate ~30% Lō`ihi component and ~70% Dm component. The distinct decrease in heterogeneity could reflect a switch in mechanisms for melt generation, which is discussed in the following section.

The Pb-Sr, Pb-Hf, Pb-Nd and Sr-Nd isotopic plots are consistent with the involvement of the Lō`ihi component in each stage of Kaua`i's eruptive history (Figures 5 and 6). Also, these plots show that not only is the Lō`ihi component evident in all Kaua`i lavas, it is a persistent contributor in lavas from Kaua`i to Lō`ihi, indicating its longevity in the Hawaiian mantle plume (~5 Ma). Other components sampled by Hawaiian volcanoes, Ko`olau and Kea, are evidently present as smaller domains in the plume and are relatively short-lived within a volcano's history. On Kaua`i, there is no contribution from the Kea component, and the contribution of the Ko`olau component was minor, and expressed most strongly during the late-shield stage. The stronger Ko`olau contribution in the late-shield stage is a phenomenon also observed on Ko`olau and volcanoes from the Maui Nui complex (Haskins and Garcia, 2004; Gaffney et al., 2005). Isotopic evidence from Kaua`i and other Hawaiian islands suggests that the Lō`ihi component constitutes the matrix of the plume (Figure 9; Gaffney et al., 2005). A ubiquitous Lō`ihi component; however, is not supported in $^{208}\text{Pb}/^{204}\text{Pb}$ vs. $^{206}\text{Pb}/^{204}\text{Pb}$ space. It is possible that another component co-exists with the Lō`ihi component in the plume matrix and accounts for the observed Pb trends. The Ko`olau component exists as "blobs" or "strings" near the periphery of the plume, and it is primarily sampled during the late stages of shield growth. The tholeiitic post-shield samples on Kaua`i were derived from a mixture of Lō`ihi and Ko`olau end-members. The Ko`olau component

Ko`olau component, but they do exhibit the presence of a larger DM contribution mixing with the Lō`ihi component (Figures 5 and 6). Similarly, during the rejuvenated stage, only the Lō`ihi plume matrix and depleted entrained asthenosphere were tapped for Kōloa magmas.

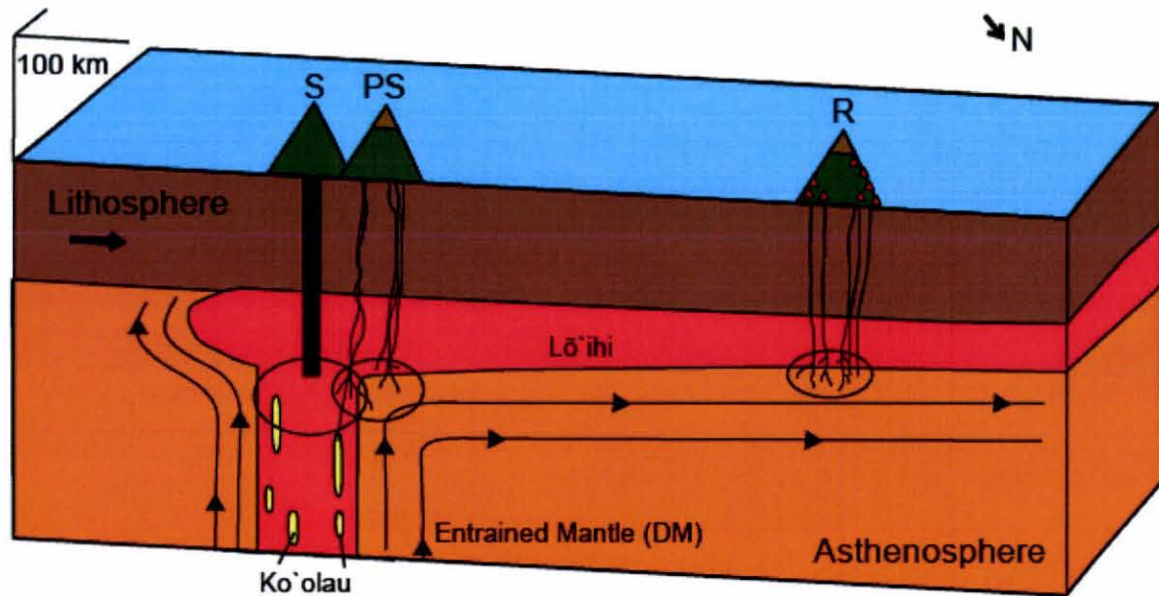


Fig. 9: Cartoon illustrating the plume structure during the evolution of the island of Kaua`i from the shield stage to the rejuvenated stage. The vertical plume stem consists of rapidly-upwelling material from the deep mantle. The plume spreads out laterally and rises as it is dragged beneath the migrating Pacific lithosphere. The vertical plume stem is surrounded by asthenospheric mantle thermally-entrained by the rising plume (indicated by the black lines and arrows around the plume). The plume consists of a matrix containing the Lō`ihi component, with “blobs” of the Ko`olau component present only in the vertical plume stem. The shield stage of Kaua`i (S) incorporates Lō`ihi, DM and Ko`olau components. East Kaua`i lavas involve a relatively larger Ko`olau and smaller DM proportion than West Kaua`i lavas. The late-shield and post-shield (PS) lavas form as Kaua`i begins to move away from the vertical plume stem. These lavas sample the periphery of the plume and the late-shield and tholeiitic post-shield samples have a higher proportion of the Ko`olau component. The alkalic post-shield lavas have no Ko`olau component and only involve the Lō`ihi and DM components. The rejuvenated volcanism (R) occurred once Kaua`i was ~300-400 km downstream from the vertical plume stem. These lavas incorporate only DM and Lō`ihi components.

5.4 Implications of Isotopic Results for Rejuvenated Volcanism Models

The lithospheric melting by conductive heating model invokes a lithospheric source component for the rejuvenated stage of volcanism. This is inconsistent with the new Pb and Hf data for both the Kōloa (this study) and Honolulu Volcanics (Fekiacova et al., 2007). The secondary zone of mantle plume melting and flexure-induced decompression melting models both advocate a plume source. Therefore, additional criteria, such as rock type distribution and isotopic evolution, are required to evaluate these two models. The secondary zone of mantle plume melting model was developed specifically to explain the 1 – 2 m.y. volcanic hiatus and the 2 – 3 m.y. duration of the rejuvenated volcanism and because it involves only a plume source, it remains viable based on the new isotopic data (Ribe and Christensen, 1999). This model advocates a horizontal melt zone at the base of the stretched plume (Ribe and Christensen, 1999), which is consistent with our plume structure model. Most of the melt in this model originates from the mantle (DM) at the base of the elongated plume; however, the isotopic signature of the Kōloa Volcanics suggests that this melt then mixes with melt from the plume core (Lō`ihi; Figures 6 and 9). The isotopic signature of the Honolulu Volcanics also fits this model (Fekiacova et al., 2007).

The flexure-induced decompression melting model of Bianco et al. (2005) was developed using a three component plume source (enriched peridotite, pyroxenite, and depleted component). This model predicts a systematic change in the rate of uplift, which should correlate directly with lava volume, % melting and melt composition during rejuvenated volcanism (Figure 10). The multi-faceted predictive capabilities of this

model make it a superior model for comparing to observed features. Faster upwelling rates are expected to produce higher degrees of partial melting creating alkali basalts, whereas slower upwelling is expected to produce lower degrees of partial melting to generate foidites (Figure 10). The flexure model predicts small volumes of lower degree melts (foidites) early and late during the rejuvenated volcanism when the rate of uplift is low, whereas larger volumes of higher degree melts (alkalic basalts) are expected in between when the rate of uplift is higher (Figures 4e and 10). This model also predicts a shorter duration of rejuvenated volcanism than observed on Kauaʻi, suggesting that it should have ended when Kauaʻi stopped experiencing uplift, about 0.75 m.y. ago (Figure 10). The 38 available ages for chemically analyzed Kōloa Volcanics show a frequency pattern similar to the predicted volumes. However, volcanism did not cease at ~0.75 Ma; instead, it persisted until at least 0.15 Ma (Tagami et al., 2005). The older Kōloa lavas are undoubtedly under-represented in our sample set due to burial by subsequent lava and their greater extent of alteration in the intense tropical setting of Kauaʻi, rendering them unsuitable for geochronology. However, based on sampling efforts, the post 1.5 Ma samples are probably indicative of the rapid decline in Kōloa volcanism during the last 1 m.y. Thus, the decreasing volume of melt predicted is consistent with the observed age trend. However, the eruption of alkali basalts and the absence of foidites during the last 1 m.y. is not predicted by the flexure model. The youngest lavas of the rejuvenated stage from other oceanic islands, such as Oʻahu (Fekiacova et al., 2007), Sao Nicolau (Cape Verde; Duprat et al., 2007), and Gran Canaria (Canary Islands; Hoernle and Schmincke, 1993) do include foidites. The absence of foidites in the younger Kōloa lavas and the extended duration of the rejuvenated stage suggest that while flexure may be an

important process in initiating rejuvenated volcanism, the observed geochemistry and the long duration of the Kōloa Volcanics are inconsistent with flexure being the sole mechanism for this volcanism. The compositional and isotopic transitions to a geochemically restricted source and the absence of younger foidites could be related to a switch in mechanisms responsible for the rejuvenated volcanism. The combination of the flexure model with a secondary zone of mantle plume melting may allow for the extended duration, the higher degrees of partial melting, producing the young alkali basalts, and the abrupt decrease in isotopic heterogeneity at 1.5 Ma. The flexure model provides a physical mechanism to initiate rejuvenated volcanism, which was subsequently sustained after the uplift of Kauaʻi ceased, by the secondary zone of mantle plume melting.

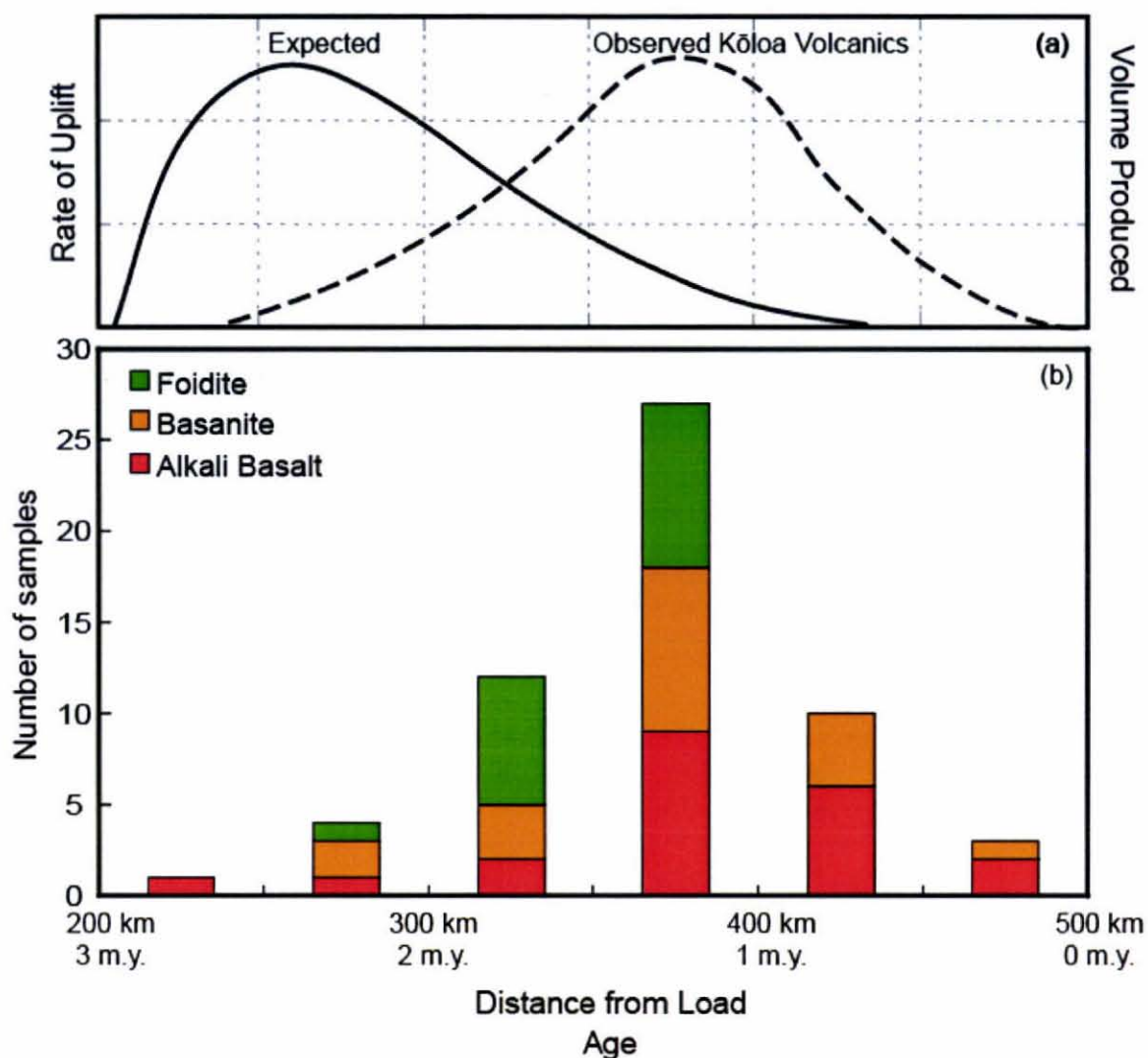


Fig. 10: (a) Qualitative representation of the predicted rate of uplift of the flexural arch with distance from the load. Kauaʻi is ~500 km from the load. The Pacific plate moves at a rate of ~100 km/m.y. (Garcia et al., 1987). The expected uplift curve is from Bianco et al. (2005). The Kōloa Volcanics began ~0.3 m.y. later than expected and continued for ~0.5 m.y. longer than predicted. (b) Histogram of rock types vs. age in 0.50 Ma bins. Oldest rocks are primarily strongly alkalic. A peak in volcanism occurs at the midpoint of the duration of rejuvenated volcanism on Kauaʻi, producing all three rock types. Volcanism rate decreased during the past 1 m.y. producing alkalic basalts and basanites rather than foidites. Age data from Clague and Dalrymple (1988) and Sano (2006).

6.0 CONCLUSIONS

Geochemical and isotopic characterization of the late-shield, post-shield, and rejuvenated stages were used to gain a better understanding of source variations during the latest volcanic stages of Kaua'i and the structure of the Hawaiian plume. Three components are responsible for most of the isotopic evolution of the shield, Lō'ihi, Ko'olau and DM. The late-shield lavas involve a greater proportion of the Ko'olau component. The post-shield stage samples analyzed are divided into two distinct geochemical groups; the tholeiitic group is geochemically similar to the shield stage whereas the alkalic group is similar to the rejuvenated stage. Isotopic heterogeneities on a small spatial scale indicate temporal fluctuations in the mixing of source components. The tholeiitic samples were derived from larger degrees of partial melting from a mixture of Lō'ihi and Ko'olau end-members. Following the eruption of the tholeiitic post-shield samples, the Ko'olau component was absent in subsequent lavas. The alkalic post-shield samples exhibit contributions from only the DM and Lō'ihi components.

The new Pb and Hf isotopic data show no genetic relationship between the Kōloa Volcanics and Pacific lithosphere, including that sampled around Hawaii at ODP Site 843, or recently at the East Pacific Rise (EPR) MOR. Thus, the lithosphere melting model cannot be used to explain the rejuvenated stage. Similarly, the Pb isotopic trend of the Honolulu Volcanics does not support the involvement of a lithospheric component (Fekiacova et al., 2007). All the isotopic systems (Pb, Hf, Sr and Nd) show that the majority of the Kōloa Volcanics comprise two source components, (1) Lō'ihi component from the plume core, and (2) depleted mantle component different from MORB. A third component is present in two Kōloa samples from the same flow that exhibit extreme

radiogenic Pb values. The depleted component could represent deep mantle material that was thermally accreted laterally to the upwelling plume stem and thus part of the overall plume structure (Fekiacova et al., 2007).

Hf and Pb isotopic systematics preclude the formation of the Kōloa Volcanics by the lithospheric melting by conductive heating. A combination of flexure-induced melting and secondary melting of the mantle plume are the most likely mechanisms for generating the voluminous and long-lived Kōloa Volcanics.

PART II

GEOCHEMICAL INFERENCES FOR THE ORIGIN OF THE SOUTH KAUA'I SWELL

7.0 INTRODUCTION

Submarine volcanism is widespread around the Hawaiian Islands. Most of this volcanism occurs either on the flexural arch surrounding the islands (North and South Arch Volcanic fields; Clague et al., 1990; Frey et al., 2000) or on the flanks of the shield volcanoes (north of Molokaʻi, northwest of Niʻihau, and south of Kauaʻi; Hanyu et al., 2005; Garcia et al., in review). The U.S.G.S. GLORIA side-scan survey of the U.S. Exclusive Economic Zone around Hawaiʻi discovered much of this volcanism (Torresan, 1990). This survey also identified a large swell south of Kauaʻi, which was interpreted as landslide deposits (Moore et al., 1994). Subsequent bathymetric mapping by numerous organizations (JAMSTEC, MBARI, SIO, SOEST, USGS, UW cruises and two R/V Kilo Moana cruises) shows the field spans $\sim 5500 \text{ km}^2$ with an estimated volume of $\sim 3000 \text{ km}^3$, and contains numerous conical shaped seamounts (Figure 11). The recognition of these seamounts on the South Kauaʻi Swell (SKS) led to additional suggestions for its origin: widespread offshore secondary volcanism contemporaneous with onshore rejuvenated activity (vents with rejuvenated lavas were found on the south flank of Kauaʻi; Clague et al., 2003) and a submarine satellite shield similar to the Southwest Oʻahu shield (e.g., Noguchi and Nakagawa, 2003; Coombs et al., 2004).

A four-week R/V Kilo Moana cruise around Kauaʻi was conducted in September 2007 to conduct bathymetric, acoustic imagery, magnetics and gravity surveys, and to extensively sample seamounts using the JASON2 ROV with the goal of evaluating the origin of the SKS. During this cruise, 169 coned shaped seamounts, typically $< 1500 \text{ m}$ wide (median = 490 m ; mean = 630 m) and many 10s to 100s m tall were identified on the swell (Garcia et al., in review). Submersible observations and sampling indicate that

the seamounts are dominantly brecciated lava with few intact pillows. Many cones contain lithologically similar angular clasts, whereas others have rounded, matrix-supported clasts. A total of 140 samples were collected from 17 seamounts on the SKS. Here we present XRF major and trace element data for 48 of the least altered basaltic samples and ICP-MS trace element and radiogenic isotope (Pb, Sr, Nd and Hf) data for 19 samples to help explain the origin of the South Kaua'i Swell.

The geochemical results indicate most (41 of 48) SKS volcanics are tholeiitic. The sparsity of submarine alkalic samples is strong evidence that the swell does not represent an extensive offshore extension of the rejuvenated volcanism on Kaua'i. The following discussion of the absence of a landslide scar in Kaua'i's southern flank, the presence of cone-shaped seamounts instead of hummocky landslide blocks, and the geochemical differences between the SKS and the Kaua'i shield lavas all suggest that a landslide origin from the island of Kaua'i is unlikely. These results imply that the SKS may represent a distinct submarine volcano.

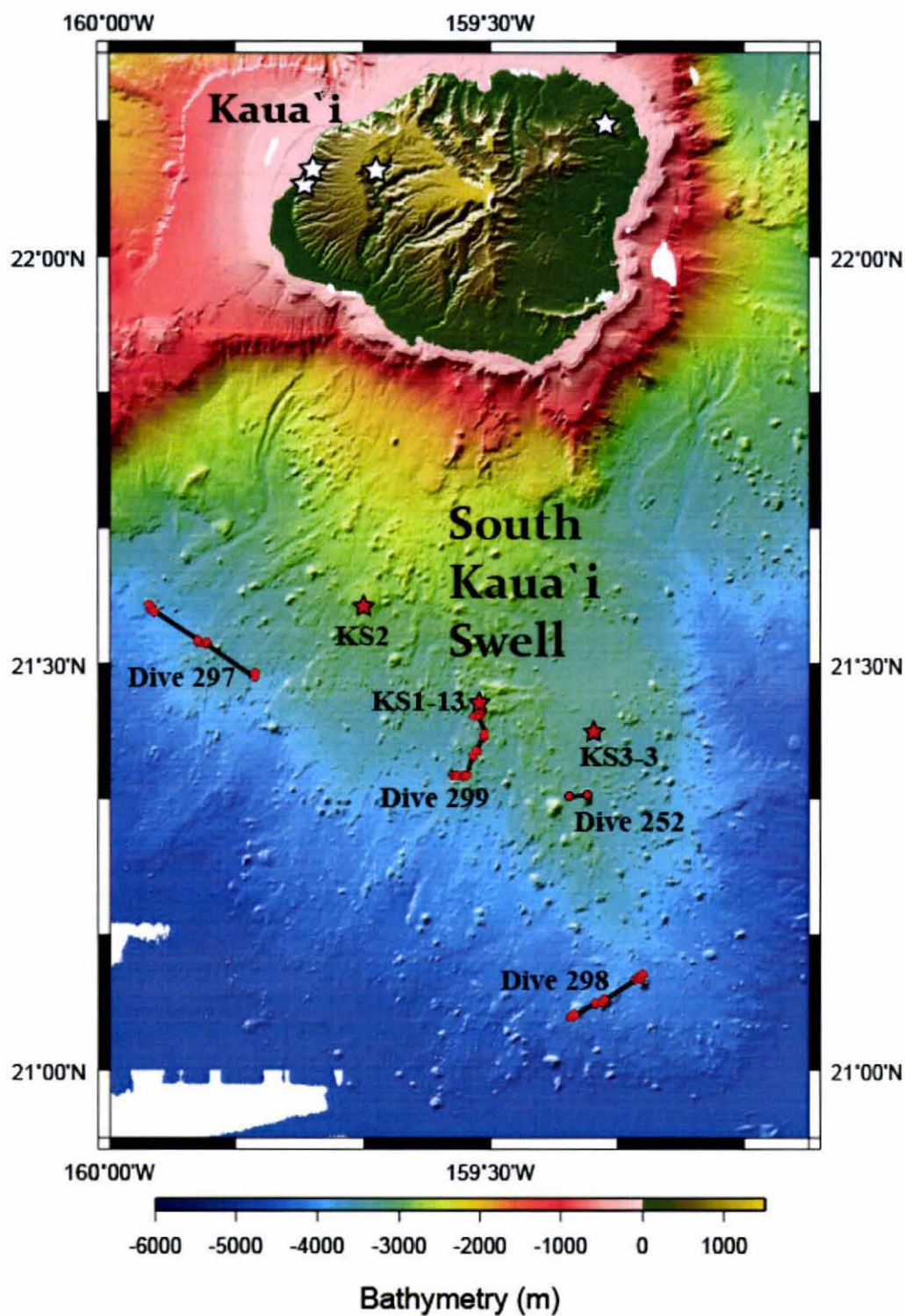


Fig. 11: Bathymetric map of the South Kaua'i Swell showing the sample locations (modified from G. Ito, pers. comm., 2008.). The white stars indicate the locations of the onshore Kaua'i shield stage samples (Bogue and Coe, 1984; Mukhopadhyay et al., 2003) discussed below.

8.0 SAMPLING AND ANALYTICAL TECHNIQUES

A total of 85 samples were recovered on three JASON2 dives (297-299) during the 2007 cruise. Locations are listed and hand specimen features of these samples are described in Appendix A. Samples from two other cruises that sampled the SKS were also included in this study. A four day JASON2 test cruise on the R/V Kilo Moana in November 2007 recovered 10 samples during Dive 252. Three dredge hauls during a student cruise in October 2005 recovered ~15 monomict breccias and volcanic rocks (Appendix A). The sample suite ranges from Mn-encrusted sediment and polymict breccias to non-encrusted lava samples. Multiple samples of adequate size (>0.6 kg) were selected from each cone or sample locality for XRF analysis and thin sectioning. A total of 48 basalt samples from 13 cones were included in this geochemical study.

Every unaltered to weakly altered SKS basalt sample was selected and prepared for XRF analysis. The samples were extensively washed prior to analysis using the method from Rhodes (1996). The crushed material was initially washed by percolating water through the sample until the water had the conductivity of the tap water (~100 micro siemens). The samples were then washed in an ultrasonic bath with deionized (D.I.) water. The samples were ultra-sonicated for several intervals of 2-5 minutes, depending on how quickly the water turned cloudy. After each interval the sample-cleaning D.I. water was changed. Once the sample-cleaning D.I. water reached a conductivity of less than two (preferably <1), the samples were deemed clean. They were then placed in a drying oven at ~1000°C and dried overnight. Once dry, the samples were slowly allowed to cool before they were powdered. Splits of the 48 samples were powdered using tungsten-carbide coated mills and analyzed by XRF for major and trace

elements at the University of Massachusetts (see Rhodes, 1996 and Rhodes and Vollinger, 2004 for analytical procedures and precision).

A subset of 19 samples, selected on the basis of a low level of alteration (e.g., low loss on ignition, LOI, <0.76 wt%) major element compositions and spatial distribution, were analyzed for the ICP-MS trace element suite, and Pb, Sr, Nd and Hf isotopes. The washed split samples were powdered in an agate mill, digested in concentrated sub-boiled HF and HNO₃ for 48 hours and then in 6N sub-boiled HCl for 24 hours. Once dried down, they were re-dissolved in concentrated HNO₃, fully dried again and then diluted 5000 times using a 10 ppb, 1% HNO₃ solution. The trace elements were analyzed using a Finnigan Element2 high-resolution inductively-coupled plasma mass spectrometer (HR-ICP-MS) at the PCIGR (Pretorius et al., 2006). For the isotopic analyses, samples were extensively acid-leached using methods outlined in Weis and Frey (1991, 1996) and Weis et al. (2005) to minimize post-eruptive alteration affects. After a 48 hour period of digestion in concentrated sub-boiled HF and HNO₃ and a 24 hour period of digestion in 6N sub-boiled HCl, the samples were purified using Pb, Sr, Nd and Hf anionic exchange columns to separate these elements (see Weis et al., 2006 and Connelly et al., 2006 for detailed procedure). The Pb, Nd and Hf isotopes were analyzed using a Nu Plasma multi-collector inductively-coupled plasma mass spectrometer (MC-ICP-MS) and the Sr isotopes were analyzed using a Finnigan Triton thermal-ionization mass spectrometer (TIMS), both at the PCIGR. Complete procedural duplicates were analyzed for one Dive 297 sample (J2-297-23) and one dredge sample (KS1-13) yielding an external reproducibility for the Pb, Sr, Nd and Hf of 69 – 131, 5-22, 1 and 16 ppm, respectively.

9.0 RESULTS

9.1 Major and Trace Element Compositions of the South Kaua'i Swell Volcanics

Forty-one of the 48 lavas analyzed for major elements are tholeiitic basalts, six samples are alkali basalts and one is a basanite (Table 6 and Figure 12). On a total alkali vs. silica (TAS) diagram, the SKS volcanics overlap with Kaua'i shield tholeiites, with the majority at the high end of the SiO₂ and total alkali range of the Kaua'i shield lavas. On MgO variation plots, the SKS lavas plot on the Kaua'i shield trend but cluster at lower MgO values (<13 wt%; Figure 13). The higher MgO contents of the Kaua'i shield lavas (up to 30 wt%) reflect substantial olivine addition based on their olivine compositions (e.g., Maaloe et al., 1989). The SKS CaO/Al₂O₃ values also overlap the Kaua'i shield lavas, suggesting they were derived from similar magma composition (Figure 13). However, K₂O contents at a given MgO are, on average, higher in the SKS volcanics. Most of the Kaua'i shield lavas studied for isotopes have lost K₂O due to post-eruptive alteration as indicated by their low K₂O/P₂O₅ values (<1.4), whereas most of the submarine SKS lavas have K₂O/P₂O₅ values of 1.5 – 2 (Table 6), the normal range for Hawaiian tholeiites (e.g., Wright, 1971). However, the most altered sample (J2-297-01) based on LOI (5.1 wt%) has an abnormally high K₂O/P₂O₅ (5.5) indicating K₂O addition. Many of the SKS samples with low K₂O/P₂O₅ have elevated LOI values but not all (Table 6). Samples with low K₂O /P₂O₅ (<1.2) and higher LOI values (>0.76) were avoided for ICP-MS and isotope analyses. Samples from a single cone exhibit large variations in MgO (10.5 – 25), SiO₂ (48.6 – 51), CaO/Al₂O₃ (0.73 – 0.91) and K₂O (0.21 – 0.53) values (Figure 13). These variations are not attributed to olivine addition (Figure

13c). The olivine addition line was determined by the step-wise addition of olivine (equilibrium composition) in small increments (0.1 wt%), using sample J2-297-04 as the starting composition.

The alkalic SKS samples plot with the alkalic rejuvenated stage of Kauaʻi on a SiO_2 vs. MgO plot and most (5 of 7) plot with Kōloa lavas in a TAS diagram and K_2O vs. MgO plot. However, all submarine alkalic samples but the basanite have lower $\text{CaO}/\text{Al}_2\text{O}_3$ than the Kauaʻi rejuvenated lavas (Figure 13).

All of the tholeiitic SKS samples, and two out of three of the alkalic samples are moderately enriched in incompatible elements, similar to the shield stage of Kauaʻi (e.g., Sr, V, Zr; Table 7). The basanite sample shows strong incompatible element enrichment, similar to Kōloa lavas. Two geochemically distinct groups can be distinguished within the SKS volcanics on a Sr/Y vs. Zr/Nb plot (Figure 14a). The tholeiitic samples have higher average Sr/Y and Zr/Nb ratios than the Kauaʻi shield lavas 14 vs. 12. The alkalic samples have a similar Sr/Y ratio to the Kōloa Volcanics, but higher Zr/Nb ratio. The rare-earth element patterns for the South Kauaʻi Swell volcanics are relatively smooth (even on a linear scale REE plot; Figure 14b) and show moderate LREE enrichment. The alkalic SKS lavas exhibit cross-cutting patterns; the basanite exhibits a steeper pattern similar to the rejuvenated stage of Kauaʻi (Figure 14b).

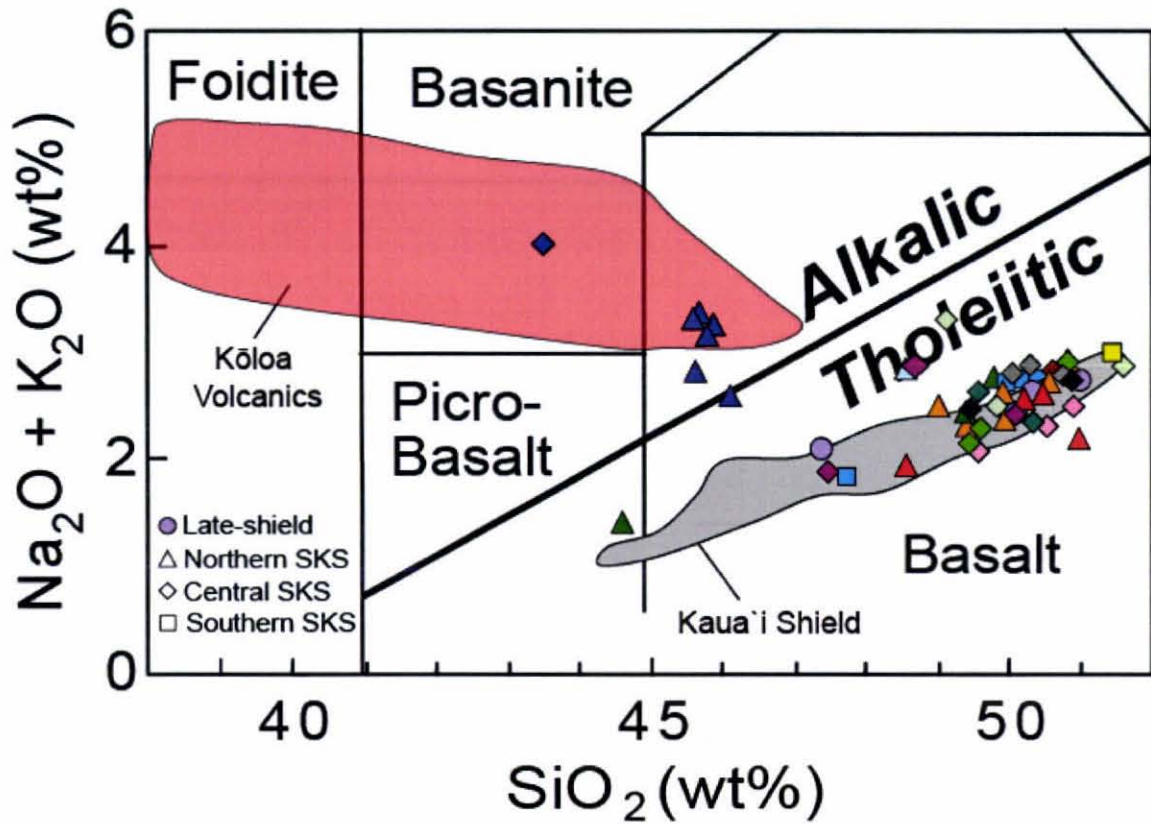


Fig. 12: Total alkalis vs. silica diagram for South Kauaʻi Swell volcanics. Each different color represents a different seamount. Each shape represents a different location on the SKS. The tholeiitic-alkalic dividing line is from Macdonald and Katsura (1964). Kauaʻi shield data from Mukhopadhyay et al. (2003). Kōloa Volcanics XRF data is from Gandy (2006). Late-shield samples plotted to show similarities with SKS lavas.

Table 6. XRF major and trace element compositions of the South Kaua'i Swell volcanics

Sample Name:	J2-297-01	J2-297-04*	J2-297-05	J2-297-06	J2-297-07*	J2-297-09	J2-297-10	J2-297-11*	J2-297-14	J2-297-17	J2-297-18*	J2-297-19
Rock type:	Thol	Thol	Thol	Thol	Thol	Thol	Thol	Thol	Thol	Thol	Thol	AB
Geology:	Cone A	Cone B	Cone B	Cone B	Cone B	Cone B	Cone B	Cone C	Cone C	Cone C	Cone C	Cone D
SiO ₂	48.58	50.60	49.43	49.94	49.04	49.97	50.85	50.49	50.24	48.59	51.01	45.82
TiO ₂	1.832	2.491	2.119	2.237	2.077	2.242	2.496	2.624	2.266	2.309	2.099	1.323
Al ₂ O ₃	9.74	13.11	11.87	12.23	11.52	12.34	14.07	13.87	13.14	13.42	13.49	15.12
Fe ₂ O ₃	12.85	12.67	12.39	12.59	13.11	12.37	12.20	12.64	12.45	12.87	12.26	12.55
MnO	0.17	0.18	0.18	0.19	0.19	0.19	0.18	0.19	0.19	0.20	0.18	0.19
MgO	18.25	8.21	12.29	10.95	12.66	11.10	6.59	6.73	9.11	10.52	8.50	10.84
CaO	5.56	9.83	9.14	9.38	8.74	9.34	10.54	10.64	10.15	10.00	10.05	11.08
Na ₂ O	1.88	2.27	2.01	2.24	2.11	1.94	2.51	2.17	2.22	1.74	1.91	2.54
K ₂ O	0.974	0.457	0.311	0.395	0.388	0.435	0.425	0.447	0.353	0.212	0.291	0.624
P ₂ O ₅	0.176	0.258	0.216	0.225	0.208	0.231	0.251	0.260	0.214	0.211	0.192	0.264
Total	100.01	100.08	99.96	100.38	100.04	100.16	100.11	100.06	100.33	100.07	99.98	100.35
LOI	5.10	0.15	0.08	-0.07	-0.12	-0.16	-0.03	0.31	0.05	0.56	-0.07	0.50
Rb	10.4	6.1	4.4	5.9	5.7	6.0	6.3	6.7	4.7	2.7	3.5	9.4
Sr	209	320	286	286	266	290	325	328	280	299	286	448
Ba	74	68	67	80	76	84	78	89	67	80	55	243
V	174	250	228	241	227	240	260	276	245	253	220	235
Cr	930	396	678	688	743	587	239	194	527	558	423	472
Ni	745	171	398	308	393	354	78	83	225	279	153	246
Zn	124	126	118	119	124	117	117	126	118	127	110	97
Ga	14	20	18	18	17	18	20	20	19	20	20	16
Y	17.5	24.5	21.7	23.0	21.8	23.1	25.7	26.4	24.3	25.2	23.1	17.8
Zr	98	150	126	135	124	134	148	160	130	135	118	62
Nb	8.8	12.3	10.3	11.6	10.5	11.1	12.9	14.7	11.4	11.6	8.9	13.8
La	4	8	7	9	8	8	8	9	8	11	8	10
Ce	18	29	21	24	23	23	26	29	26	26	23	27

Table 6. (Continued) XRF major and trace element compositions of the South Kaula'i Swell volcanics

Sample Name:	J2-297-20*	J2-297-21	J2-297-22	J2-297-23*	J2-297-24	J2-297-25	J2-297-26*	J2-297-27	J2-298-07*	J2-298-12	J2-298-16	J2-298-19
Rock type:	AB	AB	AB	AB	Trans	Thol	Thol	Thol	Thol	Thol	Thol	Thol
Geology:	Cone D	Cone D	Cone D	Cone D	Cone D	Cone E	Cone E	Cone E	Site B	Cone D	Cone D	Cone D
SiO ₂	45.66	45.91	45.63	45.71	46.14	49.41	49.81	44.64	51.47	50.18	50.43	47.76
TiO ₂	1.288	1.351	1.340	1.316	1.359	2.299	2.474	1.229	2.694	2.564	2.425	1.611
Al ₂ O ₃	14.54	15.24	15.23	15.04	15.37	12.44	12.90	7.81	13.51	12.67	13.66	9.36
Fe ₂ O ₃	13.03	12.92	12.98	13.05	12.96	12.14	11.76	12.79	12.12	12.71	11.79	13.01
MnO	0.20	0.20	0.20	0.21	0.19	0.18	0.16	0.17	0.20	0.18	0.18	0.18
MgO	11.62	9.64	9.97	10.40	9.65	10.94	10.50	24.69	6.36	9.19	7.57	18.56
CaO	10.72	11.20	11.12	10.94	11.45	9.73	9.37	7.10	10.43	9.62	10.70	7.54
Na ₂ O	2.13	2.55	2.73	2.80	2.18	2.17	2.28	1.26	2.40	2.31	2.31	1.58
K ₂ O	0.701	0.718	0.588	0.568	0.420	0.277	0.494	0.159	0.609	0.443	0.453	0.264
P ₂ O ₅	0.259	0.296	0.291	0.292	0.297	0.231	0.310	0.191	0.261	0.268	0.241	0.155
Total	100.15	100.03	100.08	100.33	100.02	99.82	100.06	100.04	100.05	100.14	99.76	100.02
LOI	0.61	0.60	0.33	0.19	1.20	-0.04	0.12	0.77	0.76	0.39	0.44	1.29
Rb	10.8	11.7	8.5	8.8	7.0	3.7	7.0	2.6	11.2	7.3	5.4	4.0
Sr	432	482	477	474	487	306	378	200	326	345	326	203
Ba	243	262	244	245	265	67	88	34	83	77	71	83
V	227	238	235	237	239	240	215	154	294	236	249	172
Cr	499	420	422	437	358	632	576	1918	129	534	357	1226
Ni	269	207	206	228	179	329	364	1263	133	193	153	922
Zn	95	97	96	96	94	118	120	112	121	128	108	119
Ga	16	16	16	16	17	19	19	11	21	21	20	14
Y	17.3	18.2	18.2	17.9	18.4	24.1	23.3	13.3	28.4	23.3	24.4	17.3
Zr	61	64	64	63	64	125	162	72	156	157	141	89
Nb	13.1	14.6	14.1	13.8	14.0	11.0	14.6	5.4	14	14	12.2	7.1
La	10	13	12	10	13	8	9	5	9	9	8	5
Ce	25	30	29	27	31	26	31	15	28	30	27	17

Table 6. (Continued) XRF major and trace element compositions of the South Kaua'i Swell volcanics

Sample Name:	J2-298-20*	J2-299-04*	J2-299-05	J2-299-12	J2-299-14	J2-299-20*	J2-299-21	J2-299-23*	J2-299-27	J2-299-28	J2-299-29*	J2-299-33
Rock type:	Thol	Thol	Thol	Thol	Thol	Thol	Thol	Thol	Thol	Thol	Thol	Thol
Geology:	Cone D	Site A	Site A	Site A	Site A	Site B	Site B	Site B	Site C	Site C	Site C	Site D
SiO ₂	49.98	50.93	49.59	50.08	50.56	51.62	49.84	49.14	50.78	50.07	50.32	50.64
TiO ₂	2.608	2.359	2.195	2.149	2.379	2.544	2.131	3.10	2.558	2.676	2.526	2.521
Al ₂ O ₃	12.90	14.24	13.91	12.62	13.90	13.29	11.48	13.36	13.72	13.89	14.15	13.25
Fe ₂ O ₃	12.42	12.26	11.62	12.55	12.11	12.36	12.37	13.32	12.38	12.48	12.06	12.14
MnO	0.18	0.18	0.17	0.18	0.19	0.19	0.17	0.19	0.20	0.19	0.18	0.18
MgO	8.90	6.78	8.43	9.66	7.36	6.89	12.22	7.30	6.95	6.60	7.32	8.34
CaO	10.22	10.72	11.26	10.19	11.06	9.98	8.90	10.09	10.55	10.64	10.50	10.02
Na ₂ O	2.22	2.21	1.87	2.04	2.06	2.25	2.07	2.62	2.42	2.40	2.44	2.31
K ₂ O	0.507	0.293	0.210	0.436	0.256	0.628	0.431	0.690	0.370	0.409	0.448	0.525
P ₂ O ₅	0.269	0.232	0.225	0.199	0.228	0.259	0.212	0.335	0.251	0.269	0.250	0.259
Total	100.20	100.20	99.48	100.10	100.10	100.01	99.82	100.15	100.18	99.62	100.19	100.19
LOI	0.70	0.61	1.65	1.04	0.51	0.58	1.24	0.15	0.00	0.00	-0.17	0.51
Rb	6.0	4.0	3.1	7.6	3.3	9.2	7.9	10.2	5.5	5.7	6.2	9.4
Sr	347	292	275	275	316	292	283	383	335	346	347	328
Ba	103	87	59	82	81	81	104	168	85	79	84	100
V	246	261	259	226	255	261	208	292	250	271	248	253
Cr	540	174	487	637	310	343	839	444	247	232	285	460
Ni	242	80	175	239	100	98	485	143	89	85	116	201
Zn	118	118	168	116	111	120	118	125	111	126	115	117
Ga	21	21	19	19	20	20	19	24	21	21	20	21
Y	24.3	27.4	29.7	22.3	25.8	25.8	21.9	29.0	25.8	27.0	24.2	25.3
Zr	155	135	121	119	129	149	118	179	142	150	141	154
Nb	13.4	10.9	10.4	9.9	11.1	11.2	9.4	17.7	12.5	14.2	12.9	12.3
La	11	8	9	9	10	7	6	14	10	10	11	10
Ce	28	24	25	27	29	23	25	42	31	28	31	28

Table 6. (Continued) XRF major and trace element compositions of the South Kaa'i Swell volcanics

Sample Name:	J2-299-37	KS-1-10	KS1-13*	KS-1-19	KS-2*	KS-3-1	KS3-3*	J2-252-04*	J2-252-05	J2-252-07	J2-252-09	J2-252-10*
Rock type:	Thol	Thol	Thol	Thol	Bas	Thol	Thol	Thol	Thol	Thol	Thol	Thol
Geology:	Site D	Site A	Site A	Site A	Site B	Site C	Site C	Cone A	Cone A	Cone A	Cone B	Cone B
SiO ₂	50.02	48.72	47.49	50.11	43.53	50.88	49.48	50.85	49.46	49.27	50.32	49.59
TiO ₂	2.265	3.547	1.568	2.351	2.342	2.570	2.148	2.536	2.276	2.338	2.343	2.385
Al ₂ O ₃	13.25	12.38	8.95	12.65	10.84	13.83	12.09	13.54	12.31	12.34	12.95	12.60
Fe ₂ O ₃	12.23	13.24	12.58	12.76	13.71	12.13	12.60	12.24	12.87	12.36	12.82	12.95
MnO	0.18	0.21	0.17	0.20	0.19	0.19	0.18	0.18	0.20	0.20	0.30	0.18
MgO	9.12	9.05	20.55	9.33	14.24	6.78	11.64	6.78	10.74	11.80	8.70	9.88
CaO	10.42	9.59	6.95	10.27	10.69	10.66	9.25	10.40	9.74	9.31	10.05	9.60
Na ₂ O	2.22	2.47	1.71	2.13	2.51	2.31	2.08	2.44	2.05	1.93	1.98	2.21
K ₂ O	0.213	0.419	0.172	0.281	1.502	0.462	0.398	0.472	0.370	0.252	0.315	0.429
P ₂ O ₅	0.206	0.402	0.149	0.220	0.423	0.255	0.219	0.249	0.231	0.250	0.224	0.252
Total	100.12	100.03	100.29	100.30	99.98	100.07	100.09	99.69	100.25	100.05	100.00	100.08
LOI	1.45	1.77	0.92	0.86	1.63	-0.53	0.00	0.15	-0.18	0.27	0.23	0.09
Rb	1.5	3.4	2.2	3.8	20.0	7.7	5.5	6.2	5.2	3.2	4.6	6.5
Sr	285	391	200	284	545	334	273	319	305	305	300	331
Ba	52	116	47	69	382	85	66	77	80	90	86	96
V	228	323	185	250	218	265	224	277	240	232	254	246
Cr	575	343	978	596	628	239	792	275	573	627	467	475
Ni	220	241	1018	256	370	84	335	76	274	431	182	192
Zn	146	146	113	124	118	111	114	118	127	124	125	124
Ga	20	23	14	19	16	20	17	20	19	19	20	19
Y	24.3	34.6	16.8	23.6	21.2	25.2	22.9	25.7	23.2	24.8	25.0	24.6
Zr	118	215	89	134	170	155	131	150	125	145	129	145
Nb	9.2	25.6	8.3	12.1	42.1	14.3	11.5	13.1	11.3	11.7	11.4	14.0
La	8	21	6	6	21	13	7	8	8	10	9	5
Ce	23	58	16	26	53	33	21	27	27	27	38	29

Samples were analyzed using XRF at University of Massachusetts (see Rhodes and Vollinger (2004) for analytical procedure)

Major element concentrations in wt%, trace element concentrations in ppm

Thol, tholeiite; Trans, transitional; Bas, basaltic; AB, alkali basalt; names from TAS diagram (Figure 12)

Samples marked with * were analyzed for rare-earth elements and Pb, Hf, Sr and Nd isotopic ratios

Table 7. ICP-MS trace element compositions of the South Kaua'i Swell volcanics

Sample Name:	J2-297-04	J2-297-07	J2-297-11	J2-297-18	J2-297-20	J2-297-23	J2-297-23 d	J2-297-26	J2-298-07	J2-298-20
Sc	27.8	25.9	31.0	29.0	27.6	28.0	28.6	23.7	31.8	27.6
Ni	151	451	83	183	303	205	205	313	117	215
Ga	20.0	16.8	19.9	19.3	15.2	15.4	15.6	18.1	19.6	18.6
Y	23.9	21.2	25.8	22.3	16.9	17.8	18.1	22.8	27.6	23.6
Zr	144	112	145	109	57	69	69	172	160	167
Ba	79	73	91	61	238	265	269	104	87	94
Nb	10.9	9.6	13.0	8.2	11.9	14.5	14.5	14.2	13.7	14.0
Cs	0.06	-	-	-	-	0.26	0.24	0.08	0.43	0.10
Ta	0.80	0.78	1.00	0.64	0.74	1.17	1.02	1.15	1.09	1.10
Th	0.74	0.62	0.85	0.53	0.94	1.08	1.10	0.93	0.82	0.83
U	0.24	0.20	0.25	0.16	0.25	0.30	0.30	0.32	2.11	0.29
La	10.2	8.7	12.0	7.7	11.4	13.0	13.2	12.6	11.1	10.8
Ce	26.3	23.0	30.4	21.0	26.3	30.0	30.7	32.7	28.8	28.6
Pr	3.89	3.29	4.26	3.05	3.37	3.90	4.06	4.67	4.29	4.17
Nd	19.3	16.0	20.6	15.1	15.2	17.5	18.1	22.7	21.3	20.8
Sm	5.33	4.45	5.49	4.36	3.52	3.94	4.03	5.92	5.79	5.59
Eu	1.87	1.49	1.86	1.54	1.16	1.36	1.36	1.99	2.00	1.86
Gd	5.73	4.79	5.88	5.01	3.60	3.94	4.38	6.20	6.67	6.21
Tb	0.90	0.77	0.90	0.79	0.57	0.60	0.66	0.94	1.02	0.93
Dy	5.35	4.40	5.34	4.67	3.37	3.79	3.88	5.50	6.12	5.53
Ho	0.94	0.85	1.00	0.86	0.65	0.72	0.78	0.95	1.14	0.99
Er	2.57	2.22	2.81	2.21	1.86	1.99	2.20	2.47	3.17	2.68
Tm	0.32	0.29	0.34	0.30	0.25	0.27	0.28	0.31	0.39	0.33
Yb	2.00	1.80	2.16	1.88	1.62	1.75	1.78	1.87	2.44	2.04
Lu	0.27	0.26	0.30	0.27	0.23	0.26	0.26	0.25	0.33	0.28

Table 7. (Continued) ICP-MS trace element compositions of the South Kaua'i Swell volcanics

Sample Name:	J2-299-04	J2-299-20	J2-299-23	J2-299-29	J2-299-33	KS1-13	KS-2	KS3-3	J2-252-04	J2-252-10
Sc	31.1	29.4	29.7	28.6	27.8	22.4	26.1	29.1	31.6	29.0
Ni	74	92	172	134	213	987	346	305	75	231
Ga	18.3	17.5	20.9	20.1	19.6	12.1	16.9	16.6	18.8	17.1
Y	26.2	24.0	26.6	23.5	24.2	16.6	21.6	23.8	26.2	24.5
Zr	140	151	164	139	145	80	158	120	142	129
Ba	92	80	134	83	97	40	425	68	77	83
Nb	11.0	11.1	16.3	12.3	11.1	7.2	34.3	9.9	11.5	11.8
Cs	0.07	0.21	0.08	0.07	0.43	0.25	0.44	0.20	0.21	0.20
Ta	0.93	0.95	1.35	0.93	0.84	0.98	2.57	0.87	1.32	1.14
Th	0.64	0.66	1.08	0.79	0.75	0.44	3.25	0.68	0.74	0.86
U	0.20	0.26	0.38	0.22	0.29	0.15	0.90	0.21	0.22	0.25
La	8.9	8.9	14.2	10.6	10.4	6.7	30.7	10.4	11.0	12.6
Ce	23.7	24.6	34.5	27.7	26.9	19.2	65.1	26.4	30.2	30.2
Pr	3.56	3.55	4.76	3.95	3.97	2.46	7.09	3.41	3.91	3.96
Nd	17.8	18.1	21.8	18.9	19.3	11.7	31.5	17.4	19.1	19.1
Sm	5.01	5.02	5.73	5.13	5.37	3.36	6.85	4.82	5.46	5.33
Eu	1.74	1.65	1.86	1.80	1.85	1.11	2.21	1.67	1.87	1.82
Gd	5.88	5.36	6.14	5.48	5.72	3.65	6.38	5.11	5.48	5.41
Tb	0.94	0.85	0.93	0.86	0.89	0.51	0.89	0.74	0.86	0.81
Dy	5.71	5.12	5.42	5.10	5.43	3.46	4.81	4.93	5.73	5.19
Ho	1.10	0.91	1.00	0.95	0.98	0.64	0.86	0.86	0.99	0.93
Er	3.04	2.56	2.68	2.41	2.59	1.66	2.03	2.29	2.56	2.36
Tm	0.38	0.34	0.34	0.32	0.33	0.20	0.25	0.28	0.28	0.25
Yb	2.48	2.09	2.10	1.98	2.05	1.43	1.62	1.95	2.14	2.01
Lu	0.34	0.28	0.29	0.28	0.29	0.21	0.20	0.27	0.31	0.27

Samples were analyzed at University of British Columbia

Trace element concentrations in ppm

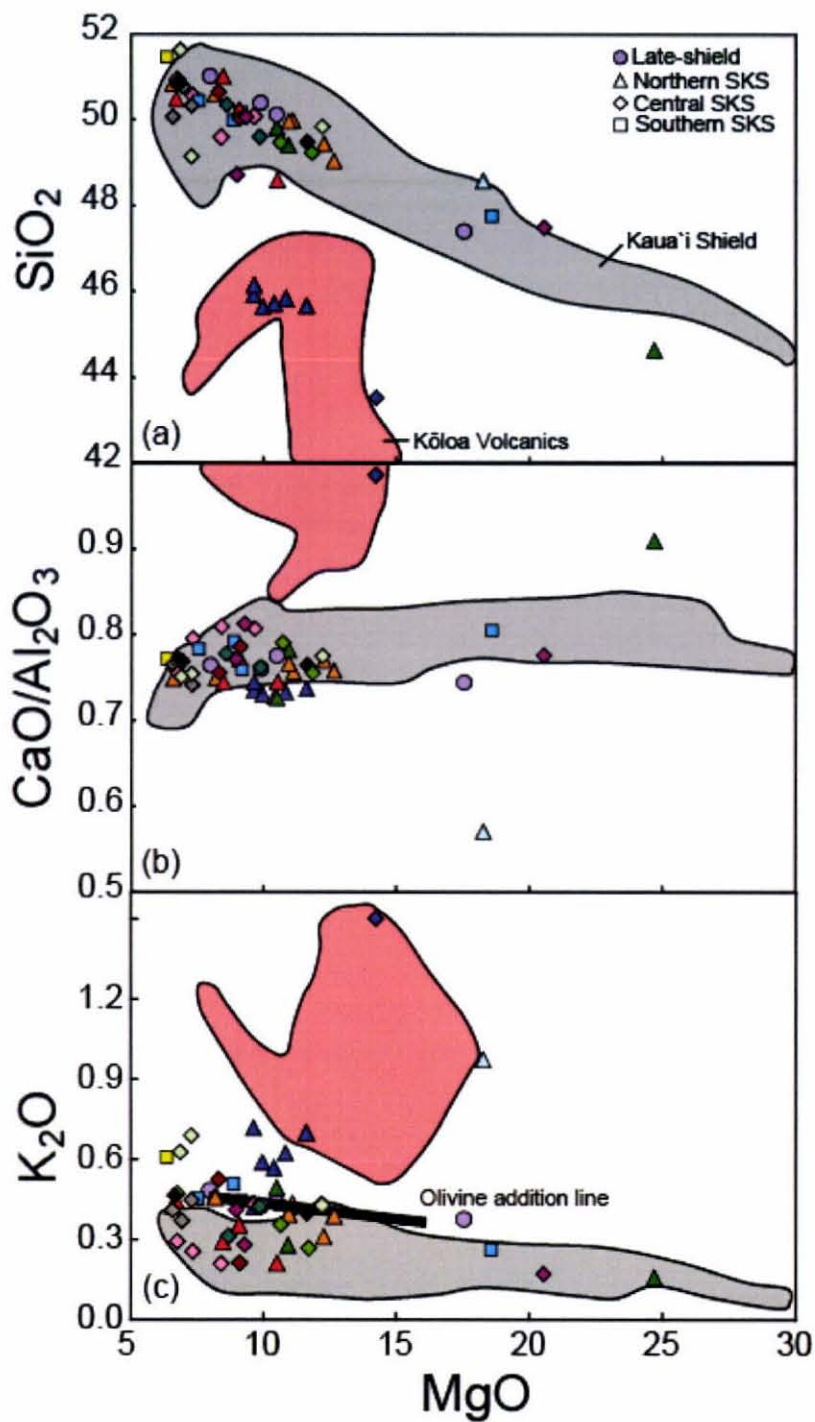


Fig. 13: Major element ratio plots comparing the South Kaua'i Swell volcanics to the different stages of volcanism on Kaua'i. (a) SiO₂ vs. MgO. (b) CaO/Al₂O₃ vs. MgO. (c) K₂O vs. MgO. Each different color represents a separate seamount. The shapes represent different locations on the SKS. All major elements analyzed using XRF. Kaua'i shield data from Mukhopadhyay et al. (2003). Kōloa Volcanics XRF data from Gandy (2006).

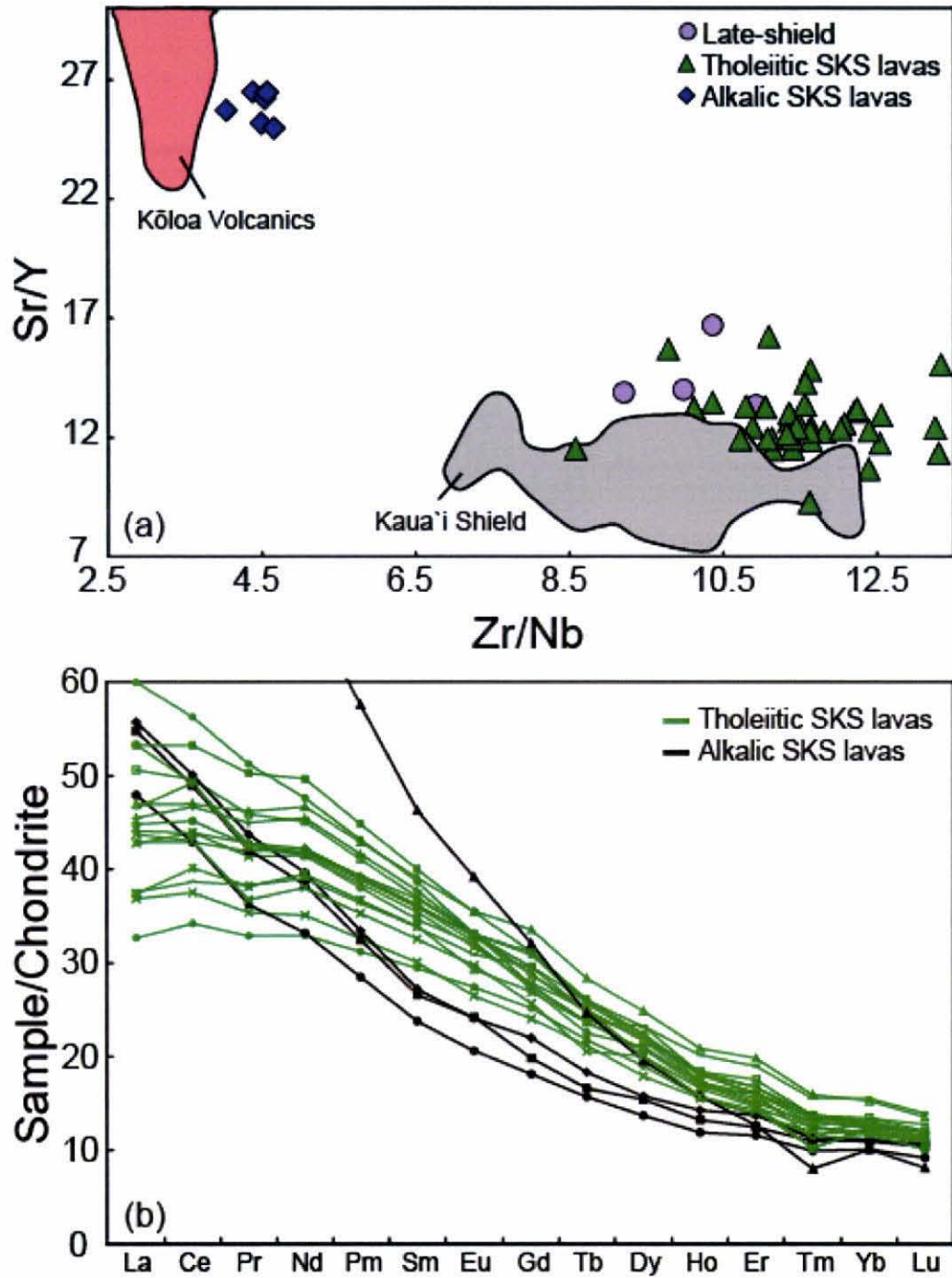


Fig. 14: Trace element ratio plots comparing the South Kaua'i Swell volcanics to the different stages of volcanism on Kaua'i. (a) Sr/Y vs. Zr/Nb (XRF data). The alkalic and tholeiitic SKS lavas define two distinct groups, which are distinct from the onshore Kaua'i lavas. Kaua'i shield field from Mukhopadhyay et al. (2003). Kōloa Volcanics XRF data from Gandy (2006). (b) Rare-earth element diagram (ICP-MS data). Alkalic lavas exhibit a steeper pattern than the tholeiitic samples. REE values normalized to chondrite values from McDonough and Sun (1995).

9.2 Isotopic Compositions of the South Kaua'i Swell Volcanics

The isotopic compositions presented here are the first for the South Kaua'i Swell volcanics (Table 8). The SKS isotopic data form two arrays that correlate with rock type; alkalic and tholeiitic. The alkalic lavas plot near the Kōloa Volcanics and the tholeiites plot with the Kaua'i shield lavas (Figure 15). The SKS tholeiitic samples form linear arrays in Pb, Sr and Nd graphs that partially overlap the Kaua'i shield field (Figure 15). There are, however, distinctions between these two rock groups. SKS tholeiites tend to have higher $^{208}\text{Pb}/^{204}\text{Pb}$ ratios for a given $^{206}\text{Pb}/^{204}\text{Pb}$ ratio than the Kaua'i shield lavas (Figure 15a). The SKS tholeiites are more geochemically similar to the late-shield stage lavas of Kaua'i. A clearer distinction between the SKS volcanics and the Kaua'i shield volcanics is seen on the $^{208}\text{Pb}^*/^{206}\text{Pb}^*$ vs. Zr/Nb plot. The SKS lavas have higher radiogenic Pb and Zr/Nb ratios (Figure 15b).

A comparison of Hf isotopes for tholeiitic SKS and Kaua'i shield samples cannot be made because no shield samples have been analyzed for Hf isotopes (Figure 15c). However, the SKS lavas resemble late-shield lavas for Hf and Nd isotope values. On an ϵ_{Hf} vs. $^{206}\text{Pb}/^{204}\text{Pb}$ graph, the alkalic SKS volcanics plot with the trend of the Kōloa volcanics, and have much higher ϵ_{Hf} values than the tholeiitic lavas (Figure 15c). A similar but less distinct pattern is seen on ϵ_{Nd} vs. $^{206}\text{Pb}/^{204}\text{Pb}$ plot (Figure 15d); the tholeiitic SKS volcanics partially overlap with the Kaua'i shield lavas, forming a positive trend, and the alkalic SKS volcanics plot near the Kōloa Volcanics (Figure 15d). The alkalic SKS lavas plot in two separate places, the dredge sample, KS-2, plots within the Kōloa Volcanics field, whereas the Dive 297 samples have higher Sr ratios (Figure 15e). On a Sr vs. Nd plot, there is a clear separation between the alkalic SKS lavas (which plot

near the Kōloa Volcanics) and the tholeiitic lavas (Figure 15f). The SKS lavas have a lower maximum ϵ_{Nd} value (6.9 vs. 7.6).

Although the Loa and the Kea Pb isotope trends have only been observed up to the Moloka'i fracture zone (Abouchami et al., 2005), our new data show this isotopic boundary to be a useful in distinguishing the SKS lavas from the Kaua'i shield lavas (Figure 15b). The Kaua'i shield, which may lie on the possible extension of the Kea trend, has lavas that plot in the Kea field. However, the lavas erupted during Kaua'i's late-shield stage are Loa-like, plotting above the Pb-Pb boundary as defined by Abouchami et al. (2005). Most (11 of 16) of the tholeiitic SKS volcanics exhibit Loa-like radiogenic Pb ratios, consistent with their geographical location on the possible extension of the Loa trend.

Table 8. Pb, Sr, Nd and Hf isotope data for the South Kaua'i Swell volcanics

Sample Name:	$^{206}\text{Pb}/^{204}\text{Pb}$	$\pm 2\sigma$	$^{207}\text{Pb}/^{204}\text{Pb}$	$\pm 2\sigma$	$^{208}\text{Pb}/^{204}\text{Pb}$	$\pm 2\sigma$	$^{87}\text{Sr}/^{86}\text{Sr}$	$\pm 2\sigma$	$^{143}\text{Nd}/^{144}\text{Nd}$	$\pm 2\sigma$	ϵ_{Nd}	$^{178}\text{Hf}/^{177}\text{Hf}$	$\pm 2\sigma$	ϵ_{Hf}
J2-297-04	18.2386	0.0005	15.4593	0.0005	37.9417	0.0012	0.703656	0.000007	0.512996	0.000007	6.98	0.283099	0.000007	11.57
J2-297-07	18.1892	0.0008	15.4578	0.0007	37.9290	0.0020	0.703718	0.000007	0.512976	0.000007	6.60	0.283083	0.000005	11.00
J2-297-07 (rep)	18.1895	0.0008	15.4586	0.0007	37.9335	0.0020	-	-	-	-	-	-	-	-
J2-297-11	18.1602	0.0007	15.4549	0.0007	37.9625	0.0017	0.703746	0.000009	0.512937	0.000008	5.84	0.283065	0.000006	10.38
J2-297-18	18.1425	0.0007	15.4549	0.0007	37.8959	0.0015	0.703710	0.000008	0.512961	0.000008	6.29	0.283083	0.000007	10.99
J2-297-20*	18.0967	0.0017	15.4614	0.0014	37.7848	0.0036	0.703312	0.000007	0.513031	0.000005	7.66	0.283180	0.000005	14.42
J2-297-23*	18.0807	0.0010	15.4571	0.0008	37.7702	0.0019	0.703307	0.000007	0.513032	0.000005	7.69	0.283180	0.000009	14.44
J2-297-23* (dup)	18.0816	0.0006	15.4586	0.0006	37.7737	0.0015	0.703312	0.000008	0.513033	0.000005	7.70	0.283177	0.000008	14.33
J2-297-26	18.1444	0.0008	15.4560	0.0008	37.8945	0.0021	0.703650	0.000007	0.512945	0.000008	5.99	0.283087	0.000007	11.13
J2-297-26 (rep)	18.1468	0.0006	15.4585	0.0006	37.9011	0.0015	-	-	-	-	-	0.283067	0.000006	10.43
J2-298-07	18.3796	0.0009	15.4674	0.0008	38.0240	0.0022	0.703589	0.000008	0.512987	0.000008	6.81	0.283109	0.000005	11.92
J2-298-07 (rep)	-	-	-	-	-	-	-	-	0.512998	0.000006	7.02	-	-	-
J2-298-20	18.2867	0.0007	15.4593	0.0005	37.9587	0.0015	0.703600	0.000007	0.512985	0.000008	6.77	0.283093	0.000006	11.36
J2-298-20 (rep)	-	-	-	-	-	-	-	-	-	-	-	0.283094	0.000005	11.39
J2-299-04	18.2408	0.0011	15.4618	0.0014	37.9640	0.0034	0.703654	0.000007	0.512982	0.000008	6.71	0.283102	0.000008	11.66
J2-299-20	18.2521	0.0011	15.4634	0.0007	37.9580	0.0010	0.703724	0.000007	0.512974	0.000007	6.54	0.283067	0.000005	10.42
J2-299-23	18.1881	0.0007	15.4564	0.0007	37.8955	0.0016	0.703600	0.000009	0.512990	0.000008	6.86	0.283085	0.000007	11.06
J2-299-29	18.1805	0.0008	15.4522	0.0007	37.9312	0.0018	0.703725	0.000009	0.512957	0.000014	6.22	0.283073	0.000008	10.65
J2-299-29 (rep)	18.1830	0.0008	15.4550	0.0007	37.9397	0.0019	-	-	-	-	-	0.283069	0.000006	10.52
J2-299-33	18.2011	0.0007	15.4592	0.0006	37.9401	0.0017	0.703686	0.000007	0.512978	0.000007	6.63	0.283080	0.000005	10.90
KS1-13 ^T	18.1323	0.0006	15.4493	0.0006	37.8649	0.0017	0.703722	0.000008	0.512946	0.000020	6.48	-	-	-
KS1-13 (dup)	18.1333	0.0006	15.4494	0.0006	37.8659	0.0015	0.703700	0.000007	0.512957	0.000006	7.51	-	-	-
KS-2*	18.2792	0.0015	15.4542	0.0016	38.0152	0.0034	0.703216	0.000008	0.513023	0.000007	6.25	0.283078	0.000005	10.81
KS3-3	18.1925	0.0007	15.4547	0.0007	37.9402	0.0017	0.703735	0.000007	0.512959	0.000006	6.01	0.283061	0.000005	10.23
J2-252-04	18.1602	0.0007	15.4531	0.0016	37.9056	0.0018	0.703692	0.000007	0.512970	0.000009	6.22	0.283057	0.000004	10.09
J2-252-10	18.1952	0.0007	15.4582	0.0006	37.9288	0.0015	0.703693	0.000006	0.512978	0.000008	6.63	0.283088	0.000004	11.17

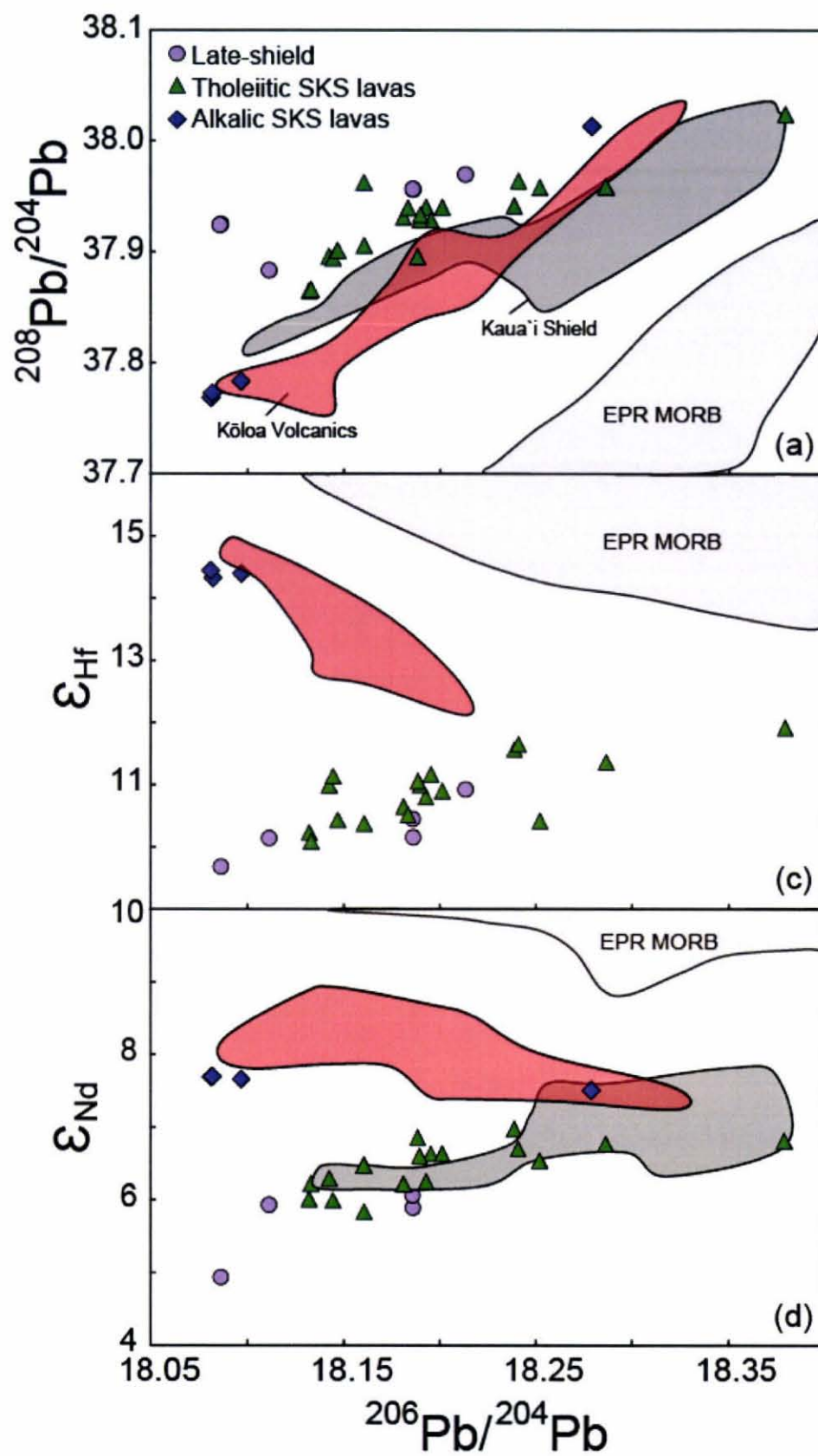
All samples were leached using method outlined in Weis and Frey (1991, 1996); Weis et al. (2005)

Samples were analyzed for Pb and Hf using the Nu Plasma Instruments MC-ICP-MS and for Sr using the Finnigan TRITON TIMS

Samples denoted with ^T were analyzed for Nd using TRITON TIMS

Remaining samples analyzed for Nd using MC-ICP-MS

Samples denoted with * are alkalic



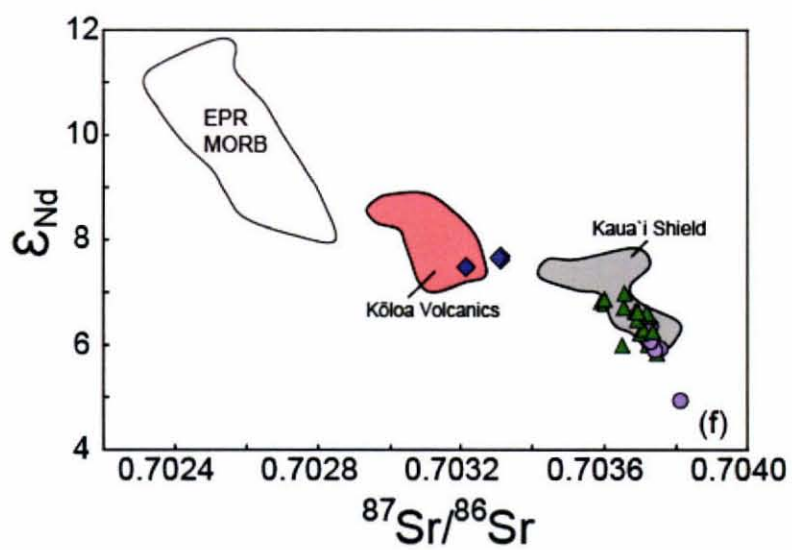
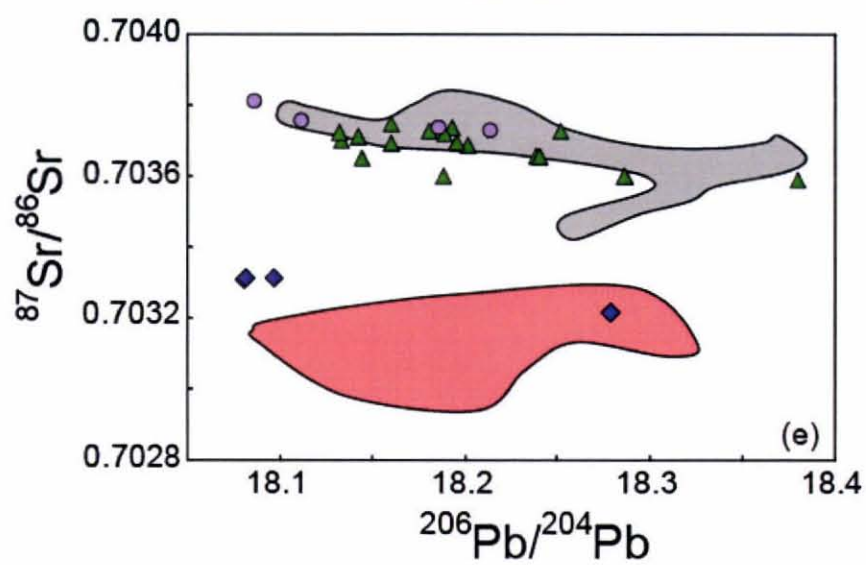
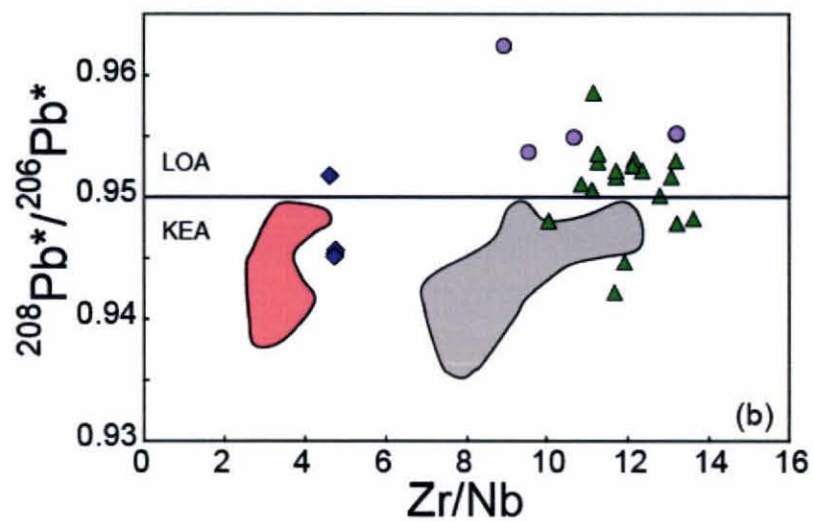


Fig. 15: Comparison of Pb, Hf, Sr and Nd isotopic ratios for the South Kaua'i Swell volcanics with the onshore Kaua'i lavas, the recent EPR MORB lavas and ~110 Ma-old Pacific lithosphere from ODP Site 843. (a) $^{208}\text{Pb}/^{204}\text{Pb}$ vs. $^{206}\text{Pb}/^{204}\text{Pb}$. The SKS volcanics form a linear array which partially overlaps with both the Kaua'i shield volcanics and the rejuvenated Kōloa Volcanics. (b) $^{208}\text{Pb}^*/^{206}\text{Pb}^*$ vs. Zr/Nb shows a clear distinction between the SKS volcanics and the Kaua'i shield volcanics. (c) ϵ_{Hf} vs. $^{206}\text{Pb}/^{204}\text{Pb}$. Kōloa Hf data from Stracke et al. (1999). No Hf isotopic data exists for the Kaua'i shield. (d) ϵ_{Nd} vs. $^{206}\text{Pb}/^{204}\text{Pb}$. (e) $^{87}\text{Sr}/^{86}\text{Sr}$ vs. $^{206}\text{Pb}/^{204}\text{Pb}$. The SKS lavas overlap the Kaua'i shield lavas, but have a smaller range in Sr ratios. (f) ϵ_{Nd} vs. $^{87}\text{Sr}/^{86}\text{Sr}$. SKS lavas overlap Kaua'i shield lavas, but have a smaller range in both Sr and Nd ratios. References for ERP MORB data from Figure 5.

10.0 DISCUSSION

The current hypotheses for the formation of the South Kaua'i Swell include: (1) landslide deposits from Kaua'i (Moore et al., 1994); (2) widespread offshore secondary volcanism contemporaneous with onshore rejuvenated activity (secondary volcanics have been reported on the submarine south flanks of Kaua'i; Clague et al., 2003); or, (3) a submarine satellite shield (Garcia et al., in review). The high proportion of tholeiitic lavas, and the trace element and isotopic characteristics of the SKS lavas are inconsistent with the secondary volcanism model for the swell. However, two cone sampled have alkalic lavas geochemically similar to Kaua'i's alkalic post-shield and rejuvenated lavas. The tholeiitic composition of most of the SKS lavas indicate they probably formed during a shield stage of volcanism (e.g., Macdonald et al., 1983), either as part of Kaua'i, or separately as a distinct shield, such as the Southwest O'ahu volcano (Noguchi and Nakagawa, 2003; Coombs et al., 2004).

The bathymetric swell south of Kaua'i was interpreted as a landslide deposit based mainly on a side-scan survey (Moore et al., 1994). There are two morphological inconsistencies with this hypothesis: (1) there is no visible large landslide scar on the submarine or subaerial south flank of Kaua'i; and, (2) the swell does not display typical hummocky landslide terrain (e.g., Nu'uuanu debris field; Clague et al., 1989; Smith and Satake, 2002), but rather has numerous cone-shaped seamounts (Figure 16). If the South Kaua'i Swell was formed due to a massive landslide off Kaua'i, it would have had to occur during the early stages of shield growth (≤ 5 Ma), to allow time for the scar to have been subsequently filled with younger lavas. It has been suggested that the west wall of Waimea Canyon represents a landslide scar and that the South Kaua'i Swell is the

landslide deposit composed of western Kauaʻi shield lavas (Holcomb et al., 1997). Such a scenario has also been proposed to have occurred on the southwest flank of Mauna Loa (Lipman et al., 1990).

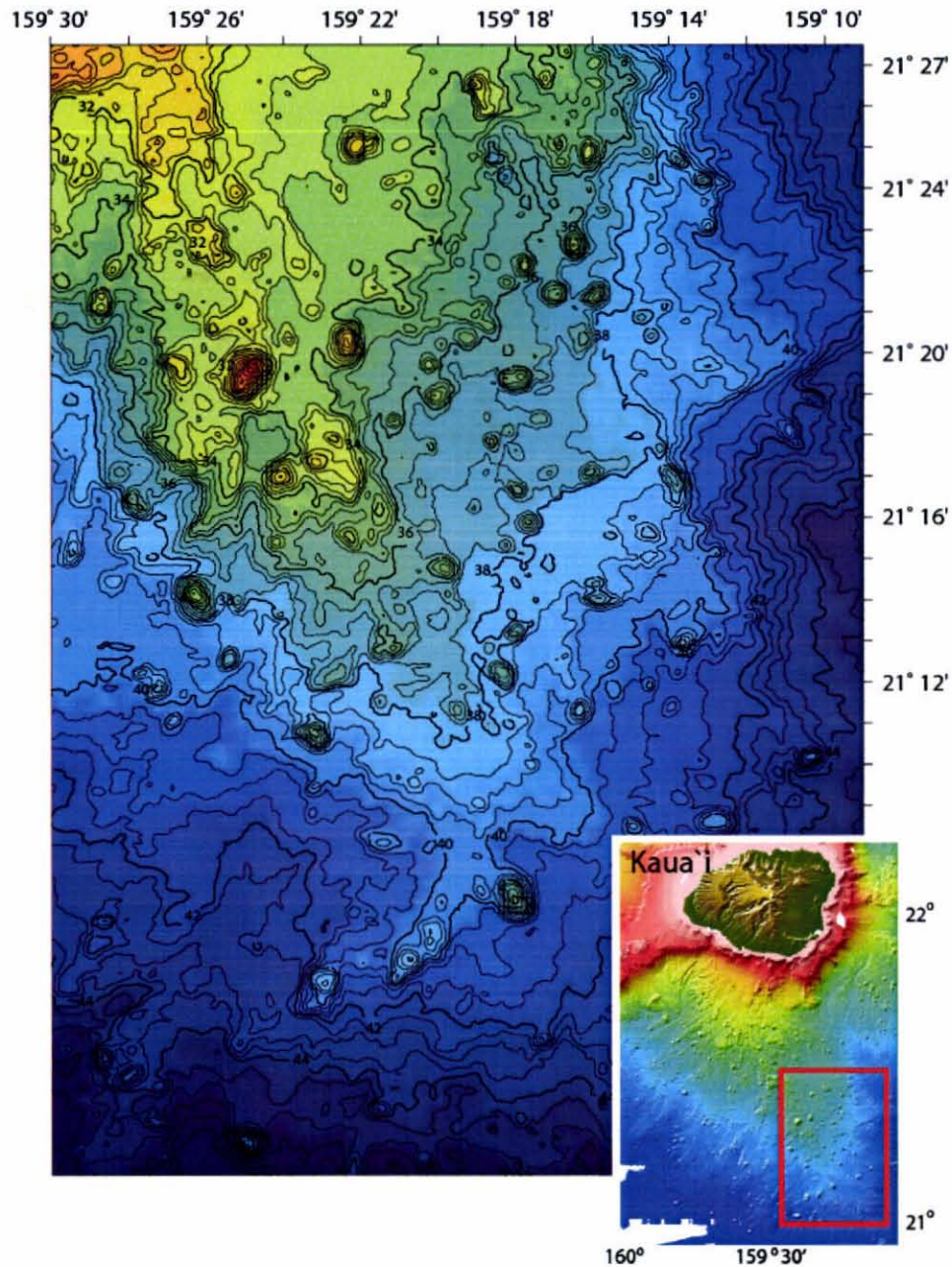


Fig. 16: Bathymetric map of the southeast part of the South Kauaʻi Swell showing the numerous conical seamounts. The numbers on the map represent depth in 100s of meters. Only a portion of the SKS enlarged to clearly show cone-shaped seamounts. Inset map shows location of South Kauaʻi Swell. Modified from B. Appelgate, pers. comm. (2008).

The geochemical differences between the SKS lavas and the Kaua'i shield stage lavas also suggest the South Kaua'i Swell was not derived as a landslide deposit from older Kaua'i lavas. Although the SKS and Kaua'i shield lavas are similar in most major elements, trace elements and isotope ratios, there are notable differences between them. The SKS lavas exhibit higher K₂O values, Zr/Nb ratios and ²⁰⁸Pb*/²⁰⁶Pb* values, and extend to lower ε_{Nd} values than the Kaua'i shield lavas. Also, while the relatively low K₂O values in the Kaua'i shield lavas most likely reflect removal of K₂O by post-eruptive subaerial alteration, rather than a different source, the higher K₂O values in the SKS lavas suggest they were not erupted and altered subaerially. The isotopic similarities between the SKS and Kaua'i shield lavas are of the of the same magnitude as similarities observed between some other adjacent Hawaiian shield volcanoes (e.g., Lāna'i and Kaho'olawe; Gaffney et al., 2005; Leeman et al., 1994; Huang et al., 2005, and West Maui and East Moloka'i; Gaffney et al., 2005), which suggests a separate submarine shield origin for the South Kaua'i Swell can still be consistent with the isotopic data.

The SKS lavas exhibit a spatial correlation in Pb isotopic ratios that is opposite to that of the Kaua'i shield (Figure 17). The Dive 297 lavas, from the upper western section of the SKS, have the lowest Pb ratios, Dive 299 lavas, from the middle of the swell, have intermediate Pb ratios, and Dive 298 lavas, from the southern part of the swell, have the highest Pb ratios (Figures 11 and 17). The Pb isotope ratio variations across the SKS lavas from west to east are opposite to that observed on Kaua'i. Pb ratios of Kaua'i shield lavas are the highest in the west and lowest in the east. The proposed origin of the landslide is western Kaua'i (Holcomb et al., 1997); however, the western Kaua'i shield lavas are isotopically dissimilar to the SKS volcanics (Figure 18). The isotopic

dissimilarities between the western Kauaʻi shield lavas and the SKS volcanics, and the contrasting shield and SKS west to east Pb ratio spatial variations suggest the SKS lavas were not derived from the adjacent Kauaʻi shield.

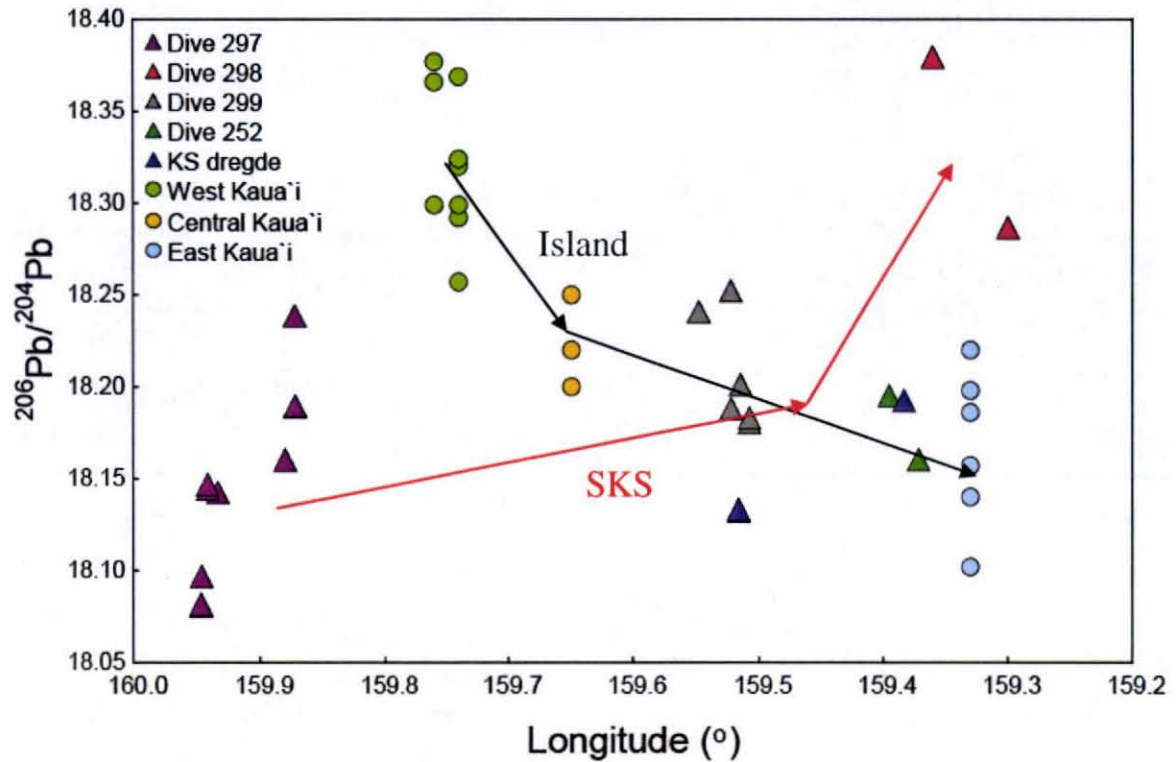


Fig. 17: $^{206}\text{Pb}/^{204}\text{Pb}$ vs. longitude for the South Kauaʻi Swell and Kauaʻi shield volcanics. The SKS volcanics exhibit a partial correlation that is opposite to that seen on the island of Kauaʻi. Longitude and Pb isotopic data for the Kauaʻi shield from Bogue and Coe (1984) and Mukhopadhyay et al. (2003), respectively.

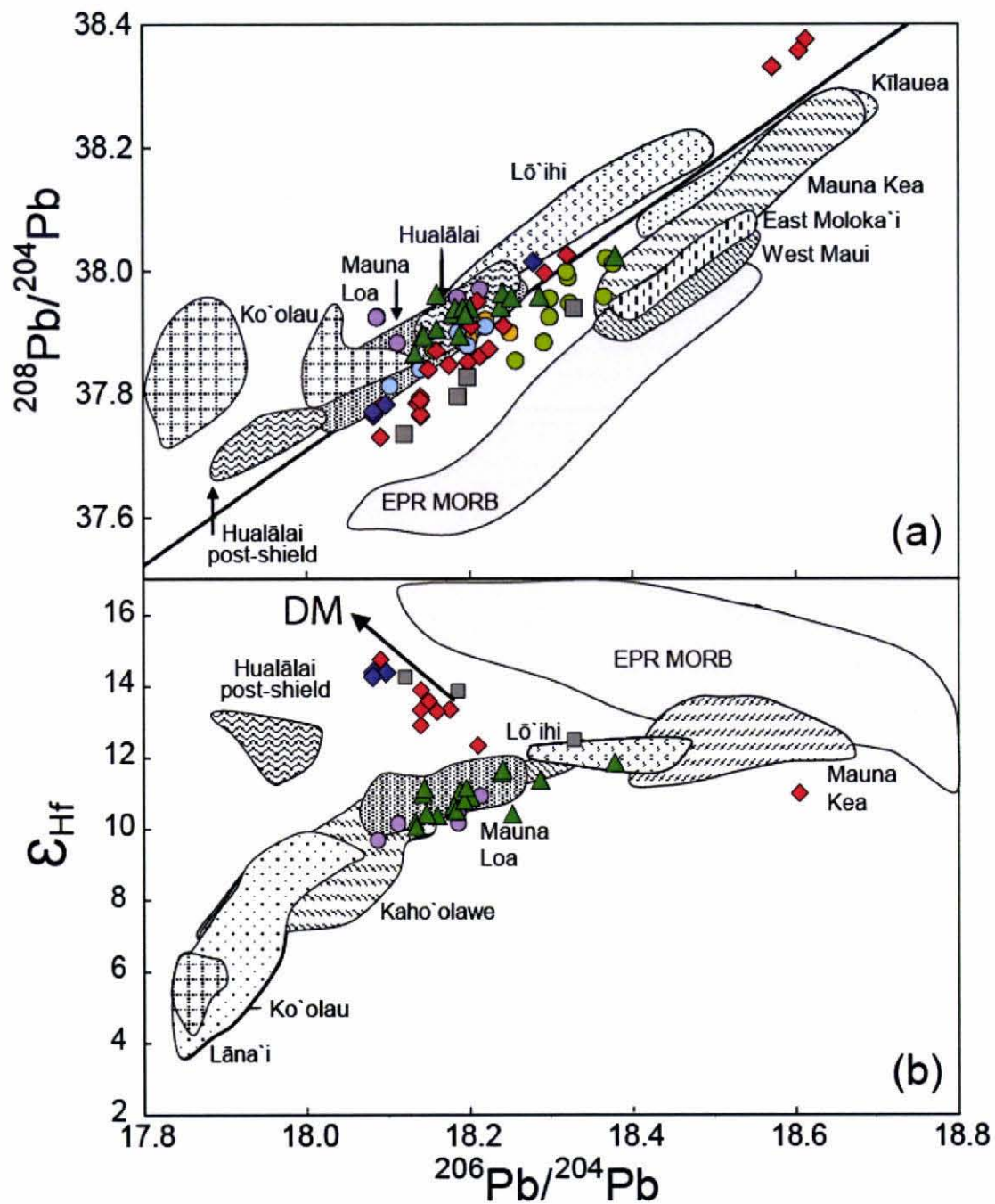
SKS samples are geochemically similar to the Kauaʻi late-shield lavas (Figure 15). They both exhibit higher $^{208}\text{Pb}^*/^{206}\text{Pb}^*$ ratios, a trend towards lower ϵ_{Nd} values and higher Sr ratios. Also, the one dated SKS tholeiite (KS1-13) has an unspiked K-Ar age of 3.9 Ma (Yamasaki and Tagami, pers. comm., 2007), consistent with some late-shield stage Kauaʻi tholeiites (McDougall, 1964; Sano, 2006; Table 2). However, a post 4.0 Ma

giant landslide of sufficient size to create the $\sim 3000 \text{ km}^3$ SKS would have left a large scar in the flanks of Kauaʻi, given the limited $<4.0 \text{ Ma}$ shield volcanism that occurred on the island (McDougall, 1964; Clague and Dalrymple, 1988). Thus, although a young slide origin would be consistent with the geochemical results, it is inconsistent with the geological history of Kauaʻi.

The only remaining viable model for the South Kauaʻi Swell is a separate submarine shield origin. The monomictic character of many of the breccia SKS samples supports a local origin. The satellite shield may have experienced a tholeiitic shield-building stage ($\sim 3.9 \text{ Ma}$). If this age is representative of the SKS, this satellite shield was built during the late-shield/post-shield stage in Kauaʻi's history. This is consistent with the isotopes from the SKS lavas being more similar to these later stages in Kauaʻi's growth than the earlier shield-building stage. If the SKS does represent a separate shield, the SKS lavas incorporated more of the Koʻolau-like component than the early Kauaʻi shield lavas, similar to the onshore late-shield Kauaʻi lavas (Figure 18). Perhaps a large, effectively homogenous, domain existed near the plume edge at this time and was simultaneously responsible for the lavas of the SKS and the onshore late-shield stage. A similar scenario was suggested for the formation of East Molokaʻi and West Maui volcanoes (Gaffney et al., 2005).

The alkalic KS-2 sample plots with the Kōloa Volcanics (Figures 13, 14, and 15) and has an age of 1.9 Ma suggesting it represents a rejuvenated stage. However, ages are needed for the samples from Dive 297 to determine whether they represent the post-shield or rejuvenated stage. The offshore alkalic lavas also do not entirely geochemically overlap with the onshore alkalic lavas (Figs 13, 14, 15 and 18); rather, they appear to

incorporate less depleted mantle component as the onshore lavas. The alkalic SKS lavas are isotopically similar to the Honolulu Volcanics (Figures 6 and 18; Fekiacova et al., 2007), suggesting they may represent the rejuvenated stage of volcanism on the South Kaua'i Swell.



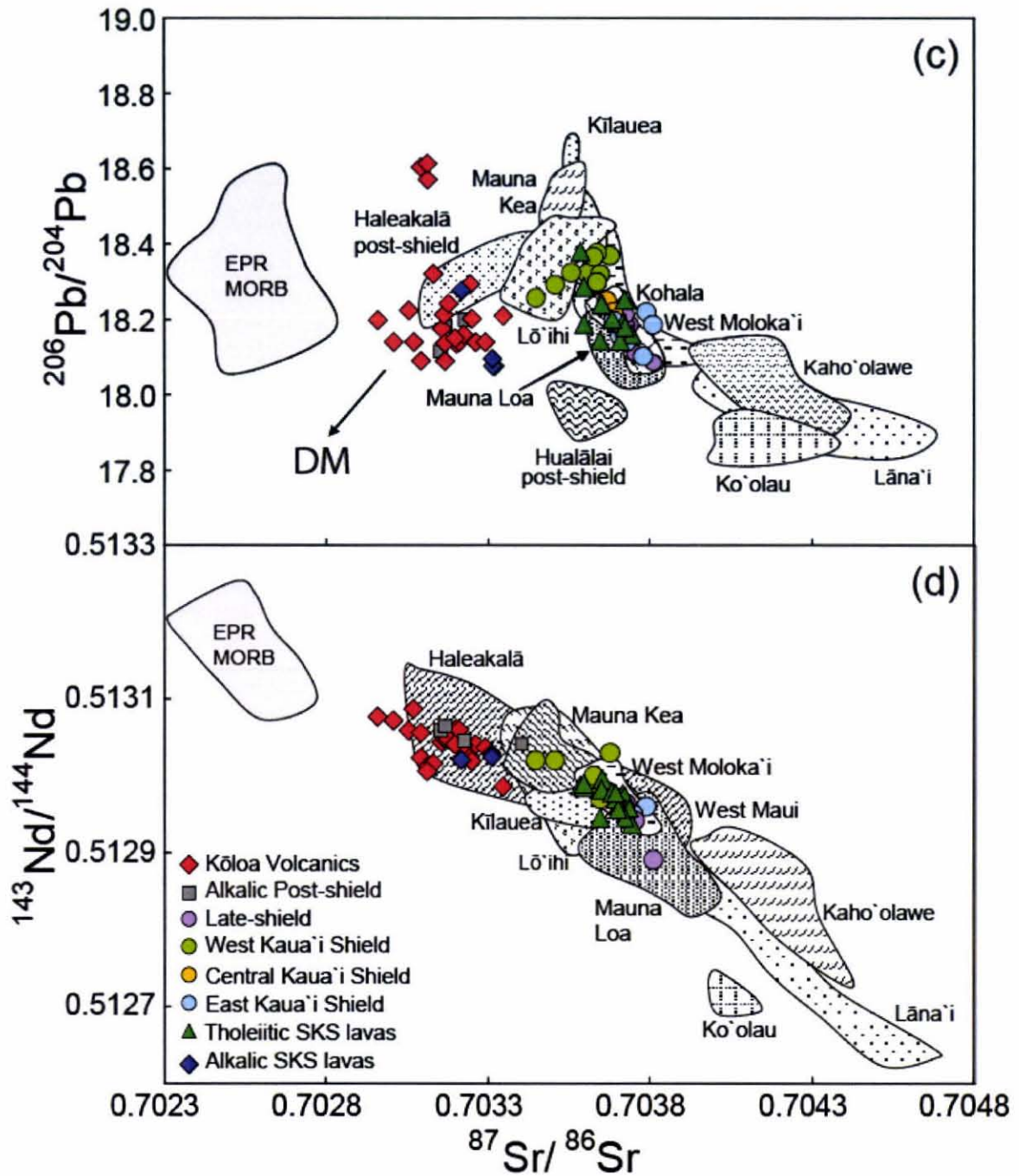


Fig. 18: Comparison of Pb, Hf, Sr and Nd isotopic ratios from the South Kaua'i Swell with other Hawaiian shield volcanoes. (a) $^{208}\text{Pb}/^{204}\text{Pb}$ vs. $^{206}\text{Pb}/^{204}\text{Pb}$. Pb isotopes show a spatial correlation, similar to the Kaua'i shield lavas. (b) ϵ_{Hf} vs. $^{206}\text{Pb}/^{204}\text{Pb}$. (c) $^{206}\text{Pb}/^{204}\text{Pb}$ vs. $^{87}\text{Sr}/^{86}\text{Sr}$. The SKS lavas show a tighter range in Sr ratios than the Kaua'i shield lavas. (d) ϵ_{Nd} vs. Sr. Several Hawaiian volcanoes overlap in Sr and Nd ratios. References for ERP MORB and Hawaiian volcanoes from Figure 6.

11.0 CONCLUSIONS

The origin of the enigmatic South Kaua'i Swell was addressed by combining geochemical, geochronological and geological results. Three models have been considered for its origin: a massive landslide deposit, extensive offshore secondary volcanism, and a submarine satellite shield. Geochemical results show that samples from 11 of 13 seamounts are tholeiitic, unlike any rejuvenated lava. Thus, the secondary volcanism model is improbable. The SKS samples are geochemically similar to Kaua'i shield lavas, although they extend to higher Zr/Nb (14 vs. 12) and $^{208}\text{Pb}^*/^{206}\text{Pb}^*$ (0.960 vs. 0.948), and lower ϵ_{Nd} (6.9 vs. 7.6) values, as do some adjacent Hawaiian shield volcanoes. These differences, the 3.9 Ma age for one tholeiitic SKS sample, and the absence of a scar on the flanks of Kaua'i suggest a landslide origin from the island of Kaua'i is unlikely for the SKS. The remaining separate submarine shield model is consistent with available geochemical and geological results (e.g., conical shape of seamounts). Thus, we conclude that a separate submarine shield is the most viable current model. Future work, including radiometric ages and refined gravity data, will be conducted by others to refine the mode of formation of the South Kaua'i Swell.

Appendix A. Sample locations and descriptions for South Kaua'i Swell volcanics for Dive 297

Sample #	Location	Rock Type	Lat (deg)	Long (deg)	Depth (m)	In Situ?	Size (x,y,z) (cm)	Weight (kgs)	glass (mm)	Mn coating (mm)	Alteration	Comments on sample location
J2-297-01*	Area A	tholeiitic basalt	29.0310	48.4970	3770	n	16,9,9	1.9	1 - 2	1 - 8	weak	small cliff section
J2-297-02	Area A	olivine basalt	29.3190	48.4700	3547	?	26,15,10	5.0	1 - 3	1 - 3	weak	small cliff section
J2-297-03	Area A	picrite	29.3420	48.4820	3504	?	16,13,10	2.5	0	<1 - 3	moderate	small cliff section
J2-297-04**	Cone B	tholeiitic basalt	31.4440	52.3380	3541	n	28,20,13	15.5	?	<1 - 2	-	indurated seds or volcanoclastic material
J2-297-05*	Cone B	tholeiitic basalt	31.4800	52.3420	3483	n	13,11,7	10.0	0	<1 - 2	weak	brecciated flow material
J2-297-06*	Cone B	tholeiitic basalt	31.5190	52.3450	3468	y	28,15,13	8.0	0	<1 - 5	weak	massively fractured flow field
J2-297-07**	Cone B	tholeiitic basalt	31.5760	52.3220	3467	?	9,8,7	0.7	0	<1	weak	from edge of brecciated ledge
J2-297-08	Cone B	basalt	31.5810	52.2910	3478	?	7,4,6	0.5	0	2	weak	6-7 cm knobby bud
J2-297-09*	Cone B	tholeiitic basalt	31.5810	52.2830	3483	?	25,23,12	9.8	0	<1 - 2	weak	slabby sample from eastern edge of summit
J2-297-10*	Cone B	tholeiitic basalt	31.5730	52.3030	3471	?	16,12,7.5	1.0	0	<1	weak	10 cm angular clast taken from top of hil
J2-297-11**	Cone C	tholeiitic basalt	21.5630	52.7960	3608	n	17,13,14	3.7	0	<2	weak	rubble layer of cobbles at base of slope
J2-297-12	Cone C	sediment	21.5650	52.8390	3583	n	multiple pieces	0.2	n/a	2 - 4	-	from dense top layer above coarser rubble
J2-297-13	Cone C	sediment	21.6740	52.9620	3384	n	10,20,7	0.1	n/a	2 - 4	-	soft crumbly sediment layer at top of terrace
J2-297-14*	Cone C	tholeiitic basalt	21.7040	52.9640	3393	n	9,6,9	1.0	0	1 - 4	weak	piece of rubble
J2-297-15	Cone C	basalt	21.7590	53.0330	3348	?	5.5,5,12	0.4	0	1 - 4	weak	sediment from stratified outcrop
J2-297-16	Cone C	basalt	21.7480	53.0420	3344	?	15.5,12,12	2.3	0	1	weak	probable sediment from spires
J2-297-17*	Cone C	tholeiitic basalt	21.7110	53.0430	3326	?	14.5,13.5,13	3.6	0	<1	weak	brick shaped sediment from talus
J2-297-18**	Cone C	tholeiitic basalt	21.7040	56.0310	3333.5	?	21,9,5,20	8.4	0	<1	weak	talus/sediment
J2-297-19*	Cone D	alkalic basalt	24.0350	56.8140	3771	n	14,8,6	1.0	0	1	weak	loose rock frag, large near pillow lava
J2-297-20**	Cone D	alkalic basalt	24.0650	56.8130	3767	y	22,17,15	7.3	~1	<1 - 2	weak	in place pillow lava
J2-297-21*	Cone D	alkalic basalt	24.0790	56.8170	3701	y	14,6,8	1.5	1.5	1	weak	in place pillow lava
J2-297-22*	Cone D	alkalic basalt	24.2090	56.8150	3650.7	y	10,8,5	1.5	1 - 2	2	moderate	in place pillow lava
J2-297-23**	Cone D	alkalic basalt	24.3160	56.8350	3613.6	y	7,7,5	1.0	5	1	moderate	in place pillow lava
J2-297-24*	Cone D	transitional basalt	24.3940	56.9450	3669	y	15,12.5,13.5	3.5	0	1	weak	in place pillow surrounded by fine sediment
J2-297-25*	Area E	tholeiitic basalt	23.8500	56.5180	3886.3	n	15,15,7	-	0	0	-	sediment outwash from cone 297E in pit
J2-297-26**	Area E	tholeiitic basalt	23.8520	56.5220	3885	n	6.5,6,7	1.0	2	1	weak	sediment outwash from cone 297E in pit
J2-297-27*	Area E	tholeiitic basalt	23.8520	56.5220	3885	n	-	-	-	-	-	sediment outwash from cone 297E in pit

Appendix A (Continued). Sample locations and descriptions for South Kaua'i Swell volcanics for Dive 298

Sample #	Location	Rock Type	Lat (deg)	Long (deg)	Depth (m)	In Situ?	Size (x,y,z) (cm)	Weight (kgs)	Mn coating (mm)	Alteration	Comments on sample location
J2-298-01	Cone A	mudstone	21.0652	159.3943	4163	?	9,24,6	1.9	8 - 11	-	elongate fragment from sheet-like surface
J2-298-02	Cone A	mudstone	21.1653	159.3923	4137	?	18,20,10	4.8	1 - 3.5	-	outcrop of ~ 0.5 m thick slabby unit
J2-298-03	Cone A	mudstone	21.0653	159.3921	4107	?	22,27,12	6	2 - 3	-	from 0.5 m thick slabby unit
J2-298-04	Cone A	mudstone	21.0674	159.3879	4019	?	23,42,10	6.2	1 - 11	-	from 0.5 m thick slabby unit
J2-298-05	Cone A	mudstone w/ basalt breccia	21.0688	159.3884	3940	?	17, 15, 9	2	0	weak	from 0.5 m thick slabby unit, top of hill
J2-298-06	Site B	volcanic sandstone	21.0814	159.3602	4090	?	20,12,6	1.6	<1	moderate	from lower slope of target B
J2-298-07**	Site B	tholeiitic basalt in breccia	21.0821	159.3605	3978	?	25,13,9	3	2 - 6	moderate	from upper portion of slope of target B
J2-298-08	Site B	mudstone	21.0827	159.3609	3982	?	25,50,17	14.8	2 - 15	-	indurated angular block from massive outcrop
J2-298-09	Cone C	mudstone	21.0835	159.3527	3980	yes	13,30,9	3.5	<1 - 10	-	from ledge of slabby rock outcrop
J2-298-10	Cone C	mudstone	21.0870	159.3487	3807	?	-	-	-	-	Sample Lost
J2-298-11	Cone C	silty mudstone	21.0869	159.3484	3797	no	22,35,10	5.3	<1 - 2	-	angular slabby block
J2-298-12*	Cone D	tholeiitic basalt	21.1117	159.3085	3944	?	11,12,10	2.2	1	moderate	collected from upper smooth unit
J2-298-13	Cone D	volcanic breccia	21.1140	159.3055	3771	no	10,6,4	0.2	3 - 12	moderate	small fragment, mostly Mn crust
J2-298-14	Cone D	mudstone/sandstone	21.1140	159.3055	3771	no	4.5,1.5,3	-	3	-	small fragment, mostly Mn crust
J2-298-15	Cone D	volcanic breccia	21.1134	159.3049	3742	no	25,20,11	5.5	3 - 13	moderate	large block from lower part of ledge
J2-298-16*	Cone D	tholeiitic basalt	21.1131	159.3039	3685	no	17,15,10	5.5	<<1	weak	from base of 0.5 m ledge
J2-298-17	Cone D	sandstone w/ breccia	21.1124	159.3020	3572	no	16,12,9	1.9	5	moderate	cemented but not in situ
J2-298-18	Cone D	conglomerate	21.1124	159.3020	3572	no	11,8,8.5	1.1	3	moderate	from base of 0.5 m ledge
J2-298-19*	Cone D	tholeiitic basalt	21.1174	159.3000	3710	no	?	2.2	<1 - 1	moderate	collected from talus breccia
J2-298-20**	Cone D	tholeiitic basalt	21.1185	159.2998	3778	no	11,10,7	1.4	0	weak	from coarse breccia outcrop

Appendix A (Continued). Sample locations and descriptions for South Kaua'i Swell volcanics for Dive 299

Sample #	Location	Rock Type	Lat (deg)	Long (deg)	Depth (m)	In Situ?	Size (x,y,z) (cm)	Weight (kgs)	Mn-coating (mm)	Alteration	Comments on sample location
J2-299-01	Site A	mudstone	21.3619	159.5495	3627	no	5,8,5	0.4	1 - 2	-	sedimentary deposit
J2-299-02	Site A	picritic basalt	21.3618	159.5480	3575	no	19,12,9	2.4	<1 - 3	moderate	talus pile
J2-299-03	Site A	basalt breccia	21.3618	159.5480	3537	no	7,6,5	0.2	<1 - 2	moderate	heavily Mn encrusted sample
J2-299-04**	Site A	tholeiitic basalt	21.3618	159.5480	3500	no	16,16,13	5.1	<1	weak	debris/talus from underlying talus
J2-299-05*	Site A	tholeiitic basalt	21.3620	159.5458	3463	no	28,23,14	8.1	<1 - 5	strong	talus pile
J2-299-06	Site A	pebbly mudstone	21.3620	159.5453	3431	no	11,26,9	2.6	6	-	talus above brecciated surface
J2-299-07	Site A	basalt breccia	21.3620	159.5448	3381	no	10,7,6	0.4	1 - 3	strong	brecciated surface - clasts well lithified
J2-299-08	Site A	basalt breccia	21.3620	159.5443	3336	no	33,18,17	12.4	<1 - 4	weak	talus pile surrounded by fine-sed
J2-299-09	Site A	basalt breccia	21.3620	159.5436	3269	no	8,6,6	0.4	<1	moderate	well cemented breccia
J2-299-10	Site A	pebbly sandstone	21.3616	159.5363	3331	no	14,20,9	2.6	5	-	base of brecciated/clastic cliff
J2-299-11	Site A	basalt breccia	21.3618	159.5358	3322	no	26,13,9	2.2	<10	-	mottled edge of pavement surface
J2-299-12*	Site A	tholeiitic basalt breccia	21.3621	159.5346	3291	no	18,13,12	3.5	<1 - 5	moderate	knobbly Mn encrusted outcrop
J2-299-13	Site A	basalt breccia	21.3624	159.5326	3214	no	7,9,13.5	1.1	3 - 11	moderate	cobbled/clastic horizon - same
J2-299-14*	Site A	tholeiitic basalt breccia	21.3626	159.5326	3204	no	21,17,11	7.0	13	moderate	cobbled/clastic horizon - same
J2-299-15	Site A	basalt breccia	21.3627	159.5327	3200	no	21,17,13	9.5	11		cobbled/clastic horizon - same
J2-299-16	Site A	basalt breccia	21.3627	159.5326	3199	no	10,15,8	1.0	<1 - 6	moderate	cobbled/clastic horizon - same
J2-299-17	Site A	pebbly mudstone	21.3629	159.5324	3199	no	9,18,7	1.5	10	-	cobbled/clastic horizon - same
J2-299-18	Site A	breccia	21.3631	159.5306	3174	no	10,9,6	0.6	2 - 6	weak	cobbled/clastic horizon - same

Appendix A (Continued). Sample locations and descriptions for South Kaua'i Swell volcanics for Dive 299

Sample #	Location	Rock Type	Lat (deg)	Long (deg)	Depth (m)	In Situ?	Size (x,y,z) (cm)	Weight (kgs)	Mn coating (mm)	Alteration	Comments on sample location
J2-299-19	Site B	pebbly sandstone	21.3869	159.5228	3162	yes	8,6,10	1.7	~8	-	debris flow/rubble outcrop
J2-299-20**	Site B	tholeiitic basalt	21.3869	159.5228	3163	no	16,13,10	5.5	1 - 5	moderate	at foot of debris flow
J2-299-21*	Site B	tholeiitic basalt	21.3870	159.5226	3147	no	12,8.5,7.5	1.5	<1	moderate	debris flow outcrop
J2-299-22	Site B	muddy sandstone	21.3870	159.5226	3147	no	soft rubble	1.2	1 - 2	-	-
J2-299-23**	Site B	tholeiitic basalt	21.3873	159.5224	3127	no	16,12,11	3.4	2 - 5	moderate	-
J2-299-24	Site B	basalt	21.3926	159.5175	3238	no	25,14,14	4.5	11	moderate	from cobbles
J2-299-25	Site B	basalt	21.3935	159.5181	3188	no	13,10,6	-	5	moderate	from base of of cobbly ledge
J2-299-26	Site C	basalt	21.4098	159.5090	3109	no	26,16,8	3.0	12	moderate	cobbled deposit under smooth sed layer
J2-299-27*	Site C	tholeiitic basalt	21.4106	159.5089	3085	no	8,9,5	0.6	5	weak	clastic fractured deposit - same as 26
J2-299-28*	Site C	tholeiitic basalt	21.4121	159.5081	3034	no	18,17,18	7.2	3 - 9	moderate	same as above
J2-299-29**	Site C	tholeiitic basalt	21.4124	159.5078	3006	no	35,18,16	24	11	weak	same as above
J2-299-30	Site C	breccia	21.4130	159.5075	3000	no	25,17,9	-	1	weak	same as above
J2-299-31	Site C	pebbly sandstone	21.4141	159.5075	2979	no	20,19,9	4.5	3 - 4	-	same as above - now at top of hill
J2-299-32	Site D	mudstone	21.4355	159.5218	3326	no	18,23,13	5.2	1 - 2	-	sitting on top of very large slab
J2-299-33**	Site D	tholeiitic basalt	21.4358	159.5151	3041	no	10.5,7,8	0.8	1 - 6	strong	talus blocks
J2-299-34	Site D	mudstone	21.4360	159.5143	2989	no	13,22,12	3.5	8 - 11	-	coarse breccia with draping sed
J2-299-35	Site D	basalt w/ mudstone	21.4424	159.5107	3027	no	9,9.5,12	0.9	1.5 - 5	moderate	talus blocks and mud
J2-299-36	Site D	lost	21.4429	159.5107	2999	no	-	-	-	-	big talus pile forming hillside
J2-299-37*	Site D	tholeiitic basalt	21.4434	159.5108	2969	no	7.5,8.5,13	1.4	1 - 4	moderate	draping talus
J2-299-38	Site D	pebble conglomerate	21.4434	159.5108	2969	no	17,33,9	5.6	9	-	draping talus

Appendix A (Continued). Sample locations and descriptions for South Kaua'i Swell volcanics for Dive 252 and dredges

Sample #	Location	Rock Type	Lat (deg)	Long (deg)	Depth (m)	In Situ?	Size (x,y,z) (cm)	Weight (kgs)	glass (mm)	Mn coating (mm)	Alteration
J2-252-01	Cone A	basalt	21.3454	159.3680	3383	no	30,21,11	6.0	0	<0.5 - 14	moderate
J2-252-02	Cone A	basalt	21.3445	159.36879	3242	no	16,10,11	1.3	0	<0.5 - 7	weak
J2-252-03	Cone A	sediment	21.3429	159.37032	3232.5	no	17.5,26,8	2.4	n/a	1 - 3	-
J2-252-04**	Cone A	tholeiitic basalt	21.3418	159.3717	3132	no	16,14,11.5	4.8	<1	<1 - 2.5	weak
J2-252-05*	Cone A	tholeiitic basalt	21.3415	159.3720	3095	no	26,18,11	5.4	0	2 - 4	weak
J2-252-06	Cone A	sediment	21.3401	159.3730	3048	no	14,13,8	0.5	n/a	<1 - 3	weak
J2-252-07*	Cone A	tholeiitic basalt	21.3388	159.3742	2993	no	18,14.2,10.5	2.7	0	1 - 6	moderate
J2-252-08	Cone B	basaltic breccia	21.3378	159.3938	3335	no	9,10,7.5	0.7	0	1 - 3	strong
J2-252-09*	Cone B	tholeiitic basalt	21.3378	159.3942	3292	no	14.5,15,13	2.2	0	0 - 1	weak
J2-252-10**	Cone B	tholeiitic basalt	21.3380	159.3951	3264	no	20,18,16	3.9	0	1 - 10	weak
J2-252-11	Cone B	basaltic breccia	21.3380	159.3955	3193	no	12,9.5,5	0.3	0	1 - 6.5	moderate
KS1-10*	Site A	tholeiitic basalt			?	no	20,14,9	?	0	1	weak
KS1-13**	Site A	tholeiitic basalt	21.4417	159.5167	?	no	35,19,14	?	0	<1	weak
KS1-19*	Site A	tholeiitic basalt			?	no	25,22,19	?	0	2 - 5	moderate
KS-2**	Site B	alkalic basalt	21.5650	159.6667	?	no	?	?	?	?	weak
KS3-1*	Site C	tholeiitic basalt			?	no	35,24,26	?	0	3 - 7	weak
KS3-3**	Site C	tholeiitic basalt	21.4167	159.3833	?	no	12,7,5	?	0	0 - 1	weak

* Rock type name from TAS diagram for samples analyzed by XRF

** Samples analyzed for XRF major and trace elements, ICP-MS trace elements and Pb, Sr, Nd and Hf isotopes

Appendix A (Continued). Vesicularity and Mineralogy of the South Kaua'i Swell volcanics for Dive 297

Sample #	% Vesicles	Vesicle size (mm)	Vesicle Comments	% Olivine	Ol Size (mm)	% Plag	Plag Size (mm)	% Others	Other Comments
J2-297-01	< 1	1 - 2	round	5 - 10	1 - 4	0	-	0	glassy matrix
J2-297-02	1 - 5	<1	< 1mm	8 - 12	1 - 4	0	-	0	glassy matrix
J2-297-03	1 - 5	1 - 2	variable	10 - 15	1 - 3	1 - 2	1	0	-
J2-297-04	10 - 15	<1 - 5	irregular	4 - 6	<1 - 3	1 - 3	< 1	0	mudstone adhering to one side of lava
J2-297-05	20 - 30	1 - 2	-	1 - 3	1 - 2	0	-	0	-
J2-297-06	30 - 40	<1 - 2	round	5 - 10	1 - 3	?	-	0	2 pieces
J2-297-07	30 - 40	<1 - 2	round	~10	<1 - 2	?	-	0	-
J2-297-08	20	1 - 2	irregular	4	2	?	1	0	Cr-spinel inclusions in Ol; scoreaceous
J2-297-09	15 - 25	1 - 20	irregular	10 - 15	1 - 5	0	-	0	elongated vesicles
J2-297-10	~ 30	<1 - 3	round	0	0	0	-	0	vesicles empty w/ brownish thin coating
J2-297-11	~ 25	<2	round	~1	1	0	-	0	top 1/4 of vesicles filled with sediment
J2-297-12	n/a	n/a	n/a	n/a	n/a	n/a	n/a	n/a	distinct Mn coated borings 6 cm x 57mm
J2-297-13	n/a	n/a	n/a	n/a	n/a	n/a	n/a	n/a	extensive borings
J2-297-14	< 5	-	-	5 - 10	<2.5	< 5	< 1	0	-
J2-297-15	< 1	-	-	<1	<<1	0	-	0	nearl aphyric, highly altered Ol
J2-297-16	15 - 20	-	irregular	<5	1	0	-	<1% spinel	some vesicles filled with mud
J2-297-17	40 - 50	0.5 - 1.5	round	10 - 15	<3	5	< 1.5	0	-
J2-297-18	30 - 40	<6	irregular	<5	<1	0	-	0	-
J2-297-19	5	1 - 2	round	3	1 - 2	5	~ 1	0	-
J2-297-20	< 5	<1 - 2	round	3 - 5	1 - 3	1 - 2	< 1	<1% cpx	-
J2-297-21	2	<2	-	4	1 - 2	4	1	0	coarser/more abundant vesicles at edge
J2-297-22	< 5	<1 - 2	round	<1	1	0	-	0	broken into numerous small pieces
J2-297-23	< 5	0.5 - 1.5	round	7 - 10	<1 - 2	5	< 1	0	palagonite interspersed in fresh glass
J2-297-24	<2	1	irregular	5 - 7	1 - 3	0	-	0	some vesicles have thin greenish coating
J2-297-25	0	-	-	0	-	0	-	0	lava and sediment
J2-297-26	2	1 - 2	irregular	5	5	10	1 - 2	0	rock coated w/ 2 mm of sediment under Mn
J2-297-27	-	-	-	-	-	-	-	-	lava and sediment

Appendix A (Continued). Vesicularity and Mineralogy of the South Kaua'i Swell volcanics for Dive 298

Sample #	% Vesicles	Vesicle size (mm)	Vesicle Comments	% Olivine	OI Size (mm)	% Plag	Plag Size (mm)	% Others	Other Comments
J2-298-01	n/a	n/a	n/a	n/a	n/a	n/a	n/a	n/a	very sandy mudstone to very muddy sandstone
J2-298-02	n/a	n/a	n/a	n/a	n/a	n/a	n/a	n/a	bioturbated sandy (vf-f grained) mudstone
J2-298-03	n/a	n/a	n/a	n/a	n/a	n/a	n/a	n/a	massive appearing, moderately indurated
J2-298-04	n/a	n/a	n/a	n/a	n/a	n/a	n/a	n/a	well indurated, v. coarse clastic unit below Mn coat
J2-298-05	5 - 10	<1 - 1	round	?	-	0	-	0	clast are of same lithology, friable basalt
J2-298-06	n/a	n/a	n/a	n/a	n/a	n/a	n/a	n/a	reddish olivine, clayey matrix, massive, dense
J2-298-07	0 - 30	<1 - 2	round	variable	-	0	-	0	reddish Ol rims, diverse clasts of lava(?), matrix supported
J2-298-08	n/a	n/a	n/a	n/a	n/a	n/a	n/a	n/a	complex; multigenerational mudstone w/ Mn-coated surface truncating burrow:
J2-298-09	n/a	n/a	n/a	n/a	n/a	n/a	n/a	n/a	complex; multigenerational mudstone w/ Mn-coated surface truncating burrow:
J2-298-10	n/a	n/a	n/a	n/a	n/a	n/a	n/a	n/a	NO SAMPLE
J2-298-11	n/a	n/a	n/a	n/a	n/a	n/a	n/a	n/a	bioturbated to burrowed, w/ possilbe slide grooves at base of slab
J2-298-12	<1	<1	round	<5	<1	0	-	0	Mn encrusted, oxidized ol
J2-298-13	<5 - 30	?	variable	0	-	0	-	0	mottled matrix, subrounded to subangular clasts of similar lithology
J2-298-14	n/a	n/a	n/a	n/a	n/a	n/a	n/a	n/a	mixed mudstone/sandstone, small areas of Fe-oxide
J2-298-15	<5-15	<1	round	?	-	0	-	0	mottled colour
J2-298-16	<1	<1		7	1-3	0	-	0	olivines altered, few fractures
J2-298-17	n/a	n/a	n/a	n/a	n/a	n/a	n/a	n/a	clasts surrounded w/ sandy matrix
J2-298-18	<5	<1	round	<2	1	0	-	0	vesicles filled, basalt clasts in sed rock
J2-298-19	<5	<1 - 1	round	>15	?	0	-	0	outer 3 cm strongly weathered
J2-298-20	<5	<1	round	5 - 10	<1 - 2	0	-	0	brownish green olivine, holocrystalline matrix

Appendix A (Continued). Vesicularity and Mineralogy of the South Kaua'i Swell volcanics for Dive 299

Sample #	% Vesicles	Vesicle size (mm)	Vesicle comments	% Olivine	Ol size (mm)	% Plag	Plag size (mm)	% Others	Other Comments
J2-299-01	n/a	n/a	n/a	n/a	n/a	n/a	n/a	n/a	bioturbated, brecciated, Mn lined 2-3 cm borings
J2-299-02	<1	<1	round	15 - 20	1 - 7	<1	1	< 1% cpx	reddish brown in holocrystalline matrix
J2-299-03	10 - 15	1 - 2	round	5 - 8	1 - 3	?	-	0	pervasive Mn, broken fragments with Mn coating
J2-299-04	15 - 25	?	irregular, elongate	5 - 10	<1	<1	<1	0	olivines tiny but seem green, matrix holocrystalline
J2-299-05	20 - 30	<1 - 2	round	4 - 6	1 - 2	1	1	0	conglomerate with basaltic clasts, altered Ol
J2-299-06	n/a	n/a	n/a	n/a	n/a	n/a	n/a	n/a	brecciated, bioturbated mudstone with pebble sized clasts
J2-299-07	20 - 30		irregular	0	-	3 - 5	<1 - 3	< 1% cpx	extensive zeolite in vesicles
J2-299-08	10 - 15	1 - 4	irregular, variable	2 - 4	1 - 2	?	-	0	clasts mostly unaltered, monoclasic clast lithology
J2-299-09	30 - 40	<1 - 3	round, irregular	1 - 3	1	0	-	0	reddish matrix, olivine green
J2-299-10	n/a	n/a	n/a	n/a	n/a	n/a	n/a	n/a	poorly sorted, pebbly, indurated
J2-299-11	0	-	-	0	-	0	-	0	-
J2-299-12	<1	<<1	round	5 - 10	<1 - 1	0	-	0	brecciated clasts of monolithic basalt
J2-299-13	5 - 10	<3	round	0	-	0	-	0	brecciated clasts of monolithic basalt
J2-299-14	20	1 - 13	irregular	0	-	0	-	0	oxidized with weathered material in vesicles
J2-299-15	0	-	-	0	-	0	-	0	breccia clasts (aphyric basalt, vesicular olivine basalt)
J2-299-16	65	1 - 3	round, irregular	0	-	0	-	0	layer of coating mudstone with adjoining breccia
J2-299-17	n/a	n/a	n/a	n/a	n/a	n/a	n/a	n/a	< 2 cm rounded basalt pebbles
J2-299-18	<5	<<1	round	0	-	0	-	0	4 pieces

Appendix A (Continued). Vesicularity and Mineralogy of the South Kaua'i Swell volcanics for Dive 299

Sample #	% Vesicles	Vesicle size (mm)	Vesicle comments	% Olivine	Ol size (mm)	% Plag	Plag size (mm)	% Others	Other Comments
J2-299-19	n/a	n/a	n/a	n/a	n/a	n/a	n/a	n/a	poorly sorted, relatively soft rock
J2-299-20	<2	3 - 5	irregular	5	1 - 2	2	<1.5	5% cpx	cpx crystals surrounding plag crystals
J2-299-21	<1	-	-	~10	<4	0	-	5% cpx	diabase texture
J2-299-22	n/a	n/a	n/a	n/a	n/a	n/a	n/a	n/a	poorly indurated (soft), pebbles up to 1cm
J2-299-23	5	<1 - 5	round	5 - 7	1 - 3	0	-	0	holocrystalline matrix
J2-299-24	1	-	-	2	1	0	-	0	~2% coarse grained ultramafic (harzburgite) xenoliths
J2-299-25	2	1	irregular	2	1	0	-	0	limonite-coated fractures
J2-299-26	2	1	round	3	2	1	1	0	outside could be clastic but mostly basalt frags
J2-299-27	10 - 12	1 - 10	round, irregular	0	-	0	-	0	-
J2-299-28	40 - 50	<2	round	0	-	0	-	0	2 aphyric basalt clasts held together in Mn coating
J2-299-29	0	-	-	0	-	0	-	0	fractured basalt clasts in tan mud matrix
J2-299-30	0	-	-	0	-	0	-	0	vesicular basalts clasts to 5.5cm in matrix of brown mud
J2-299-31	n/a	n/a	n/a	n/a	n/a	n/a	n/a	n/a	v. poor sorting, vague stratification; brittly deformed?
J2-299-32	n/a	n/a	n/a	n/a	n/a	n/a	n/a	n/a	bioturbated mudstone, Mn coating borings, 2-3mm
J2-299-33	<1	-	-	5	<3	<5	<4	0	v. weathered minerals, pervasive fractures
J2-299-34	n/a	n/a	n/a	n/a	n/a	n/a	n/a	n/a	prominent fractures from lithification & brittle deformation
J2-299-35	40 - 50	1	-	<1	-	<1	-	0	vesicles filled with mud, half rock is sedimentary
J2-299-36	n/a	n/a	n/a	n/a	n/a	n/a	n/a	n/a	-
J2-299-37	50	1 - 3	round	5	1	0	-	0	ol weathered to rustic colour, vesicles filled with sand
J2-299-38	0	-	-	0	-	0	-	0	mainly basaltic clasts up to 5cm, poorly sorted

Appendix A (Continued). Vesicularity and Mineralogy of the South Kaua'i Swell volcanics for Dive 252 and dredges

Sample #	% Vesicles	Vesicle size (mm)	Vesicle Comments	% Olivine	Ol Size (mm)	% Plag	Plag Size (mm)	% Others	Other Comments
J2-252-01	10	1 - 6	round	<1	1 - 2	0	-	<1% pyx	many vesicles filled with red/brown alteration/mud
J2-252-02	30	1 - 5	round, elongate	5	<1 - 4	0	-	0	core is highly vesicular
J2-252-03	n/a	n/a	n/a	n/a	n/a	n/a	n/a	n/a	mud w/small basalt clasts
J2-252-04	<1	<<1	round	<<1	<1	0	-	0	Ol only in hyaloclastite edge
J2-252-05	30	1 - 7	round, elongate	20	1 - 5	0	-	0	abundance of vesicles change in bands across sample
J2-252-06	n/a	n/a	n/a	n/a	n/a	n/a	n/a	n/a	mud w/small basalt clasts
J2-252-07	1	<1 - 5	round	1	<1 - 2	0	-	0	clastic rock? Basalt w/ mud matrix
J2-252-08	0	-	-	1 - 5	1 - 2	0	-	0	highly fractured and deeply weathered
J2-252-09	30	<1 - 5	round	3	<1	0	-	0	vesicles filled with clay and basalt clasts
J2-252-10	25	1 - 7	irregular	~5	<1	0	-	0	vesicles partly filled with clay on one end
J2-252-11	0	-	-	0	-	0	-	0	basalt clasts (~2-5mm)
KS1-10 ^D	?	?	?	~ 5 - 10	?	?	?	?	fractured, mud in fractures
KS1-13 ^D	<1	<<1	-	15	<2	0	-	<5% cpx	minor alteration only at the edge
KS1-19 ^D	?	?	?	?	?	?	?	?	altered surface, fresh interior
KS-2 ^D	?	?	?	?	?	?	?	?	-
KS3-1 ^D	<1	<<1	-	0	-	0	-	0	very dense and aphyric, fractured
KS3-3 ^D	0	-	-	0	-	0	-	0	very dense and aphyric

^D Collected using a dredge as opposed to the JASON2 ROV

? Data unavailable

APPENDIX B LEACHING INFORMATION

Part I. Leaching data for the subaerial rejuvenated, post-shield and late-shield stages of Kaua`i and standard

Sample Name:	Sample Weight (g)	Weight of dried leached sample (g)	Number of leaching steps	Percentage Loss (%)
<i>Koloa Volcanics</i>				
KR-11	0.1597	0.0175	8	89.0
0301-1	0.1952	0.1011	8	48.2
KV05-8	0.3043	0.1492	10	51.0
PV-2	0.3037	0.1273	9	58.1
KV01-3	0.2803	0.1146	13	59.1
KR-2 (Pb)	0.2981	0.0854	18	71.4
KR-2 (Sr, Nd)	0.2937	0.0907	14	69.1
KR-5	0.2859	0.0536	11	81.3
KR-5 (2)	0.2136	0.0409	12	80.9
KV03-17	0.2020	0.0602	14	70.2
KV04-4	0.1870	0.0675	8	63.9
KV03-21	0.1531	0.0387	10	74.7
KV04-1	0.3148	0.1263	10	59.9
KV03-15	0.2546	0.0417	9	83.6
KV05-1	0.3177	0.1113	10	65.0
KV05-2	0.1476	0.0659	7	55.4
KV03-11	0.1101	0.0321	8	70.8
KV03-11 (dup)	0.1378	0.0508	7	63.1
<i>Post-Shield Kaua`i Volcanics</i>				
KV05-10	0.4157	0.0674	11	83.8
GA650	0.2732	0.2039	12	25.4
GA566	0.1672	0.0315	14	81.2
KV03-5	0.2625	0.0487	10	81.4
KV05-13	0.1569	0.0429	9	72.7
GA565	0.2761	0.2106	12	23.7
<i>Late-Shield Kaua`i Volcanics</i>				
KV04-22	0.4048	0.1448	11	64.2
KV04-16	0.4426	0.1097	12	75.2
KV04-16 (dup)	0.4205	0.0953	12	77.3
KV04-19	0.4123	0.1130	9	72.6
KV04-21	0.4255	0.1633	10	61.6
<i>Standard</i>				
BHVO-2	0.2932	0.2218	10	24.4

Part II. Leaching data for the South Kaua'i Swell volcanics and standard

Sample Name:	Sample Weight (g)	Weight of dried leached sample (g)	Number of leaching steps	Percentage Loss (%)
J2-297-04	0.3792	0.0870	11	77.1
J2-297-07	0.3846	0.1454	15	62.2
J2-297-11	0.3789	0.0951	16	74.9
J2-297-18	0.3943	0.1432	15	63.7
J2-297-20	0.3941	0.0804	13	79.6
J2-297-23	0.4065	0.0840	11	79.3
J2-297-23 (dup)	0.3926	0.0392	9	90.0
J2-297-26	0.4084	0.1282	11	68.6
J2-298-07	0.4053	0.0347	9	91.4
J2-298-20	0.4023	0.1081	12	73.1
J2-299-04	0.3868	0.0348	7	91.0
J2-299-20	0.3965	0.0501	10	87.4
J2-299-23	0.4010	0.0758	13	81.1
J2-299-29	0.3929	0.1385	8	64.7
J2-299-33	0.4009	0.0734	13	81.7
KS1-13	0.4027	0.1926	13	52.2
KS1-13 (dup)	0.4457	0.2038	14	54.3
KS-2	0.2614	0.146	14	44.1
KS3-3	0.2587	0.1904	12	26.4
J2-252-04	0.2816	0.0984	9	65.1
J2-252-10	0.2522	0.0893	10	64.6
<i>Standard</i>				
Kilauea '93	0.3994	0.2733	8	31.6

APPENDIX C
POINT COUNTING PETROGRAPHY FOR DIVE 252 VOLCANICS

*Appendix C. Modes in volume % for Dive 252 South Kaua`i Swell volcanics
based on 500 counts/sample calculated vesicle-free*

Sample	Rock type	Olivine	Plagioclase	Matrix	Vesicles (%)
J2-252-02	Olivine basalt	9.0	0.8	90.2	28.6
J2-252-04	Basalt	1.4	1.6	97.0	0.8
J2-252-05	Picritic basalt	19.2	3.8	77.0	20.8
J2-252-10	Olivine basalt	5.4	0.3	94.3	26
J2-252-11	Plag-oliv basalt	4.5	2.7	92.8	2.4

REFERENCES

- Abouchami, W., Galer, S.J.G., Hofmann, A.W., 2000. High precision lead isotope systematics of lavas from the Hawaiian Scientific Drilling Project. *Chem. Geol.* 169, 187–209.
- Abouchami, W., Hofmann, A.W., Galer, S.J.G., Frey, F.A., Eisele, J., Feigenson, M., 2005. Lead isotopes reveal bilateral asymmetry and vertical continuity in the Hawaiian mantle plume. *Nature* 3402, doi:10.1038.
- Bianco, T.A., Ito, G., Becker, J.M., Garcia, M.O., 2005. Secondary Hawaiian volcanism formed by flexural arch decompression. *Geochem. Geophys. Geosyst.* 6, doi:10.1029/2005GC000945.
- Blichert-Toft, J., Frey, F.A., Albarède, F., 1999. Hf isotope evidence for pelagic sediments in the source of Hawaiian basalts. *Science* 285, 879–882.
- Blichert-Toft, J., Weis, D., Maerschalk, C., Agraniér, A., Albarède, F., 2003. Hawaiian hot spot dynamics as inferred from the Hf and Pb isotope evolution of Mauna Kea volcano. *Geochem. Geophys. Geosyst.* 4, doi:10.1029/2002GC00340.
- Bogue, S.W., Coe, R.S., 1984. Transitional paleointensities from Kauai, Hawaii, and geomagnetic reversal models. *J. Geophys. Res.* 89, 10,341–10,354.
- Bryce, J.G., DePaolo, D.J., Lassiter, J.C., 2005. Geochemical structure of the Hawaiian plume: Sr, Nd and Os isotopes in the 2.8 km HSDP-2 section of Mauna Kea volcano. *Geochem. Geophys. Geosyst.*, 6, doi:10.1029/2004GC000809.
- Castillo, P., Klein, E., Bender, J., Langmuir, C., Shirley, S., Batiza, R., White, W., 2000. Petrology and Sr, Nd, and Pb isotope geochemistry of mid-ocean ridge basalt glasses from the 11°45'N to 15°00'N segment of the East Pacific Rise. *Geochem. Geophys. Geosyst.*, 1, doi:10.1029/1999GC000024.
- Chen, C.-Y., Frey, F.A., Garcia, M.O., Dalrymple, G.B., Hart, S.R., 1991. The tholeiite to alkalic basalt transition at Haleakala Volcano, Maui, Hawaii. *Contrib. Mineral. Petrol.* 106, 183–200.
- Chen C.-Y., Frey F.A., Rhodes J.M., Easton R.M., 1996. Temporal geochemical evolution of Kilauea volcano: comparison of Hilina and Puna basalt, *Earth Processes, Reading to isotopic code.* (Basu, A; Hart, S.R.) AGU, Washington DC, 161–181.
- Clague, D.A., Cousens, B.L., Davis, A.S., Dixon, J.E., Hon, K., Moore, J.G., Reynolds, J.R., 2003. Submarine rejuvenated-stage lavas offshore Molokai, Oahu, Kauai, and Niihau, Hawaii. *Eos, Trans., AGU* 84, Suppl., Abstract V11B-01.
- Clague, D.A., Dalrymple, G.B., 1988. Age and petrology of alkalic postshield and rejuvenated-stage lava from Kaua'i, Hawaii. *Contrib. Mineral. Petrol.* 99, 202–218.
- Clague, D.A., Frey, F.A., 1982. Petrology and trace element geochemistry of the Honolulu Volcanics, Oahu; implications for the oceanic mantle below Hawaii. *J. Petrol.* 23, 447–504.
- Clague, D.A., Holcomb, R.T., Sinton, J.M., Detrick, R.S., Torresan, M.E., 1990. Pliocene and Pleistocene alkalic flood basalts on the seafloor north of the Hawaiian Islands. *Earth Planet. Sci. Lett.* 98, 175–191.
- Clague, D.A., Holcomb, R. T., Torresan, M. E., Ross, S. L., 1989. Shipboard report for Hawaii GLORIA ground-truth cruise F11-88-HW, 25 Oct. - 7 Nov., 1988. Open-File Report - USGS Report: OF 89-0109, 33 pp.

- Connelly, J.N., Ulfbeck D.G., Thrane K., Bizzarro M., Housh, T., 2006. A method for purifying Lu and Hf for analyses by MC-ICP-MS using TODGA resin. *Chem. Geol.* 233, 126-136.
- Coombs, M.L., Clague, D.A., Moore, G.F., Cousens, B.L., 2004. Growth and collapse of Waianae Volcano, Hawaii, as revealed by exploration of its submarine flanks. *Geochem. Geophys. Geosyst.* 5, doi:10.1029/2004GC000717.
- Duprat, H.I., Friis, J., Holm, P.M., Grandvoinet, T., Sorensen, R.V., 2007. The volcanic and geochemical development of Sao Nicolau, Cape Verde Islands; constraints from field and (super 40) Ar/ (super 39) Ar evidence. *J. Volcanol. Geotherm. Res.* 162, 1-19.
- du Vignaux, N. M., Fleitout L., 2001. Stretching and mixing of viscous blobs in Earth's mantle. *J. Geophys. Res.* 106, 30,893–30,908.
- Eisele, J., Abouchami, W., Galer, S.J.G., Hofmann, A.W., 2003. The 320 kyr Pb isotope evolution of Mauna Kea lavas recorded in the HSDP-2 drill core. *Geochem. Geophys. Geosyst.* 4, doi:10.1029/2002GC000339.
- Feigenson, M.D., 1984. Geochemistry of Kaua'i volcanics and a mixing model for the origin of Hawaiian alkalic basalts. *Contrib. Mineral. Petrol.* 87, 109–119.
- Fekiacova Z., Abouchami, W., Galer, S.J.G., Garcia, M.O., Hofmann, A.W., 2007. Temporal evolution of Ko'olau Volcano: inferences from isotope results on the Ko'olau Scientific Drilling Project (KSDP) and Honolulu Volcanics. *Earth Planet. Sci. Lett.* 261, 65–83.
- Frey, F.A., Clague, D.A., Mahoney, J.J., Sinton, J.M., 2000. Volcanism at the edge of the Hawaiian plume; petrogenesis of submarine alkalic lavas from the North Arch volcanic field. *J. Petrol.* 41, 667–691.
- Frey, F.A., Garcia, M.O., Wise, W.S., Kennedy, A., Gurriet, P., Albarede, F., 1991. The evolution of Mauna Kea Volcano, Hawaii; petrogenesis of tholeiitic and alkalic basalts. *J. Geophys. Res.* 96, 14,347–14, 375.
- Frey, F. A., Huang, S., Blichert-Toft, J., Regelous, M., Boyet, M., 2005. Origin of depleted components in basalt related to the Hawaiian hot spot: Evidence from isotopic and incompatible element ratios. *Geochem. Geophys. Geosyst.* 6, doi:10.1029/2004GC000757.
- Gaffney, A.M., Nelson, B.K., Blichert-Toft, J., 2004. Geochemical Constraints on the Role of Oceanic Lithosphere in Intra-Volcano Heterogeneity at West Maui, Hawaii. *J. Petrol.* 45, 1663–1687.
- Gaffney, A.M., Nelson, B.K., Blichert-Toft, J., 2005. Melting in the Hawaiian plume at 1–2 Ma as recorded at Maui Nui: the role of eclogite, peridotite, and source mixing. *Geochem. Geophys. Geosyst.* 6, doi:10.1029/2005GC000927.
- Gandy, C., 2006. Volume and petrological characteristics of the Kōloa Volcanics, Kaua'i, Hawai'i. University of Hawai'i, Unpublished M.S. thesis, 107 pp.
- Gandy, C.E., Garcia, M.O., Blay, C., Implications of the volume of Kaua'i's Kōloa Volcanics for the origin of Hawaiian rejuvenated volcanism. *Geology*, in review
- Garcia, M.O., Frey, F.A., Grooms, D.G., 1986. Petrology of volcanic rocks from Kaula Island, Hawaii; implications for the origin of Hawaiian phonolites. *Contrib. Mineral. Petrol.* 94, 461–471.

- Garcia, M.O., Grooms, D.G., Naughton, J.J., 1987. Petrology and geochronology of volcanic rocks from seamounts along and near the Hawaiian Ridge; implications for propagation rate of the ridge. *Lithos* 20, 323–336.
- Garcia, M.O., Ito, G., Weis, D., Geist, D., Swinnard, L., Bianco, T., Flinders, A., Appelgate, B., Taylor, B., Blay, C., Hanano, D., Nobre Silva, I., Naumann, T., Maerschalk, C., Harpp, K., Christensen, B., Sciaroni, L., Tagami, T., Yamasaki, S., Widespread secondary volcanism around the northern Hawaiian Islands. EOS, in review.
- Garcia, M.O., Pietruszka, A.J., Rhodes, J.M., Swanson, K., 2000. Magmatic processes during the prolonged Pu'u 'O'o eruption of Kilauea Volcano, Hawaii. *J. Petrol.* 41, 967–990.
- Gurriet, P., 1987. A thermal model for the origin of post-erosional alkalic lava, Hawaii. *Earth Planet. Sci. Lett.* 82, 153–158.
- Hanano, D., Weis, D., Aciego, S., Scoates, J.S., DePaolo, D.J., 2005. Geochemical Systematics of Hawaiian Post-shield Lavas: Implications for the Chemical Structure of the Hawaiian Mantle Plume. *Eos, Trans., AGU*, 86(52), Suppl., Abstract V41D-1497.
- Hanyu, T., Clague, D.A., Kaneoka, I., Dunai, T.J., Davies, G.R., 2005. Noble gas systematics of submarine alkalic lavas near the Hawaiian Hotspot. *Chem. Geol.* 214, 135–155.
- Haskins, E.H., Garcia, M.O., 2004. Scientific drilling reveals geochemical heterogeneity within the Ko'olau shield, Hawai'i. *Contrib. Mineral. Petrol.* 147, 162–188.
- Hauri, E.H., 1996. Major-element variability in the Hawaiian mantle plume, *Nature* 382, 415–419.
- Hauri, E.H., Whitehead, J.A., Hart, S.R., 1994. Fluid dynamic and geochemical aspects of entrainment in mantle plumes. *J. Geophys. Res.* 99, 24,275–24,300.
- Hoernle, K., Schmincke, H.-U., 1993. The petrology of the tholeiites through melilitite nephelinites on Gran Canaria, Canary Islands; crystal fractionation, accumulation, and depths of melting. *J. Petrol.* 34, 573–597.
- Holcomb, R.T., Reiners, P.W., Nelson, B.K., Sawyer, N.E., 1997. Evidence for two shield volcanoes exposed on the island of Kauai, Hawaii. *Geology* 25, 811–814.
- Huang, S., Frey, F.A., Blichert-Toft, J., Fodor, R.V., Bauer, G.R., Xu, G., 2005. Enriched components in the Hawaiian plume: evidence from Kahoolawe Volcano, Hawaii. *Geochem. Geophys. Geosyst.* 6, doi:10.1029/2005GC001012.
- Jackson, M.C., Frey, F.A., Garcia, M.O., Wilmoth, R.A., 1999. Geology and geochemistry of basaltic lava flows and dikes from the Trans-Koolau tunnel, Oahu, Hawaii. *Bull. Volcanol.* 60, 381–401.
- Jackson, E.D., Wright, T.L., 1970. Xenoliths in the Honolulu volcanic series, Hawaii. *J. Petrol.* 11, 405–430.
- Kennedy, A.K., Kwon, S.-T., Frey, F.A., West, H.B., 1991. The isotopic composition of postshield lavas from Mauna Kea volcano, Hawaii. *Earth Planet. Sci. Lett.* 103, 339–353.
- King, A.J., Waggoner, D.G., Garcia, M.O., 1993. Geochemistry and petrology of basalts from Leg 136, Central Pacific Ocean. In: Wilkens, R.H., Firth, J., Bender, J., et al. (Eds.), *Proc. ODP Sci. Res.* 136, 107–118.

- Kogiso, T., Hirschmann, M. M., Pertermann M., 2004. High-pressure partial melting of mafic lithologies in the mantle. *J. Petrol.* 45, 2407–2422.
- Kurz, M. D., Kenna, T. C., Kammer, D. P., Rhodes, J. M., Garcia, M. O., 1995. Isotopic evolution of Mauna Loa Volcano: A view from the submarine southwest rift zone, in *Mauna Loa Revealed*, AGU Monograph, 92, edited by J. M. Rhodes and J. P. Lockwood, 289–06.
- Lassiter, J.C., DePaolo, D.J., Tatsumoto, M., 1996. Isotopic evolution of Mauna Kea volcano: Results from the initial phase of the Hawaiian Scientific Drilling Project. *J. Geophys. Res.* B101, 11,769–11,780.
- Lassiter, J.C., Hauri, E.H., Reiners, P.W., Garcia, M.O., 2000. Generation of Hawaiian post-erosional lavas by melting of mixed lherzolite/pyroxenite source. *Earth Planet. Sci. Lett.* 178, 269–284.
- Leeman, W.P., Gerlach, D.C., Garcia, M.O., West, H.B., 1994. Geochemical variations in lavas from Kahoolawe Volcano, Hawaii; evidence for open system evolution of plume-derived magmas. *Contrib. Mineral. Petrol.* 116, 62–77.
- Li, X., Kind, R., Yuan, X., Wolbern, I., Hanka, W., 2004. Rejuvenation of the lithosphere by the Hawaiian plume. *Nature* 427, 827–829.
- Maaloe, S., James, D., Smedley, P., Petersen, S., Garmann, L.B., 1992. The Kōloa Volcanics Suite of Kauaʻi, Hawaii. *J. Petrol.* 33, 761–784.
- Maaloe, S., Tumyr, O., James, D., 1989. Population density and zoning of olivine phenocrysts in tholeiites from Kauai, Hawaii. *Contrib. Mineral. Petrol.* 101, 176–186.
- Macdonald, G.A., Davis, D.A., Cox, D.C., 1960. Geology and groundwater resources of the island of Kauaʻi, Hawaii. *Bulletin 13*, Hawaii Division of Hydrography.
- Macdonald, G.A., Katsura, T., 1964. Chemical Composition of Hawaiian Lavas. *J. Petrol.* 5, 82–133.
- Macdonald, G. A., 1968. Composition and origin of Hawaiian lavas. *Mem. Geol. Soc. Am.* 116, 477–522.
- Macdonald, G.A., Abbott, A.T., Peterson, F.L., 1983. *Volcanoes in the Sea: The Geology of Hawaii*. University of Hawaii Press, 528 pp.
- Marske, J.P., Pietruszka, A.J., Weis, D., Garcia, M.O., Rhodes, J.M., 2007. Rapid passage of a small-scale mantle heterogeneity through the melting regions of Kilauea and Mauna Loa volcanoes. *Earth Planet. Sci. Lett.* 259, 34–50.
- McDonough, W.F., Sun, S.-s., 1995. The composition of the Earth. *Chem. Geol.* 120, 223–253.
- McDougall, I., 1964. Potassium-Argon Ages from Lavas of the Hawaiian Islands. *GSA Bull.* 75, 107–128.
- McDougall, I., 1979. Age of shield-building volcanism of Kauaʻi and linear migration of volcanism in the Hawaiian island chain. *Earth Planet. Sci. Lett.* 46, 31–42.
- Moore, J.G., Normark, W.R., Holcomb, R.T., 1994. Giant Hawaiian landslides. *Annu. Rev. Earth Planet. Sci. Lett.* 22, 119–144.
- Mukhopadhyay, S., Lassiter, J.C., Farley, K.A., Bogue, S.W., 2003. Geochemistry of Kauaʻi shield-stage lavas: Implications for the chemical evolution of the Hawaiian plume. *Geochem. Geophys. Geosyst.* 4, doi:10.1029/2002GC000342.

- Noguchi, N., Nakagawa, M., 2003. Geochemistry of submarine Southwest-Oahu volcano, Hawaii: new type of Hawaiian volcano? *Geochim. Cosmochim. Acta*, 67, A341.
- Ozawa, A., Tagami, T., Garcia, M.O., 2005. Unspiked K-Ar ages of Honolulu rejuvenated and Koolau shield volcanism on Oahu, Hawaii. *Earth Planet. Sci. Lett.* 232, 1–11.
- Palmiter, D. B., 1975. The Geology of the Kōloa Volcanic Series of the South Coast of Kauaʻi, Hawaii. M.S. Thesis, University of Hawaii, Honolulu.
- Paris, R., Guillou, H., Carracedo, J.C., Perez-Torrado, F.J., 2005. Volcanic and morphological evolution of La Gomera (Canary Islands), based on new K-Ar ages and magnetic stratigraphy; implications for oceanic island evolution. *J. Geol. Soc. London* 162, 501–512.
- Paul, D., White W.M., Blichert-Toft, J., 2005. Geochemistry of Mauritius and the origin of rejuvenescent volcanism on ocean island volcanoes. *Geochem. Geophys. Geosyst.*, 6, doi:10.1029/2004GC000883.
- Pertermann, M., Hirschmann, M.M., 2003. Anhydrous partial melting experiments on MORB-like eclogite: phase relations, phase compositions and mineral-melt partitioning of major elements at 2–3 GPa. *J. Petrol.* 44, 2173–2201.
- Pretorius, W., Weis, D., Williams, G., Hanano, D., Kieffer, B., Scoates, J., 2006. Complete trace elemental characterisation of granitoid (USGS G-2, GSP-2) reference materials by high resolution inductively coupled plasma-mass spectrometry. *Geostandards and Geoanalytical Research* 30, 39–54.
- Regelous, M., Niu, Y., Wendt, J.L., Batiza, R., Greig, A., Collerson, K.D., 1999. Variations in the geochemistry of magmatism on the East Pacific Rise at 10°30'N since 800 ka. *Earth Planet. Sci. Lett.* 168, 45–63.
- Reiners, P.W., Nelson, B.K., 1998. Temporal-compositional-isotopic trends in rejuvenated-stage magmas of Kauaʻi, Hawaii, and implications for mantle melting processes. *Geochim. Cosmochim. Acta* 62, 2347–2368.
- Reiners, P.W., Nelson B.K., Izuka, S.K., 1999. Geologic and petrologic evolution of the Lihue Basin and eastern Kauaʻi, Hawaii. *GSA Bull.* 111, 674–685.
- Rhodes, J.M., 1996. Geochemical stratigraphy of lava flows sampled by the Hawaii Scientific Drilling Project. *J. Geophys. Res.* 101, 11,729–11,746.
- Rhodes, J.M., Vollinger, M.J., 2004. Composition of basaltic lavas sampled by phase-2 of the Hawaii Scientific Drilling Project: Geochemical stratigraphy and magma types. *Geochem. Geophys. Geosyst.* 5, 1–38.
- Ribe, N.M., 2004. Through thick and thin. *Nature* 427, 793–795.
- Ribe, N.M., Christensen, U.R., 1999. The dynamical origin of Hawaiian volcanism. *Earth Planet. Sci. Lett.* 171, 517–531.
- Roden, M.F., Trull, T., Hart, S.R., Frey, F.A., 1994. New He, Nd, Pb, and Sr isotopic constraints on the constitution of the Hawaiian plume: Results from Kōlolu volcano, Oahu, Hawaii, USA. *Earth Planet. Sci. Lett.* 69, 141–158.
- Sano, H., 2006. Unspiked K-Ar dating of the rejuvenated and shield-building volcanism on Kauaʻi. Hawaiʻi, Kyoto University, Unpublished M.S. thesis.

- Smith, J.R., Satake, K., 2002. Multibeam bathymetry and sidescan data of the Hawaiian islands, 1998–1999. In: E. Takahashi, P.W. Lipman, M.O. Garcia, J. Naka and S. Aramaki, Editors, *Hawaiian Volcanoes: Deep Underwater Perspectives*, Am. Geophys. Union Geophys. Monogr. 128, 3–9.
- Staudigel, H., Zindler, A., Hart, S.R., Leslie, T., Chen, C.-Y., Clague, D.A., 1984. The isotopic systematics of a juvenile intraplate volcano: Pb, Nd, and Sr isotope ratios of basalts from Loihi Seamount. *Earth Planet. Sci. Lett.* 69, 13–29.
- Stille, P., Unruh, D.M., Tatsumoto, M., 1983. Pb, Sr, Nd and Hf isotopic evidence of multiple sources for Oahu, Hawaii basalts. *Nature* 304, 25–29.
- Stille, P., Unruh, D.M., Tatsumoto, M., 1986. Pb, Sr, Nd and Hf isotopic constraints on the origin of Hawaiian basalts and evidence for a unique mantle source. *Geochim. Cosmochim. Acta* 50, 2303–2319.
- Stracke, A., Salters, V., Sims, K., 1999. Assessing the presence of garnet-pyroxenite in the mantle sources of basalts through combined hafnium-neodymium-thorium isotope systematics. *Geochem. Geophys. Geosyst.* 1, doi:10.1029/1999GC000013.
- Tagami, T., Sano, H., Blay, C., Gandy, C.E., 2005. Unspiked K-Ar dating of the Kōloa rejuvenated volcanism and shield Waimea Canyon Basalt on Kauai. *Eos Trans. AGU* 86, V51A-1473.
- Tanaka, R., Makishima, A., Nakamura, E., 2008. Hawaiian double volcanic chain triggered by an episodic involvement of recycled material: Constraints from temporal Sr-Nd-Hf-Pb isotopic trend of the Loa-type volcanoes. *Earth Planet. Sci. Lett.* 265, 450–465.
- Tanaka, R., Nakamura, E., 2005. Boron isotopic constraints on the source of Hawaiian shield lavas. *Geochimica et Cosmochimica Acta*. 69, 3385–3399.
- Tanaka, R., Nakamura, E., Takahashi, E., 2002. Geochemical evolution of Koolau volcano. In: Takahashi, E., Lipman, P.W., Garcia, M.O., Naka, J., and Aramaki, S. (eds.), *Hawaiian Volcanoes: Deep Underwater Perspectives*, Geophys. Monogr. Ser., 128, 311–332.
- Torresan, M.E., 1990. GLORIA mosaic of the U.S. Hawaiian Exclusive Economic Zone. *AAPG Bull.* 74, 1005 pp.
- van Keken, P., Zhong S., 1999. Mixing in a 3D spherical model of present-day mantle convection. *Earth Planet. Sci. Lett.* 171, 533–547.
- Wanless, V.D., Garcia, M.O., Rhodes, J.M., Weis, D., Norman, M.D., 2006. Shield-stage alkalic volcanism on Mauna Loa Volcano, Hawaii, *J. Volcanol. Geotherm. Res.* 151, 141–155.
- Weis, D., Frey, F.A., 1991. Isotopic geochemistry of Ninetyeast Ridge basement basalts: Sr, Nd and Pb evidence for involvement of the Kerguelen hot spot. In Weissel, J., Pierce, J., Taylor, E., Alt, J., (eds). *Proc. ODP, Scientific Results 121*. Ocean Drilling Program, College Station, Tex, 591–610.
- Weis, D., Frey, F.A., 1996. Role of the Kerguelen plume in generating the eastern Indian Ocean seafloor. *J. Geophys. Res.* 101, 13,381–13, 849.
- Weis, D., Frey, F.A., Giret, A., Cantagrel, J.M., 1998. Geochemical characteristics of youngest volcano (Mount Ross) in the Kerguelen Archipelago; inferences for magma flux, lithosphere assimilation and composition of the Kerguelen Plume. *J. Petrol.* 39, 973–994.

- Weis, D., Kieffer, B., Maerschalk, C., Pretorius, W., Barling, J., 2005. High-precision Pb-Sr-Nd-Hf isotopic characterization of USGS BHVO-1 and BHVO-2 reference materials. *Geochem. Geophys. Geosyst.* 6, doi:10.1029/2004GC000852.
- Weis, D., Kieffer, B., Maerschalk, C., Barling, J., de Jong, J., Williams, G.A., Hanano, D., Pretorius, W., Mattielli, N., Scoates, J.S., Goolaerts, A., Friedman, R.M., Mahoney, J.B., 2006. High-precision isotopic characterization of USGS reference materials by TIMS and MC-ICP-MS. *Geochem. Geophys. Geosyst.* 7, doi:10.1029/2006GC001283.
- Weis, D., Kieffer, B., Hanano, D., Nobre Silva, I., Barling, J., Pretorius, W., Maerschalk, C., Mattielli, N., 2007. Hf isotope compositions of U.S. Geological Survey reference materials. *Geochem. Geophys. Geosyst.* 8, doi:10.1029/2006GC001473.
- West, H.B., Leeman, W.P., 1987. Isotopic evolution of lavas from Haleakala Crater, Hawaii. *Earth Planet. Sci. Lett.* 84, 211–225.
- Woods, M. T., Leveque, J.-J., Okal, E. A., Cara, M., 1991. Two station measurements of Rayleigh wave group velocity along the Hawaiian swell. *Geophys. Res. Lett.* 18, 105–108.
- Wright, T.L., 1971. Chemistry of Kilauea and Mauna Loa lava in space and time. USGS Professional Paper, Report: P 0735, 40 pp.
- Wright, E., White, W.M., 1987. The origin of Samoa; new evidence from Sr, Nd, and Pb isotopes. *Earth Planet. Sci. Lett.* 81, 151–162.
- Xu, G., Frey, F.A., Clague, D.A., Weis, D., Beeson, M.H., 2005. East Molokai and other Kea-trend volcanoes: Magmatic processes and sources as they migrate away from the Hawaiian hot spot. *Geochem. Geophys. Geosyst.* 6, doi:10.1029/2004GC000830.
- Xu G., Frey, F.A., Clague, D.A., Abouchami, W., Blichert-Toft, J., Cousens, B., Weisler M., 2007. Geochemical characteristics of West Molokai shield- and postshield-stage lavas: Constraints on Hawaiian plume models. *Geochem. Geophys. Geosyst.* 8, doi:10.1029/2006GC001554.